

Response to Reviewer Comments on Nickless et al.,

Reviewer 1:

Main comments:

The authors present an atmospheric inversion result over Cape Town focusing on sensitivity analyses related to the technical aspects of the inversion method. I can easily see the authors did a lot of work. However, the presentation needs substantial improvement as well as revisions in technical details.

First, the authors definitely need to rewrite the abstract. Simply it is too long and not organized well (please see my specific comments below).

Response: Following a rewrite of the manuscript, the abstract has been substantially modified.

The introduction section also needs lots of changes or rewriting. Please see my comments below.

Basically, it is too technical from the beginning of the section, not providing a gentle overview of the study presented. I recommend that the section be shortened.

Response: The Introduction has been substantially rewritten to give a fuller introduction to city-scale inversions, and details of the sensitivity tests have been kept brief. The purpose of the paper is made clearer.

The writing is below average compared to many papers I have reviewed. I understand that the authors did a lot of work but in many places, but the result/discussion presented is not so clear. The paper is too long for the reader to read in current form while there is no exciting scientific findings - this does not mean that the material is not important (it is a different paper). I wonder if the authors can reduce the number of sensitivities cases by (re)moving some of the insignificant results to the supplement.

Response: The manuscript has been rewritten to improve clarity, and more emphasis is given to those aspects to which the inversion was most sensitive, and sections on tests which had little impact on the result of the inversion have been shortened. We feel that it is important to highlight these aspects of low sensitivity, as this is important information for those who may be concerned about these attributes in similar inversion studies.

Please see the detailed comments below and address them before I consider any suggestion for publication.

Detailed comments:

Abstract.

Simply put, the abstract is too long while not conveying useful information in a succinct way.

Needs significant improvement in writing (and selecting the most useful pieces of information to be presented here).

Response: The abstract has been rewritten. It is shorter with better explanation of the purpose and greater emphasis on the main result of the paper.

Please try to rephrase "A carbon assessment product of natural carbon fluxes, used in place of CABLE, and the Open-source Data Inventory for Anthropogenic CO₂ product, in place of the fossil fuel inventory, resulted in prior estimates that were more positive on average than the reference configuration." - a little awkward.

Response: This is no longer in the abstract. It now reads: "Alternative prior products were considered in the form of a carbon assessment analysis to provide biogenic fluxes and the ODIAC

(Open-source Data Inventory for Anthropogenic CO₂ product) fossil fuel product. These were used in place of the reference inversion's biogenic fluxes from CABLE (Community Atmosphere Biosphere Land Exchange model) and fossil fuel emissions from a bespoke inventory analysis carried out specifically for the Cape Town inversion.”

Also, the authors need to divide the following sentences into two (unless made clearer):

“For the Cape Town inversion we showed that, where our reference inversion had aggregated prior flux estimates that were made more positive by the inversion, suggesting that the CABLE was overestimating the amount of CO₂ uptake by the biota, when the alternative prior information was used, fluxes were made more negative by the inversion.”

Response: This has been amended to “Where the reference inversion had aggregated prior flux estimates that were made more positive by the inversion – suggesting that CABLE was overestimating the amount of CO₂ biogenic uptake – the carbon assessment prior fluxes were made more negative by the inversion.”

Please remove the following (you can state in the results or discussion section): “As the posterior estimates were tending towards the same point, we could deduce that the best estimate was located somewhere between these two posterior fluxes. We could therefore restrict the best posterior flux estimate to be bounded between the solutions of these separate inversions. “

Response: This has been amended to: “As the posterior estimates were tending towards the same point, we could infer that the best estimate was located somewhere between these two posterior fluxes”. We have not removed the sentence entirely because this is one of the important points we are trying to make from our conclusions.

What is the main conclusion we can gain from the abstract? The authors need to emphasize it. Currently, I only see many small points and cannot determine which one to take home.

Response: The main conclusion from this paper are that spatial and temporal correlations in the flux uncertainties can dictate the solution of an inversion, particular in the typical city-scale inversion framework where high-resolution fluxes are solved for in the inversion. We need to take advantage of these uncertainty correlations in order to propagate the information from the observations further into the domain. To the abstract we have added:

“In summary, estimates of Cape Town fluxes can be improved by using better and multiple prior information sources, particularly on biogenic fluxes. Fossil fuel and biogenic fluxes should be broken down into components, building in knowledge on spatial and temporal consistency in these components into the control vector and uncertainties specified for the sources for the inversion. This would allow the limited observations to provide maximum constraint on the flux estimates.”

P 2, L12: Please remove “where estimates of CO₂ fluxes can be derived from measurements of CO₂ concentrations at a point location”, which does not represent the general atmospheric inversion.

Response: The introduction has been rewritten. This section has now been changed to “Bayesian inverse modelling provides a top-down technique for verifying emissions and uptake of carbon dioxide (CO₂) from both natural and anthropogenic sources. It relies on accurate measurements of CO₂ concentrations at suitably located sites which can collect information about these sources at different spatial and temporal scales. The concentration measurements on their own are not sufficient to solve for the emission sources as there are many more sources of CO₂ than there are measurements of the concentrations. Therefore well-informed initial estimates of the biogenic and anthropogenic emissions are required, together with uncertainty estimates, which are used to regularise the problem.”

P2, L17: Not all of inversions do that; depends on the study. It could be fossil fuel only.

Response: This has been reworded as above. An inversion does not necessarily need to solve for both, but both anthropogenic and biogenic fluxes need to be taken into account (either through design, such as limiting the period over which the inversion is performed to be during the dormant season, or by setting one of these components as fixed, or solving for both components of the total flux).

Introduction: The authors are more focused on the technical aspects of the inversion method considered here by starting describing what atmospheric inversion means in terms of technique, even in the first paragraph of the introduction! Please reframe the introduction so that the authors approach the problem from the urban greenhouse gas (GHG) perspective. People may be interested in Cape Town GHG emissions (more generally), which I haven't heard much before.

Response: The introduction has been rewritten to give a fuller introduction to the use of inverse modelling for the purpose of solving for greenhouse gas fluxes at the city-scale. The details on the sensitivity analysis in the introduction have been kept light. A summary of the Cape Town reference inversion results have been included at the beginning of the Results section.

Also, please reduce the introduction section because it includes too many technical details/terms. It should be a gentle "introduction" to the paper.

Response: The technical details in the introduction have been reduced.

P2, L25: covariance matrices => uncertainty (or error) covariance matrices

Response: Corrected

P6, L10: "s" should be the surface fluxes, not including the background (i.e., CO₂ concentration at the boundary). This is because "Hs" is from the model, not the measurements.

Response: In our inversion framework, the sources include the concentrations at the boundary, which is possible as shown in Ziehn et al 2014 and Nickless et al 2018. This avoids the need to set as fixed what the boundary concentrations are (which are usually modelled with significant errors), which is usually subtracted from the observed concentrations, and these differences used as the observations in the inversion. Because we worked with a rectangular domain, it made sense to use the boundaries at the four cardinal directions. We do not have modelled concentrations at the boundaries. Instead, we were fortunate to have a GAW measurement site in the domain which observed background conditions for the majority of the time, and due to the homogeneity of the region around Cape Town, these measurements could be taken as representative of boundary conditions on all sides. By solving for the concentrations, but imposing small uncertainties on these concentrations, the inversion can make small corrections to the boundary concentrations, but these corrections would not dominate the inversion solution.

Also, c_{mod} should be Hs_0 (s_0 is prior fluxes in Eq. 1), right?

Response: In this case c_{mod} should be equal to Hs . Even if we know exactly what s are, Hs only gives us modelled concentrations, and difference between these modelled concentrations and the true concentrations are then the observation errors.

P6, L13: Change s to s_0 . Is s_0 hourly or weekly? Even if you solve for the weekly mean surface fluxes, for CO₂, I would expect that hourly prior fluxes were used. Please clarify.

Response: s has been changed to s_0 . We have provided more details on the Bayesian inversion framework. The fluxes are weekly fluxes. It is possible to calculate a sensitivity matrix to solve for a flux in any time step. We chose to solve for weekly fluxes (i.e. we assumed that the day and night fluxes remained constant over a period of a week) since daily fluxes would lead to much larger

matrices than would be manageable in the current framework, and there are not enough observations available to resolve fluxes at an hourly time step.

P6, L17: “The boundary concentrations in s ”? Why “ s ” when you talk about concentration. “ s ” can only be linked to concentrations via H . When you refer to concentrations, it should be “ c ”, not “ s ”; “ s ” is fluxes. Right?

Response: The boundary concentrations are included in s_0 since we solve for these concentrations in the inversion. Ziehn et al (2014) shows the derivation of the sensitivity matrix for boundary concentrations solved for in a limited domain regional inversion.

P6, L20: Change “can be added to the measurement errors contained in C_c ” to “can be added to the error covariance matrix C_c that includes measurement errors”. Mathematically, C_c includes all different error sources, but, to be specific/accurate, we want to separate transport errors from those of measurements.

Response: This has been reworded and the section expanded.

P6, L23: Are 4 and 16 ppm^2 the total variance (i.e., including transport error, background error, etc.) in the diagonal elements of C_c that the authors actually used in the inversion? Then, do the authors have any scientific/statistical evidence that these numbers really represent the total irreducible variance in the error covariance matrix?

In other words, how did the authors come up with these number?

Response: These are only the minimum observation errors. Further terms are added for the observation errors based on the observed variability in the measurements at the site within each hour and the average wind speed at the site during each hour. More information has been added to the methods section on the derivation of the observation errors.

P7, L3: Why is 1-hour assumed for L ? It seems too short. After an hour, are the errors uncorrelated? Usually, following synoptic scales of meteorology, it could go hours and days.

Response: A 1 hour correlation length leads to non-zero correlations between observations at least seven hours apart. Most city-scale and mesoscale inversions do not include observation error correlations, and work with diagonal matrices, although it is known that observation errors are correlated. We have included an additional case using a 7 hour correlation length, which leads to non-zero correlations between observations further than 24 hours apart.

P7, L7: Please add a subsection for the transport model because in current form the authors try to combine the Bayesian inversion method with everything (transport, prior flux, etc.) that is part of the inversion system; not convenient for the reader to follow.

Response: The description of the inversion framework has been expanded and divided into subsections.

P7, L19: Please add information of temporal and spatial resolutions of the prior flux, as a minimum detail.

Response: These additional details have been added.

P7, L32 - 34: Related to this, please add a few sentences about C_{s_0} (prior error covariance) including the structure (e.g., dimension, etc.). In this way, the reader should be able to better understand how the authors treated the prior error covariance.

Response: These additional details have been added.

P8, L2-4: Any concern of aggregation of hourly to weekly? If the authors aggregated into monthly, I would be definitely concerned, but weekly aggregation is in the gray area, it seems to me. The way I

would do it is that you still use prior predictions in hourly (i.e., Hs_0 in hourly in eq. 1) while solving for weekly mean “s”. CABLE is originally 1 x 1 km? If not, please say so.

Response: Hs_0, which are the modelled concentrations, is hourly. The sensitivity matrix H relates weekly fluxes to hourly concentrations (i.e. assume that the day and night fluxes remain constant during the week). CABLE was dynamically coupled to the regional climate model, and therefore was driven by inputs on a 1 x 1 km spatial grid. Additional details on the inversion framework have been added.

P8, L29: “in place of” => “in addition to”. Both bio prior emissions are used?

Response: The sentence referred to here is “We used these estimates of NEE and NPP in place of those from CABLE (inversion Carbon Assess).” The reference inversion used the net ecosystem exchange from CABLE as the biogenic flux prior and the net primary productivity as the estimate of the uncertainty in the biogenic flux. As a sensitivity test, the estimates from CABLE were replaced with those from a carbon assessment product (NEE for the biogenic flux prior and NEP as the uncertainty in this flux).

This sentence has been changed to “As a sensitivity test, the NEE and NPP from CABLE estimates used for the biogenic flux priors and their uncertainties were replaced with NEE and NPP from the carbon assessment product and the inversion rerun with these priors”.

P9, L6: Where is this standard deviation coming from?

Response: This estimate was calculated as the standard deviation between the fynbos biome pixels from the carbon assessment product. This information has been added. This sentence has been changed to: “The carbon assessment estimated the GPP flux for the year in the fynbos biome to be 521 g CO₂ m⁻² year⁻¹ with a standard deviation of 492 g CO₂ m⁻² year⁻¹ across pixels with 1 km² resolution.”

P9, L9: Please add a few sentences about Figure 1. How are the two bio prior fluxes are different (e.g., in total)? How has the uncertainty in the two priors been estimated?

Response: These details have been added in the section on the priors. The uncertainties are taken as the NPP estimate from the products, as has been done in previous mesoscale inversions. We favour this approach over assigning a percentage uncertainty, as biogenic fluxes in many of South Africa’s biomes are often close to carbon neutral, resulting from large productivity and respiration fluxes during the growing seasons. Therefore if a percentage uncertainty was assigned to the NEE flux, these uncertainties would be close to zero, which would be unrealistic.

After Figure 1 we have added: “The biogenic CO₂ fluxes are more homogeneous across the domain in the carbon assessment product. This can be explained by the products used as inputs for the estimation of the carbon stock components, such as FAPAR, which would not be expected to differ considerably from pixel to pixel in this domain. CABLE predicts greater CO₂ uptake. The average CO₂ flux over the course of the study period and across the domain, was -41 g CO₂ m⁻² week⁻¹ according to the carbon assessment and -172 g CO₂ m⁻² week⁻¹ according to CABLE. The true flux is likely to be highly variable but close to carbon neutral over a long period of time (several years).”

P10, L4-16: This paragraph can be shortened because it does not include any specifics on the author’s work. Does Hestia have anything to do with this work? Except for the product description, I don’t see any point here.

Response: This has been shortened. The discussion on the Hestia product was to show how ODIAC compared to alternative inventory data available in other settings.

P10, L21: Please spare your space more on Figure 2 where you compare the two products for prior fossil fluxes. Are they different? If so, how much, in the bottom-up inventory perspective?

Response: This figure has been modified and additional statistics comparing the products have been provided. A paragraph below the figure has been added:

“The ODIAC product gave similar fossil fuel fluxes over pixels in the CBD area compared with the inventory estimates. The inventory estimates were concentrated over the road network, point sources, and areas of high population density, whereas the ODIAC product dispersed emissions over the domain, with an area of high concentration over the CT metropolitan area and decreasing emissions away from this region. The average fossil fuel flux for the domain over the study period was $134 \text{ g CO}_2 \text{ m}^{-2} \text{ week}^{-1}$ according to the inventory and $274 \text{ g CO}_2 \text{ m}^{-2} \text{ week}^{-1}$ according to the ODIAC product.”

P13, L10: The naming is quite confusing. When I started reading the result section, it was confusing and I had to come back here to check the definition. “an inversion which assumed no temporal error correlation in the specification of C_c ” := NEE Corr. But no hint of “NEE” in this definition. In Table 1, it says NEE Corr is defined as “no observation error correlation”. I understand this is the case without off-diagonal elements. Right?

Response: We have decided to use sensitivity case numbers instead, to avoid any confusion. A table is provided that gives the details of each case. Yes, No Corr means that the uncertainty covariance matrix of the fluxes is diagonal.

There is a disconnection between L9 and L10 of P13.

Response: This has been reworded. The sentences have been rewritten as:

“To assess the sensitivity of the posterior flux estimates, their uncertainties, and their distribution in space to the specification of the uncertainty correlations, we ran inversions where the non-zero off-diagonal elements of C_{s0} and C_c in the reference inversion were systematically set to zero. We considered an inversion which assumed no temporal observation uncertainty correlation in the specification of C_c (inversion S3), an inversion where no spatial uncertainty correlations were assumed for C_{s0} (inversion S4) and an inversion which assumed no uncertainty correlations in the specification of C_{s0} and C_c (inversion S5).”

P13, L33: What is the difference between “Simp Obs No Corr” and “No Corr”. As written, it is not clear.

Response: Simp Obs is the scenario where the observation error is set as either 4 ppm^2 or 16 ppm^2 (excluding the additional components for within-hour measurement variability and within-hour wind speed that were specified in the reference inversion). Both of these cases used diagonal observation error covariance matrices.

To improve clarity, this paragraph has been modified to:

“We considered an inversion where the uncertainties in C_c were set at 2 ppm for the day and 4 ppm at night (inversion S13), excluding the additional components for the error due to wind speed and observation variability that were used in the reference inversion. In this case all the errors in the modelled concentrations are contained within these values, and we disregard the climatic conditions under which the measurements were taken. We tested the impact of increasing the night-time uncertainty in the observation errors to 10 ppm (inversion S14). We further simplified C_c by using the simplified uncertainties of 2 ppm for the day and 4 ppm at night and also set the temporal observation uncertainty correlation to zero (inversion S15).”

P14, L1: Please use “state vectors” instead of “control vectors” because “s” (flux) really means the state, which is commonly used in the timeseries model. In GHG inversion work, I have never heard of control vectors.

Response: The use of control vector is quite commonly used in mesoscale and city-scale inversion studies (e.g. Lauvaux et al 2012 and Oda et al 2017). We would prefer to continue to use control vector to be consistent with the companion paper already published.

We have included a sentence earlier in the manuscript “Additionally we were interested in the composition of the control vector, also referred to as the state vector, which specifies the surface fluxes and domain boundary concentrations to be solved for by the inversion.”

P14, L11-12: I don’t think I have seen a clear description of the background concentration (or boundary concentration). Why only four corners? Since a Lagrangian approach is used, why not sampling boundary conditions for each of the particles? Reading “The inversion solved for $4 \times 2 \times 4 = 32$ boundary concentrations” I understand that the authors seem to solve (as in “s”) for the a single boundary condition for day or night for each week. 4 corners x 2 (day and night) x 4 weeks? Ideally, each (hourly or sub hourly) CO₂ observation has to be associated with the boundary condition. It looks like weekly mean boundary conditions were used, which is not quite okay. Only four corners were used? If so, this is too much simplification. Please clarify how the authors treated the upstream boundary conditions.

Response: We did not have modelled concentrations of CO₂ at the boundaries of the domain. We used the cardinal directions because our limited domain was gridded. We would not expect great variations in the CO₂ concentrations at the boundaries of this domain as there are no close sources either near the ocean borders or the terrestrial borders. The differences between the concentrations at the boundary and the concentration measured at the background site (Cape Point) located within the domain are expected to be very small, certainly smaller than errors in modelling CO₂ concentrations if a chemical transport model had been used.

We have added a full description of the treatment of the boundary concentrations in a new section on the reference inversion. With regards to the sensitivity tests, which is the focus of this paper, all of the inversions used the same prior boundary concentrations and solved for the same 32 boundary concentrations. As these sensitivity tests were focused on the uncertainty covariance matrices, we did not consider any sensitivity tests listed here which changed the way we treated the boundary concentrations, but kept this as a constant between all inversions tested.

Even if the authors used a simple one-valued boundary condition for day and night, I am doubtful about the robustness of the estimation of those 32 values of boundary conditions when solved together with “s”. In a sense, Bayesian inversions use regularization methods via prior assumptions, which means a state vector of 244,824 (huge) can still be solved with a small number of observations. But here because the authors are solving for hundreds thousands of parameters, the posterior is highly dependent on the prior. Related to boundary conditions, what this means is that the posterior boundary conditions (if the authors really estimated the posterior boundary conditions while doing inversions, not pre-subtracting; please clarify) is significantly affected by the prior. If so, what prior did the authors use for the boundary condition?

Response: The prior for the boundary condition was the average concentration taken from the background signal at Cape Point during the course of a week. Variations in this concentration are expected to be small during the course of a week, and there are no large nearby sources outside the domain. The concentration at the boundary is solved for in the inversion, but only a small uncertainty is placed on these concentrations, informed by the observed hourly concentrations, which means that the inversion has to correct the modelled concentration predominantly through making changes to the fluxes within the domain. This was shown to be the case in the reference

inversion (Nickless et al. 2018), and a full discussion on the use of this approach is provided in the companion paper. Where the inversion did make corrections to the boundary concentrations, these corrections were usually made to the terrestrial boundary, which is what we expected.

For the purposes of this paper, which focuses on sensitivity analyses, the boundary condition was set to be the same for all cases, therefore for each sensitivity test any sensitivity shown in the inversion solution in comparison with the reference inversion should be due to the adjustment made to the inversion for this test, and not due to the approach used for accounting for the boundary concentrations.

P15, L27: It is okay to use χ^2 for assessing the goodness-of-fit, but please state the assumption related to this test and whether the data used in the inversion meet the test assumptions. Also, state that what χ^2 results mean. χ^2 itself does not guarantee the accuracy of the results.

Response: This has been changed to: "In order to assess the suitability of the prior uncertainty estimates contained in C_{s0} and C_c , the χ^2 statistic as described in Tarantola (2005), was calculated". More explanation on the statistical assumptions and caveats of this statistic for making this assessment are provided in a new section relating to the use of the χ^2 statistic for the reference inversion.

P18, 3. Results: Please add a subsection here; it looks like an introduction to the Results section but it is a mix of many things. I strongly recommend that the authors remove some to other sections or rewrite it. Basically, what is the main topic for this whole page?

Response: The results section has been rewritten to more succinct and to focus on the main finding of the sensitivity analysis. The description of non-significant tests has been made much shorter. The first section of the results gives a summary of the reference inversion for Cape Town.

P21, L2: Please define bias (obs - model?) if it has not been done somewhere else.

Response: The definition for bias has been added in Section 2.2.5.

P21, L11: Then what does it suggest? The model (Gaussian here) and data using ODIAC are more consistent : : :?

Response: This suggests that the uncertainty estimates for the prior fluxes taken from the ODIAC product, which were set at 100% of the ODIAC estimate, are consistent with the statistical assumptions of the inversion. The uncertainties used for the ODIAC product are much larger than those used for the estimates derived from the inventory in the reference inversion. As χ^2 is not less than one, it indicates that these larger uncertainties are needed in order to adjust the prior flux estimates so that the modelled concentrations better match the observed concentrations.

P21, L14: That's because the prior uncertainty was extremely small. Is it a correct prior assumption? It is over-confident!

Response: The same approach for assigning uncertainties to the prior biogenic fluxes in the reference inversion (using the NPP fluxes as the uncertainty) was applied to the carbon assessment inversion. In this case, the uncertainty estimates are too narrow (if we assume the observation errors are large enough). We wanted to show what the inversion would look like if we swapped out the reference biogenic component for an alternative without making any further changes.

P22, L2: Which uncertainty? Please be specific.

Response: This was referring to the total flux uncertainty. This has been made more specific.

P22, L7: Typically, biospheric fluxes are much more uncertain. This near-zero uncertainty on the prior suggests to me that the prior assumption is wrong.

Response: The uncertainty is not near-zero, but closer to zero than those for the reference inversion. This has been made clearer. It is the difference in the uncertainty from the prior to posterior uncertainty that is small. As you have stated, the prior uncertainties are too small, and therefore the Bayesian inversion has not been able to provide sufficient correction to the prior fluxes, and as a consequence, the difference between the prior and posterior fluxes and the difference between the observed and modelled concentrations are too large and are not centred around zero. Therefore, the χ^2 statistic is greater than one. The uncertainty in the fluxes after the inversion is almost as great as the uncertainty before the inversion.

P22, L9: Before moving to spatial distribution, do we have any conclusion from this time series comparison? What does all this comparison mean?

Response: The figure for the time series has been changed to one which shows the time series of the posterior flux estimates on one step of axes for all three inversions. This shows better how much each set of posterior fluxes has been adjusted from the prior estimates, and in which direction the inversion has shifted the fluxes. The time series shows that under the carbon assessment inversion, the uncertainty limits are too narrow, and so very little adjustment by the inversion was possible. The width of the uncertainty bounds of the ODIAC inversion was similar to those for the reference inversion. The inversion has shifted the more positive prior fluxes under the ODIAC inversion to be closer to zero, and in the reference inversion, the more negative fluxes have been shifted towards zero as well. The figure of the time series plots suggests that the inversion process is consistently shifting the time series of the prior fluxes towards the same ideal time series.

P27, L12: How small is the χ^2 value? Ideally χ^2 should be close to 1. Is it good or bad? This sounds like ignoring temporal correlation is okay?

Response: The temporal observation error correlations did not change the χ^2 very much, with statistics remaining close to one. Therefore, if it is assumed that the other components of the covariance matrices are correct, then removing these temporal correlations is consistent with the statistical assumptions of the inversion.

P27, L13-15: This needs some clarification. What is the difference between Ref with positive covariance (L13) and just Ref (L15). Which one is compared with which one here. This result suggests “no correlation” has a minimal impact on the posterior?

Response: There is no difference, as Ref contains these positive covariances. It is the test cases Obs Corr and No Corr where these positive covariances were made zero. The sentence referred to here has been corrected. What we meant to say here was:

In the reference inversion the positive covariances specified between neighbouring NEE flux uncertainties led to large prior and posterior uncertainty around the aggregated weekly fluxes. If these positive covariances are removed from **C_s0** then the uncertainty around the aggregated total flux was much smaller. On the other hand, the test case which retained the positive covariances in **C_s0** (S3) had uncertainty bounds around the prior and posterior aggregated fluxes that were indistinguishable from those in the reference inversion.

This section has now been shortened to: “In comparison, the removal of the temporal correlation in the observation errors in S3 had only a small penalty in the χ^2 statistic. The spatial distribution of the fluxes and uncertainty reductions achieved remained similar to the reference inversion S0 as well. Increasing the temporal correlation length in the observation errors from one hour to seven hours for the S6 inversion had little impact on the posterior flux estimates or the uncertainty reduction achieved,…”

P27, L17 - L22: The author should be able to explain why there is a such a big difference between weekly and monthly. I don't quite understand why.

Response: There is no difference between weekly and monthly uncertainty reduction. In this paragraph we have focused on the uncertainty reduction, and this is summarised for each month in the supplementary material (Table S2), and summarised over the whole study period in Table S1. The flux estimates are aggregated over a month (aggregated over space and time). If we look at the relative difference between inversions in the spatially aggregated estimates over a week, this relationship is similar to what we get if we aggregated over the month.

P27, L23 - 27: The paragraph starts with Ref and NEE Corr and then mixed up with Obs Corr and No Corr. It is really hard to follow; this happens in many places throughout the paper. Not a smooth reading at all.

Response: The labelling of the inversions has been changed. These cases are all being referred to here, in this final paragraph of the section, because we intended to compare the inversions which had modified uncertainty correlations, which in the previous version were inversions NEE Corr, Obs Corr and No Corr (now inversions S3, S4 and S5).

P27, L 27: This result seems to be important in terms of error reduction. Please add a couple of sentences for this. From Figure 7, I see the central estimates between No Corr and Ref are similar while the error reductions are different.

Response: We have changed the text here to: "The inversion solution was sensitive to the uncertainty spatial correlations assigned to the prior biogenic fluxes. This impacted on the spatial distribution of the fluxes, the magnitude of the total aggregated flux, and the uncertainty reduction achieved by the inversion. By not accounting for the spatial correlations in the biogenic flux uncertainties, this led to uncertainties that were too small, illustrated by average χ^2 statistics above 2 for inversions S4 and S5, which set the spatial correlation of the uncertainties in the biogenic fluxes to zero (see supplementary material Table S1). These inversions also showed little innovation or uncertainty reduction in comparison to the reference, leaving the posterior fluxes to be similar to the priors (Figure 7)."

Section 3.3 & 3.4: I don't have much comment except for the fact that it is somewhat boring to read - please try to convey in a clearer and succinct way!

Response: The results section has been rewritten.

P38, L9: Please clarify what "and could not react to local climate conditions" means.

Response: This sentence has been reworded. "The direction of the correction to the prior fluxes made by the inversion using NEE fluxes from the carbon assessment product suggested that the amount of carbon uptake was insufficient. The NEP fluxes were also smaller compared to those from CABLE, leading to uncertainties that were too small, and therefore an ill-specified inversion. The inversion could not correct the fluxes sufficiently so that modelled concentrations could match better with observed concentrations, and therefore certain localised events (i.e. spikes in the CO₂ signal) were not well represented in posterior fluxes from the carbon assessment inversion."

P38, L13 - 15: Not clear what the authors mean by "The ODIAC product extended the fossil fuel fluxes much further a field from the CBD region than the reference inventory. This led to aggregated estimates that were much larger under the ODIAC inversion than the reference inversion." How is the first sentence is related to the second sentence?

What do the authors mean by the statement in the first sentence?

Response: The ODIAC product has fossil fuel emissions that non-zero for pixels further away from the Cape Town central business district compared with the Cape Town inventory, where the

emissions were localised and concentrated around road networks and point sources, and within regions where the census information located the majority of the population. There are many terrestrial pixels on the outskirts of the domain, near the terrestrial boundaries of the domain where the population size is small, there are no point sources nor a substantial road network, and so the fossil fuel emissions are close to zero. The ODIAC product smoothed the emissions further from the central area, with most pixels having non-zero fossil fuel emissions. If the emissions are aggregated over the domain, the ODIAC product had a larger aggregated flux compared with the Cape Town inventory, and this persisted in the posterior fluxes as well. This is expected as the Cape Town inventory only account for the major point sources in the domain. The aggregation of the smaller point sources that are unknown is almost certainly significant.

We have changed this to: “The comparison of inversion results using different prior products provides useful information regarding which direction the true flux estimates are likely to be. A pixel within the CBD limits had similar fossil fuel flux estimates from the ODIAC product compared with the reference inventory product, but the ODIAC product had emissions that were more widespread across the domain away from the CBD. This led to aggregated estimates that were larger under the ODIAC inversion than the reference inversion. Compared to the reference, the ODIAC inversion attempted to reduce the aggregated flux for most months – and to a greater degree – to better match the observations, indicating that compared with the reference inventory, the ODIAC prior was most likely overestimating the amount of fossil fuel emissions from Cape Town to a greater extent for most parts of the study period.”

P38, L15: “The inversion attempted to reduce the aggregated flux” means when the model tries to match the observations?

Response: In order to better match the observations, the inversion needed to reduce the fossil fuel fluxes implied by the ODIAC product, leading to a reduced aggregated flux over the domain. See above response.

P38, L18-20: Please provide estimates (in numbers) for both in the text so that the reader can clearly see the likely true emission estimates. Each inversion should have a uncertainty bound and then I don't understand what it means by “a much narrower uncertainty region than for either inversions.”

Response: This statement has been modified as follows, and the figure of the time series for this set of sensitivity tests has been updated to illustrate this idea and what the likely flux is: “When the two prior information products provide divergent prior flux estimates, such that the inversion reduced the flux for one product but increased the flux for the other, it suggests that the true flux lies somewhere between the posterior flux estimates from these two inversions. When the posterior aggregated flux was made smaller than the ODIAC prior but larger than the reference prior aggregated flux, such as during February and March 2013, the true aggregated flux should lie between these two posterior estimates. When the posterior flux was made smaller than the prior for both inversions, we could deduce that the true aggregated flux must be below the minimum of these two posterior estimates, and if we have accurate uncertainty estimates, the true flux should be no smaller than the lower uncertainty limit. Making use of the posterior uncertainties and the direction away from the prior in which the inversions made corrections, a region is suggested where the true flux is most likely to lie (Figure 9). For the CT domain, the inversion results suggest that over the spatial domain investigated, the flux is close to carbon neutral for the majority of the year.”

P38, L26-28: 1 hour is too short. It should be useful to see the results based on 6 hours or 24 hours. I expect the length scale would be hours or even a couple of days.

Response: An additional case is added with correlation length of 7 hours. With a correlation length of 1 hour, the non-zero error correlations persist for observations at least 7 hours apart. We felt that there certainly should be error correlations, and therefore did not want to ignore these temporal

correlations, as is done for most of the urban inversions to date, but we also did not want make these correlations too long so that correlations would persist beyond a day, at least for the reference inversion.

P39, L17: This is not correct. Prior is just prior. Your sampling from a prior distribution with a fixed mean and a fixed covariance is still a priori info. It does not require the prior sample to be accurate.

Response: The sentence in reference here is: "The posterior uncertainties reflect the reduction in uncertainty achieved by the inversion given that the prior uncertainties are accurate." What we meant here is that the inversion requires appropriate uncertainty limits in order to have the freedom to correct the prior fluxes such that the uncertainty limits around the posterior flux include the true flux. If the uncertainty limits are incorrectly specified such that they are too narrow, the inversion will still correct the flux in the right direction, but the uncertainty limits may not include the true flux. The way this paragraph is written in the original manuscript may be creating some confusion. Two issues are important here: 1.) The prior mean estimate. The inversion should always nudge the posterior mean closer to the true value. 2.) The uncertainty bounds placed around the prior mean estimate. The inversion will always result in a posterior uncertainty that is smaller than or equal to the prior uncertainty, even if the prior uncertainty is ridiculously small. In terms of the inversion's ability to push the posterior solution closer to the truth, this is determined by the prior uncertainty. Ideally, one would like to be able to set the prior uncertainty just large enough to allow the inversion to still be able to achieve a posterior solution close to the truth. The trick, of course, is getting the right uncertainty estimate.

P39, L19 - 20: This is because your data points are too small compared to the number of parameters to be solved. In other words, your inversion system is more dependent on the prior rather than observations. In this case, the posterior estimate for the individual pixels won't have much constraint; only the regional total emission may be estimated more or less independently, in the best case. From the Bayesian perspective, the only thing you can do is to report what your assumption was, what model was used and what the result is.

Response: The sentence referred to is: "It can be shown that in the absence of observation error, doubling or halving the prior uncertainty in the fluxes results in a respective doubling or halving of the posterior uncertainty." We agree that the observations only weakly constrain the fluxes. This is going to be the case for most urban inversions. There are few cities which have the luxury of being well constrained by observations. And that it is why it so important to get the uncertainty covariance parameters correct, particularly uncertainty correlation lengths, as these expand the influence of the observations onto surface pixels that may not be viewed directly by the observation network.

P39, L23 - 27: Not a Bayesian way of thinking, subject to criticism from frequentists.

Response: The paragraph in question here is "This set of sensitivity tests demonstrated that if we wish to ensure that the uncertainty bounds around the posterior fluxes are within a prespecified margin, say 10% of the aggregated flux estimate, then we have to ensure that prior uncertainty that we begin with is sufficiently small. Assuming no large shifts in the mean estimate, it can be shown that if we wish to obtain an uncertainty estimate that is within 10% of the aggregated flux estimate, and we are able to reduce the uncertainty by 25% through the inversion, then the prior uncertainty estimate would need to be within 13.3% of the prior aggregated flux estimate."

We disagree that this is not a Bayesian way of thinking. In a Bayesian setting, we take advantage of the information we have to reduce the problem space to a narrower region. Normally when we assess a Bayesian inversion framework, we consider how much uncertainty reduction can the observations provide. The other side of the Bayesian solution is the prior information. We are considering by how much can we reduce the uncertainty of the posterior solution by ensuring that the prior information we start with in the inversion has sufficiently reduced the problem space.

For this methodology to be useful in the policy setting, the posterior estimates obtained from the inversion should ideally 1.) contain the true flux estimates, and 2.) the uncertainty limits should be narrow enough to determine if mitigation efforts are reducing emissions to a desired level with sufficient confidence. Since a great deal of resources already goes into the information used to provide prior flux estimates, the typical “expert-estimate” based approach of deciding on the uncertainty limits may never be good enough. Therefore alternative methods of determining the uncertainty parameters, such as the ML method mentioned in the next comment, or the Hierarchical Bayesian approach proposed, may be the best route forward.

P42, L14 - 15: Since the authors are using an analytical solutions for a Gaussian Likelihood function, they could use a simple maximum likelihood estimator for the length scale.

Response: Michalak et al. (2005) and Wu et al. (2013) provides an ML approach for estimating the correlation length and other covariance parameters in an inversion. For a single inversion this requires an iterative method, such as the Gauss-Newton method, to derive these covariance parameters, even when uncertainty covariance matrix is assumed to be diagonal. That would not be feasible for this inversion frame-work, as the number of unknowns is much larger, and we have not assumed a constant uncertainty for all sources, or assumed a single uncertainty scaling factor.

P42, L25 - 29: Please correct the sentences. Also, I don't know what the authors are trying to say here, except for the fact that a hierarchical approach may be better.

Response: The point we are trying to make here is that the approach used for historical global and mesoscale inversions, whereby uncertainty covariance terms and uncertainty correlation lengths are driven by expert opinion, may not be feasible for a high resolution city-scale inversion due to sensitivity of the solution on these estimates. Instead, robust, data-driven estimates of these terms should be considered, such as the ML method described by Michalak et al (2005) or a Hierarchical Bayesian approach described by Ganesan et al (2009). This has not so far been done for city-scale high resolution inversions due to computational constraints. We showed that running weekly inversions solving for an average weekly flux gave a very similar solution to running a monthly inversion solving for average weekly fluxes. Computational costs could therefore be reduced by running shorter inversions, which is more feasible for the ML or Hierarchical Bayesian approach requiring iterations of the inversion.

Reviewer 2

Nickless et al review

This manuscript describes a sensitivity study of an inversion of CO₂ fluxes in and around Cape Town based on measurements at 3 sites. Cape Town is a city with a strong influence from biogenic fluxes and so provides a good case study for separating the anthropogenic influence from the biogenic influence. The main results from the inversion were published in a previous paper (Nickless et al., 2018). This manuscript concentrates on sensitivity studies on various aspects of the inversion, including the priors used for the biogenic and anthropogenic fluxes and the period over which inversions are averaged. This type of sensitivity analysis is undoubtedly important since cities emit such a large fraction of the global CO₂, and there is a need to have robust and well understood inversion methodologies.

The paper is however hard to read. This is partly because it is pretty technical material and partly because so much information is included. This makes it difficult for an interested reader, let alone a casual one, to extract the main points, even after a careful reading. I do not get a feel for the main results from reading the abstract and do not think that the introduction sets the scene for the rest of the paper. I should note that the current discussion and conclusions do a better job of this.

Response: We have rewritten the Introduction and Methods sections in response to comments from the Editor and Reviewer. The introduction now contains a light introduction to Bayesian inversion studies in the context of city-scale inversions, and gives more discussion on the original Cape Town inversion study. We give a clearer explanation of why these sensitivity analyses were performed. The methodology section contains more of the details from the original paper, although we have kept this as lean as we can to avoid repeating too much of what is already described in Nickless et al 2018.

Overall, I think the manuscript could be publishable but only after major revision. I am not making many detailed suggestions as I think a considerable amount of work is needed and the first reviewer has made extensive and well thought out comments. My main comments are as follows:

1. The authors should clarify what the main findings are and then decide what material is needed to back that up in the introduction and in the main body of the manuscript. This should provide a firm basis on which to give a good understanding of the uncertainties and the implications described in the conclusions. That should result in a much tighter and probably shorter manuscript whose contents can be reflected in a clear abstract.

Response: Agreed. The introduction has been rewritten with this in mind.

2. In deciding what the main points are, the authors should consider whether ACP or GMD is the more appropriate home for the work. The ACP description includes the statement “The journal scope is focused on studies with general implications for atmospheric science rather than investigations that are primarily of local or technical interest.” GMD “is an international scientific journal dedicated to the publication and public discussion of the description, development, and evaluation of numerical models of the Earth system and its components.” Models include “geoscientific model descriptions, from statistical models to box models to GCMs.”

Response: Having read through the remit of GMD, I don't believe the type of sensitivity tests we have performed falls into the subject matter that is normally covered by this journal. If I was making changes to the atmospheric transport model it may be appropriate, but I think these types of statistical aspects of the inversion fit better into ACP. Previous studies on sensitivity analyses for city-scale inversions (focusing in this case on the observations used and the atmospheric transport model) have been published in ACP by Stauer et al. 2016 and on different priors used for a mesoscale inversion by Lauvaux et al. 2012. We have also made sure that the results and discussion now also emphasize what information the sensitivity tests provide about the flux of CO₂ from this region.

3. I think that moving to GMD would allow the manuscript to be completely focussed on the technical aspects and might well make it easier to prepare.

Response: We have reduced the amount of technical detail in the manuscript and focussed more on the science and how these sensitivity tests inform future inversions.

4. The supplementary material largely consists of a series of plots which I am not sure are helpful, though I could be persuaded. I would think that some of the current paper could be put into a revised and reduced supplementary material.

Response: The purpose of the plots and tables in the supplementary material was to provide a type of look-up table so that if anyone were interested in a particular sensitivity test case, they could inspect exactly what the solution of the inversion looked like under these conditions, particularly for those cases which are only discussed briefly in the main text because the inversion solution was not sensitive to that particular change. This also avoids any issues related to selective reporting.

5. The present tense should be used for all the new results presented here, and the past tense should be used for previous work and much of the description of the measurements. I am not sure if I am typical, but the mixed use of tense misled me on a few occasions.

Response: We have corrected the tense in the manuscript. Thank you for this guidance.

6. Some comment should be made about the important differences are present in the emissions products in sections 2.2 and 2.3. As it stands, it is hard to know what to keep in mind for later in the manuscript.

Response: More details have been added on the difference between the reference emission product and the alternative products, as described in the response to the first reviewer.

7. It would help to have a short summary of the results from Nickless et al (2018) at the start of Section 3.

Response: We have included in the new results section of the manuscript a brief summary of the results from the original Cape Town inversion.

8. Can percentages be included in the discussion of the changes vs the reference case?

Response: We have included percentages when discussing the difference between the reference and alternative cases, at least when related to the change in the uncertainty. Reporting percentage changes with the total flux is difficult because the solution swings between being positive and negative for different inversions.

9. The aspect ratio in Figs 3, 4, and 9 should be increased. They are hard to read at the moment.

Response: The figures have been replotted to be clearer and to focus only on the important aspects. The number of figures in the main manuscript has been reduced.

An atmospheric inversion over the city of Cape Town: sensitivity analyses

Alecia Nickless^{1,2}, Peter J. Rayner³, Robert J. Scholes⁴, Francois Engelbrecht⁴, and Birgit Erni^{2,5}

¹Atmospheric Chemistry Research Group, School of Chemistry, University of Bristol, Bristol, BS8 1TS, UK

²Department of Statistical Sciences, University of Cape Town, Cape Town, 7701, South Africa

³School of Earth Sciences, University of Melbourne, Melbourne, VIC 3010, Australia

⁴Global Change Institute, University of the Witwatersrand, Johannesburg, 2050, South Africa

⁵The Centre for Statistics in Ecology, the Environment and Conservation, University of Cape Town, Cape Town, 7701, South Africa

Correspondence: Alecia Nickless alecia.nickless@bristol.ac.uk

Abstract. ~~We present sixteen different sensitivity tests applied to the Cape Town atmospheric Bayesian inversion analysis from~~
~~An atmospheric inversion was performed for the City of Cape Town for the period~~ March 2012 ~~until June 2013. The reference~~
~~inversion made use of a fossil fuel inventory analysis and estimates of biogenic fluxes from CABLE (Community Atmosphere~~
~~Biosphere Land Exchange model). Changing to June 2013, making use of in situ measurements of CO₂ concentrations at~~
5 ~~temporary measurement sites located to the North East and South West of Cape Town. This paper presents results of sensitivity~~
~~analyses which tested assumptions regarding~~ the prior information ~~product and the assumptions behind the uncertainties in the~~
~~biogenic fluxes had the largest impact on the inversion results in terms of the spatial distribution of the fluxes, the aggregated~~
~~fluxes and the uncertainty reduction achieved. A carbon assessment product of natural carbon fluxes, used in place of CABLE,~~
~~and the and the uncertainty covariance matrices associated with the prior and with the observations. Alternative prior products~~
10 ~~were considered in the form of a carbon assessment analysis to provide biogenic fluxes and the ODIAC (Open-source Data In-~~
~~ventory for Anthropogenic CO₂ product-) fossil fuel product. These were used in place of the fossil fuel inventory, resulted in~~
~~prior estimates that were more positive on average than the reference configuration. The use of different prior flux products to~~
~~inform separate inversions provided better constraint on the posterior fluxes compared with a single inversion. For the Cape~~
~~Town inversion we showed that, where our reference inversion's biogenic fluxes from CABLE (Community Atmosphere~~
15 ~~Biosphere Land Exchange model) and fossil fuel emissions from a bespoke inventory analysis carried out specifically for the~~
~~Cape Town inversion. Our results confirmed that the inversion solution was strongly dependent on the prior information, but~~
~~by using independent alternative prior products to run multiple inversions, we were able to infer limits for the true domain flux.~~
~~Where the~~ reference inversion had aggregated prior flux estimates that were made more positive by the inversion ~~, suggesting~~
~~that the – suggesting that~~ CABLE was overestimating the amount of CO₂ uptake ~~by the biota, when the alternative prior~~
20 ~~information was used, biogenic uptake – the carbon assessment prior~~ fluxes were made more negative by the inversion. As the
posterior estimates were tending towards the same point, we could ~~deduce~~ infer that the best estimate was located somewhere
between these two posterior fluxes. ~~We could therefore restrict the best posterior flux estimate to be bounded between the~~
~~solutions of these separate inversions.~~

~~The assumed~~ The inversion was shown to be sensitive to the spatial error correlation length for NEE fluxes played a major role in in the biogenic fluxes – even a short correlation length – influencing the spatial distribution of the posterior fluxes and in the size of the aggregated flux estimates, where ignoring these correlations led to posterior estimates more similar to the priors compared with the reference inversion. Apart from changing the prior flux products, making changes to the error correlation length in the NEE fluxes resulted in the greatest contribution to variability in the aggregated flux estimates between different inversions across the domain, and the uncertainty reduction achieved by the inversion. Taking advantage of expected spatial correlations in the fluxes is key to maximising the use of a limited observation network. Changes to the temporal correlations in the observation errors had very minor affects on the inversion.

~~Solving for four separate weekly inversions resulted in similar results for the~~ The control vector in the original version consisted of separate day and night-time weekly fluxes for fossil fuel and biogenic fluxes over a four-week inversion period. When we considered solving for mean weekly fluxes compared with the single monthly inversion, while reducing computation time by up to 75%. Solving for a mean weekly flux within a monthly inversion did result in differences in the aggregated fluxes fluxes over each four week period – i.e. assuming the flux remained constant over the month – larger changes to the prior fossil fuel and biogenic fluxes were possible, as well as further changes to the spatial distribution of the fluxes compared with the reference inversion, but these difference were mainly during periods with data gaps. The uncertainty reduction from this inversion was almost double that of the reference inversion (47.2% versus achieved in the estimation of the overall flux increased from 25.6%). Taking advantage of more observations to solve for one flux, such as allowing the inversion% for the reference inversion to solve for separate slow and fast components of the fossil fuel and NEE fluxes, as well as taking advantage of expected error correlation between fluxes of homogeneous biota, would reduce the uncertainty around the posterior fluxes. The sensitivity tests demonstrate that going one step further and assigning a probability distribution to these parameters, for example in a hierarchical Bayes approach, would lead to more useful estimates of the posterior fluxes and their uncertainties -47.2% for the mean weekly flux inversion. This demonstrates that if flux components that change slowly can be solved for separately in the inversion, where these fluxes are assumed to be constant over long periods of time, the posterior estimates of these fluxes substantially benefit from the additional observational constraint.

In summary, estimates of Cape Town fluxes can be improved by using better and multiple prior information sources, particularly on biogenic fluxes. Fossil fuel and biogenic fluxes should be broken down into components, building in knowledge on spatial and temporal consistency in these components into the control vector and uncertainties specified for the sources for the inversion. This would allow the limited observations to provide maximum constraint on the flux estimates.

1 Introduction

~~Bayesian atmospheric inversion, where estimates of fluxes can be derived from measurements of concentrations at a point location, inverse modelling provides a top-down technique for verifying emissions and uptake of carbon dioxide (CO₂) from both natural and anthropogenic sources. It relies on accurate measurements of CO₂ concentrations at suitably located sites which can collect information about these sources at different spatial and temporal scales. The concentration measurements~~

on their own are not sufficient to solve for the emission sources as there are many more sources of CO₂ than there are measurements of the concentrations. Therefore well-informed initial estimates of the biogenic and anthropogenic emissions are required, together with uncertainty estimates, which are used to regularise the problem. This technique is a useful tool for monitoring, reporting and verification (MRV) of CO₂ emissions from cities (Bellassen and Stephan, 2015; Wu et al., 2016; Lauvaux et al., 2016; Oda et al., 2017a). While cities represent only 2% of the global land surface area, they are responsible for approximately 70% of anthropogenic greenhouse gas emissions (UN-Habitat, 2011; Seto et al., 2014), with annual urban CO₂ emissions averaging more than double the size of net terrestrial or ocean carbon sinks (Le Quéré et al., 2013).

Estimates of city-level CO₂ emissions are usually obtained using bottom-up techniques, which usually requires some require knowledge of what activities produce CO₂ emissions and the fuel usage of these activities. These estimates are strongly dependent on accurate reporting, accurate and representative emission factors, and on assumptions regarding temporal or spatial disaggregation of these emissions (Andres et al., 2012). Ascertaining the uncertainty in these inventory-based estimates is not trivial, and these uncertainties increase as the spatial and temporal spatio-temporal resolution of these estimates is increased (Turnbull et al., 2011). The inversion solves for both the anthropogenic and biogenic contributions, usually expressed as fluxes of . This approach attempts to correct prior estimates of these fluxes such that the misfit between the observed and modelled concentrations at the measurement sites is minimised. Therefore, if an inventory analysis of fossil fuel emissions from the city is used as the prior information, the inversion will provide corrections to these emissions. (Turnbull et al., 2011; Andres et al., 2014).

Inversions used for investigating city-level emissions are carried out at kilometric resolutions (Bréon et al., 2015; Lauvaux et al., 2016). Such an inversion was carried out Verifying the accuracy of inventory-based estimates of emissions has become essential (NRC, 2010). This requires transparency, quality and comparability of information, with narrow uncertainty estimates (Wu et al., 2016), but currently uncertainties associated with urban emissions far exceed emission reduction goals, and therefore verification remains challenging. The uncertainty is due to factors such as incomplete data, inconsistency in reporting between different institutions or facilities, fugitive emissions from point sources such as those caused by gas leaks, and methodology which is rarely checked against scientific standards and procedures (Hutyra et al., 2014). Recently several inverse modelling studies aimed at resolving CO₂ emissions have been conducted at the city-scale in Europe and North America (Strong et al., 2011; Duren and Miller, 2012), and more recently for the city of Cape Town (CT) in South Africa (Nickless et al., 2018). As is required for all atmospheric inversions, decisions need to be made regarding what prior information should be used; for which unknown fluxes will the inversion solve; and what the structure of the covariance matrices will be (Bréon et al., 2015; Lauvaux et al., 2016; Stauder et al., 2016; Oda et al., 2017a). Sensitivity tests on the impact of these decisions are necessary, and provide information on the robustness of the inversion results. This paper presents the results of sensitivity tests applied to these decisions for the Cape Town inversion.

The prior information required for an atmospheric inversion are the initial estimates of the unknown fluxes. For a city-level inversion, this means initial estimates of South Africa is the gridded fossil fuel emissions, at the spatial and temporal scale at which the inversion is to be performed. The inversion described in Nickless et al. (2018) made use of a bespoke inventory analysis carried out for the purpose of the inversion (Nickless et al., 2015a). Information on the uncertainty in these prior fluxes is also required. The uncertainties applied to the estimates of the fossil fuel fluxes for Cape Town were based on

~~error propagation techniques. Here the uncertainties in the emission factors and activity data were combined to obtain an overall uncertainty in the flux estimate (Nickless et al., 2015a). single largest emitter of CO₂ on the continent of Africa, and the 13th largest emitter in the world (Boden et al., 2011). South African cities are home to 63% of the present population (Statistics South Africa, 2011), and by 2030 this is predicted to be 71%. Cape Town saw its population increase from 2,563,095~~
5 ~~in 1996 to 3,740,026 in 2011, an increase of 46% (City of Cape Town, 2011).~~

~~Atmospheric inversions at the city-scale are limited by available CO₂ concentration observations – due to insufficient monitoring sites, but also a limited number of locations for suitable monitoring sites (Bréon et al., 2015). Atmospheric transport is complex in the urban environment and challenging for atmospheric transport models to resolve. This may result in large representation errors in the modelled concentrations at the measurements sites. To avoid these errors, a further reduction in the~~
10 ~~number of observations is often made, as observations are excluded based on when the models are likely to perform poorly (Lauvaux et al., 2016; Staufer et al., 2016). The observed concentration data ,as measured at atmospheric monitoring sites and which is the data used by an atmospheric inversion, is a consequence are as a result of aggregated fluxes from all sources of CO₂ along the path of the air flow. Sources refer to anything which may have a positive (i.e. emit) or negative (i.e. uptake) contribution to the overall CO₂ concentration. Even if biogenic fluxes are not necessarily of interest in the city-level inver-~~
15 ~~sion, they need to be accounted for in the inversion model as these fluxes will be inducing induce changes to the observed concentration. For the Cape Town inversion, net CO₂ concentration.~~

~~Atmospheric monitoring sites targeting CT air masses were not available, therefore temporary measurement sites were installed at Robben Island and Hangklip lighthouses, located to the North West and South East of the metropolis (Nickless et al., 2018) . A fossil fuel emission inventory analysis was performed for the city which spatially and temporally disaggregated these~~
20 ~~fluxes to provide prior estimates of the fossil fuel fluxes, with uncertainty estimates determined by means of error propagation techniques (Nickless et al., 2015a). Net ecosystem exchange (NEE) fluxes from biogenic processes were obtained from the land atmosphere exchange model CABLE (Community Atmosphere Biosphere Land Exchange)(Nickless et al., 2018). This model. Uncertainty estimates were based on the estimates of net primary productivity (NPP). CABLE was dynamically coupled to the regional climate model ,CCAM (Conformal Cubic Atmospheric Model), from which climatic variables, required~~
25 ~~for the atmospheric transport model, were obtained. Uncertainties in the prior fluxes were specified to be large due to the large amount of variation in modelling ecosystem productivity and respiration from the fynbos biome by dynamic vegetation models (Monerieff et al., 2015). Fynbos is the dominant naturally occurring vegetation type in the area. Cape Town city is also surrounded by large agricultural areas, particularly vineyards. The uncertainties in the prior NEE fluxes were set at the estimate of net primary productivity (NPP). $NEE = NPP + R_h$, where R_h is the heterotrophic respiration. Therefore NEE~~
30 ~~is a balance of two large fluxes, which are both non-trivial to model (Archibald et al., 2009). The uncertainty in set as the productivity component of the NEE flux as the error in the estimate of NEE can be as large as either the productivity or respiration component. Therefore, for the Cape Town inversion, the uncertainty was much larger than the accompanying NEE estimate. We emphasize these details, as the sensitivity analyses will demonstrate the importance of the approach adopted for assigning uncertainties and error correlations to these natural fluxes.~~

Using the inversion described in Nickless et al. (2018) as the reference inversion, we carried out sensitivity analyses which considered alternative products for the prior information. For the prior fossil fuel fluxes, we substituted the estimates from the bespoke inventory analysis with those from the ODIAC (Open-source Data Inventory for Anthropogenic)product (Oda and Maksyutov, 2011). For the biogenic fluxes, we performed a test where the CABLE estimates were replaced with those from a carbon assessment study (Scholes et al., 2013). The carbon assessment study aimed to map terrestrial carbon stocks for South Africa and provided estimates of NPP and NEE at a spatial resolution of 1×1 , and was used for a previous optimal measurement network design study for South Africa (Nickless et al., 2015b). Sensitivity tests were performed where the original products were used for the prior fossil fuel and NEE fluxes, but the uncertainties prescribed to these fluxes were either individually doubled or halved, which therefore changed the relative contribution of each flux to the uncertainty in the total prior flux.

The structure of the uncertainty covariance matrices for the observations and for the prior fluxes can have a significant effect on the resulting flux estimates from the inversion, as well as on the spatial distribution of these fluxes (Lauvaux et al., 2016). We investigated the impact of the prescribed off-diagonal covariances in these prior covariance matrices. In the reference inversion we allowed a small correlation length of one hour between observation errors. For the prior NEE uncertainty estimates, a correlation length of one kilometre was specified for NEE fluxes from the same week. No spatial correlation was specified between fossil fuel flux uncertainties as many of the larger sources from the inventory analysis were point sources. As we did not solve for fossil fuel fluxes from different sectors separately, we decided it would be better to keep fossil fuel flux uncertainties uncorrelated. This would avoid implausible correlations between uncertainties; for example, between a large industrial source and a residential source. As sensitivity tests, we removed each of these correlations from the prescribed uncertainty covariance matrices; individually as well as the case where the uncertainty covariance matrices for both the observations and for the prior fluxes were specified as diagonal matrices.

We were interested in the composition of the control vector, which contains the unknown surface fluxes and domain boundary concentrations. For the reference inversion we carried out thirteen monthly inversions which solved for weekly fluxes from each of the 101×101 surface pixels. The weekly fluxes consisted of working week and weekend fossil fuel fluxes, which provided the climate inputs required to drive the Lagrangian particle dispersion model (LPDM). The Bayesian inversion framework included a control vector where fossil fuel and NEE fluxes for the full week; each separated into day and night fluxes. Each monthly inversion solved for four sets (i. e. a period of four weeks) of these six distinct weekly fluxes from each pixel. We tested whether solving for an average of each of these weekly fluxes over the course of the month would achieve similar results compared with the reference inversion. We also compared the reference inversion with the approach of carrying out separate inversions for each week. Therefore instead of performing 13 monthly inversions, we performed 13×4 weekly inversions; four inversions per month. Each of these cases requires less computational resources to perform an individual inversion. Under our computational configuration, which made use of high performance computing, this resulted in a saving of 75% of the computational time needed for the reference inversion. If either of these alternative control vectors provides sufficiently similar results to the reference case, this would provide a more efficient means of conducting the inversion. This would allow more alternative configurations of other components of the inversion framework to be tested in the same period of time. were solved for separately.

~~The Cape Town inversion differs from recent city-scale inversions carried out over mega-cities (Bréon et al., 2015; Stauffer et al., 2016) due to~~ One way that CT differs from the mega cities that previous inversions have targeted (Bréon et al., 2015; Stauffer et al., 2016) is through the high integration of natural areas ~~in around~~ the city borders of ~~Cape Town~~CT (Nickless et al., 2018). Natural fluxes are an important contributor to the CO₂ budget of the region. For example, Table Mountain National Park is located directly adjacent to the city bowl ~~-In fact the city wraps around the base of the mountain. This national park and~~ covers an area of 221 km². For this reason, the gradient method ~~used by Bréon et al. (2015) and Stauffer et al. (2016)~~, which relies on the difference between pairs of measurement sites when the wind is blowing from one site, over the target region, to the second site, would not be appropriate given locations of our two measurement sites. ~~In our~~ For the CT case, if the air travelled between the two sites, it would pass directly over Table Mountain National Park, and therefore the gradient method would not have the desired effect of diminishing the impact of biogenic fluxes along the transect between the two sites. In addition, the wind fields showed that air did not travel in a straight path between our two sites (Nickless et al., 2018).

We adopted the approach usually used from regional inversions, where the inversion modelled the concentrations at the measurement sites (Lauvaux et al., 2012). Instead of subtracting the background CO₂ concentration from the measurements, which would have arrived from one of the domain boundaries, we solved for the concentrations at the boundary as an additional unknown, and therefore included these in the control vector, similar to the approach of Lauvaux et al. (2016). We kept tight constraints on ~~what these concentrations could be~~ these concentrations, and used the background measurements obtained from Cape Point, a Global Atmospheric Watch (GAW) background station, as prior estimates of these concentrations. We were able to do this as there are no large anthropogenic sources near the boundary of the domain. We showed in the reference inversion that the variation in the total CO₂ was largely driven by the variation in the NEE flux ~~-In these sensitivity analyses we investigate the impact of reduced uncertainty assigned to the prior NEE estimates.~~ (Nickless et al., 2018).

~~The purpose of this paper is to present the results of these sensitivity tests in comparison with the Cape Town reference inversion. Based on these tests, conclusions can be drawn on how well the reference inversion was specified, and which components could be improved with highest priority to give the greatest improvement in~~ Nickless et al. (2018) was a first attempt at estimating CO₂ fluxes at the high resolution of 1 km by 1 km over CT, solving for separate fossil fuel and biogenic sources. The inversion increased the domain emission of CO₂ from -83.5 kt per month to -19.8 kt. The inversion was able to reduce uncertainty of the total flux within a pixel by up to 97.7%, and was able to reduce the uncertainty in the total weekly flux over the whole domain by up to 50.5%. The largest innovation to a fossil fuel flux was applied to the pixel with the largest point-source fossil fuel flux over an oil-refinery. We found that the optimal solution for the posterior fluxes was one which made the overall flux in this pixel less positive by reducing the fossil fuel flux and by creating areas of more negative fluxes around this pixel. This indicated that either the prior fossil fuel flux was over-estimated, or the atmospheric transport model was not correctly indicating sensitivity of the measurement site to this flux. Compared with the fossil fuel emissions, relative innovations to the NEE fluxes were much larger, due to the large uncertainty assigned to these fluxes. The largest innovations were made to natural areas near the central business district (CBD) of CT, as well as to agricultural regions within the domain, particularly those close to the measurement sites.

Nickless et al. (2018) demonstrated the advantage of using the Bayesian inverse modelling approach to solve for disaggregated fluxes within each pixel when the ultimate goal was to solve for the aggregated flux within each pixel or within a region of interest. The inversion created negative covariances in the posterior uncertainty covariance matrix for those fluxes that were viewed simultaneously at the atmospheric measurement site. When we summed these fluxes, the effect of these negative covariances was to reduce the uncertainty of the aggregated flux – over and above the uncertainty reduction achieved by the inversion for the individual fluxes.

The specification of the uncertainty covariance matrices substantially influences the inversion result (Lauvaux et al., 2016). This paper investigates a series of adjustments to the estimation of inversion which impact on the uncertainty covariance matrix of the fluxes and the observation error covariance matrix. We considered sensitivity tests which halved and doubled the uncertainties of the individual sources, and investigated the impact of the uncertainty correlations in the posterior fluxes. Section ?? inversion. We also manipulated the prior products, either by smoothing the products used in the reference inversion, or using alternative sources for the fossil fuel and biogenic prior fluxes and uncertainties.

Additionally we were interested in the composition of the control vector, also referred to as the state vector, which specifies the surface fluxes and domain boundary concentrations to be solved for by the inversion. The composition of this vector is determined by the size of the source pixels and the time length over which we assume the fluxes are homogeneous. This in turn impacts on the assigned uncertainty covariance matrix. For the reference inversion we carried out thirteen four-week inversions which solved for weekly fluxes from each of the 101×101 surface pixels. The weekly fluxes consisted of working week and weekend fossil fuel fluxes, and NEE fluxes for the full week; each separated into day and night fluxes. We tested whether solving for an average weekly flux over the course of four weeks would achieve similar results compared with the reference inversion, which allowed the four weekly fluxes within a monthly inversion to differ. We also compared the reference inversion with the approach of carrying out separate inversions for each week. Each of these cases requires considerably less computational resources to perform an individual inversion. If either of these alternative control vectors provides sufficiently similar results to the reference case, this would provide a more efficient means of conducting the inversion.

The purpose of this paper is to present the results of these sensitivity tests in comparison with the CT reference inversion presented in Nickless et al. (2018), with the aim of determining the best course of action to improve the ability to resolve fluxes for CT through the inversion method. Section 2 briefly introduces the Bayesian inversion framework. Details of used in the reference inversion can be found in Nickless et al. (2018) (Nickless et al., 2018). This is followed by a description of the alternative prior information products. The and a presentation of the details of the sensitivity analysis are provided analyses. The results of the sensitivity analyses are provided in section ??-3, followed by discussion of these results in section ??, and conclusions in section 5-4, and a final concluding section.

2 Methods

Characterisations of the two observational sites installed at Robben Island and Hangklip lighthouses, and the background monitoring site at Cape Point, are provided in (Nickless et al., 2018). Measurements of concentrations were obtained between

March 2012 and June 2013 by means of a Picarro Cavity Ring-down Spectroscopy (CRDS) (Picarro G2301) instrument. Sufficient data for 13 of the 16 months were available to perform monthly inversions. Robben Island site viewed predominantly air influenced by the Cape Town city bowl whereas Hangklip viewed air influenced by biogenic fluxes from nearby fynbos vegetation and agricultural areas.

5 2.1 Reference Inversion and Bayesian Inverse Modelling Framework

2.1.1 Bayesian Inverse Modelling Approach

The Bayesian synthesis inversion method, as described by Tarantola (2005) and Enting (2002), was used to solve for the fluxes in this study. The observed concentration (c) at a measurement station results from contributions from the surface in the form of fluxes, from the domain boundaries, and from the initial concentration at the site. Concentrations at the measurement site can be modelled as:

In the next section we describe the Bayesian inverse modelling framework and

$$\underline{c}_{mod} = \mathbf{H}\mathbf{s} \quad (1)$$

where \underline{c}_{mod} are the modelled concentrations and \mathbf{s} a vector of source fluxes or concentrations. \mathbf{H} is the Jacobian matrix representing the first derivative of the modelled concentration at the observational site and dated with respect to the coefficients of the source components (Enting, 2002). It provides the sensitivity of each observation to each of the sources, where the sources can be fluxes or concentrations of CO₂. Estimates of the details of the reference Cape Town inversion (referred to in short-hand as inversion **Ref**). In sections 2.2.1 to 2.2.1 we describe the alterations we considered to the reference inversion, and how we compared the results between different inversions.

20 2.2 Bayesian inverse modelling framework and the reference inversion

Nickless et al. (2018) used the Bayesian inverse modelling framework to model hourly concentrations at Robben Island and Hangklip measurement sites. This approach solves for the unknown sources \mathbf{s} , as defined in the control vector, \mathbf{s} , using the Bayesian least squares solution as described in Tarantola (2005), can be obtained by minimising the following cost function with respect to \mathbf{s} :

$$\underline{s} = \underline{s}_0 + \mathbf{C}_{s_0} \mathbf{H}^T (\mathbf{H} \mathbf{C}_{s_0} \mathbf{H}^T + \mathbf{C}_c)^{-1} (c - \mathbf{H} \underline{s}_0)$$

$$J(\mathbf{s}) = \frac{1}{2} ((\underline{c}_{mod} - \mathbf{c})^T \mathbf{C}_c^{-1} (\underline{c}_{mod} - \mathbf{c}) + (\mathbf{s} - \underline{s}_0)^T \mathbf{C}_{s_0}^{-1} (\mathbf{s} - \underline{s}_0)) \quad (2)$$

and the solution for the posterior error covariance matrix for the sources, C_s ,

$$C_s \equiv \frac{(H^T C_c^{-1} H + C_{s_0}^{-1})^{-1}}{C_{s_0} - C_{s_0} H^T (H C_{s_0} H^T + C_c)^{-1} H C_{s_0}}$$

- 5 where c is the vector of concentration measurements from Robben Island and Hangklip measurement sites, s_0 where s is the control vector of unknown surface fluxes and boundary concentrations we wish to solve for, s_0 is the vector of prior estimates of these sources, C_c the error flux and boundary concentration estimates, C_c is the uncertainty covariance matrix of c , and C_{s_0} the prior the observations, and C_{s_0} is the uncertainty covariance matrix of s_0 . H is the Jacobian matrix representing the first derivative of the modelled concentration, c_{mod} , at the observational site and dated with respect to the elements of s . H projects the elements of s into the observation space of c the fluxes and boundary concentrations (Tarantola, 2005).

Minimising this cost function leads to the following solution:

$$c_{mod} = Hs.$$

$$15 \quad s = s_0 + C_{s_0} H^T (H C_{s_0} H^T + C_c)^{-1} (c - H s_0) \quad (3)$$

- The sources, s , consisted of gridded surface fluxes contained within the domain and concentrations of at the boundary. The spatial resolution of inversion was set at 1 by 1 and the extent of the domain was between 34.5° and 33.5° south and between 18.2° and 19.2° east. with posterior covariance matrix:

$$C_s \equiv \frac{(H^T C_c^{-1} H + C_{s_0}^{-1})^{-1}}{C_{s_0} - C_{s_0} H^T (H C_{s_0} H^T + C_c)^{-1} H C_{s_0}} \quad (4)$$

$$\equiv C_{s_0} - C_{s_0} H^T (H C_{s_0} H^T + C_c)^{-1} H C_{s_0}. \quad (5)$$

- 25 Separate monthly inversions were performed. s contained six surface fluxes from each of

2.1.1 Control Vector - s

The total CO₂ flux from a single surface pixel can be thought of as being made up of the following individual fluxes:

$$s_{sf}; i = s_{ff \text{ week day}; i} + s_{ff \text{ week night}; i} + s_{ff \text{ weekend day}; i} + s_{ff \text{ weekend night}; i} + s_{NEE \text{ day}; i} + s_{NEE \text{ night}; i} \quad (6)$$

where $s_{sf;i}$ is the total weekly surface flux from the i^{th} pixel, $s_{ff\ week\ day;i}$ is the total fossil fuel flux during the working week day, $s_{ff\ week\ night;i}$ is the total night-time fossil fuel flux during the working week, $s_{ff\ weekend\ day;i}$ is the total weekend daytime fossil fuel flux, $s_{ff\ weekend\ night;i}$ is the total weekend night-time fossil fuel flux, and $s_{NEE\ day;i}$ and $s_{NEE\ night;i}$ are the total day and night-time biogenic fluxes for the full week from the i^{th} pixel. The reference inversion solved for each of these separate fluxes for each week. There are 101×101 surface pixels for each of the four weeks. The surface fluxes included working week and weekend fossil fuel fluxes and weekly NEE fluxes, each separated into day and night fluxes = 10,201 surface pixels. Over the 16 month period from March 2012 to June 2013, separate monthly inversions were carried out for all months with sufficient valid concentration observations; a total of 13 inversions. Each monthly inversion solved for four weekly fluxes. Therefore a monthly inversion solves for $10,201 \times 4 \times 4 = 244,824$ surface fluxes. The boundaries were considered as the edge of the domain at each cardinal direction (north, east, south, and west). The boundary concentrations in s consisted of four average-

The mean day and night-time concentrations at each of the four domain boundaries for each week are included in the control vector. The inversion solved for $4 \times 2 \times 4 = 32$ boundary concentrations (4 boundaries, day/night, 4 weeks). We solved for weekly concentrations at the four boundaries, separated into day and night averages, therefore 32 boundary concentrations boundaries as we expected these concentrations to show small changes on synoptic time scales, particularly inflow from the ocean boundaries. We avoided solving for too short a period so that the percentile filtering technique (see section 2.1.7) would never discard all measurements for a period. The maximum standard deviation in the hourly background CO_2 concentrations for a week was 0.8 ppm.

The observed concentrations, c , consisted of hourly averaged concentrations derived from the instantaneous measurements obtained-

2.1.2 Concentration Measurements - c

The reference inversion made use of two CO_2 monitoring sites that were established at Robben Island and Hangklip. As the parameters of the atmospheric transport model are not constrained by the inversion, the resulting errors in the modelled concentrations can be added to the measurement errors contained in C_c (Tarantola, 2005). The diagonal elements of the observation error covariance matrix, C_c , consisted of daytime error variances of 4 and night-time errors of lighthouses. Each site was equipped with a Picarro Cavity Ring-down Spectroscopy (CRDS) (Picarro G2301) instrument. Sufficient data for 13 of the 16. Night-time errors are set higher as errors in atmospheric transport are known to be larger as the planetary boundary layer height is lower at night and less stable (Feng et al., 2016; Lauvaux et al., 2016). These error variances accounted for measurement errors, atmospheric transport modelling errors, representation errors and aggregation errors. As described in Nickless et al. (2018), to account for meteorological conditions, these error variances were inflated by up to 1 during day and 4 at night depending on the wind speed, with still conditions leading to the maximum error inflation. An additional inflation factor was added equal to the observed variance of the instantaneous concentration measurements made within the hour. These additional inflations represented periods when the atmospheric transport model would have been most likely to

~~misrepresent the atmospheric transport.~~ months were available to perform monthly inversions. The Robben Island site viewed predominantly air influenced by the Cape Town city bowl whereas Hangklip viewed air influenced by biogenic fluxes from nearby fynbos vegetation and agricultural areas. Details about these measurement sites are provided in Nickless et al. (2018). Rigorous calibration was performed on a regular basis, ensuring that these sites measured on the same scale as the Cape Point background site, which is calibrated to the WMO-X2007 scale. The high frequency observations were processed into hourly concentrations which provided the observed data for the inversion.

The off-diagonal elements of C_c were calculated, based on the Balgovid correlation model as used in Wu et al. (2013), as:

$$C_c(c_i, c_j) = \sqrt{C_c(c_i)} \sqrt{C_c(c_j)} \left(1 + \frac{h}{L}\right) \exp\left(-\frac{h}{L}\right)$$

where c_i and c_j are the average concentrations during hours i

2.1.3 System Meteorology

CCAM is a variable-resolution global atmospheric model developed by the Commonwealth Scientific and Industrial Research Organisation (CSIRO) (McGregor, 1996; McGregor and Dix, 2001; McGregor, 2005a, b; McGregor and Dix, 2008), and j , $C_c(c_i)$ and $C_c(c_j)$ the corresponding error variances for the concentrations in hours i and j , the characteristic correlation length L was assumed to be 1, and h is the length in time between observations i and j . The impact of this, albeit short, correlation length was assessed in a sensitivity test where no correlation between the observation errors was assumed. No consensus has yet been reached on how these correlations between model errors in the concentrations should be treated (Lauvaux et al., 2016).

~~We used the~~ has been validated over South Africa (Engelbrecht et al., 2009; Roux, 2009; Engelbrecht et al., 2011, 2013, 2015). Full details are provided in Nickless et al. (2018). CCAM was applied in stretched-grid mode to function as a regional climate model ~~CCAM, run in variable-resolution mode with Cape Town at its centre and driven by NCEP~~ (A multiple-nudging approach was followed to downscale the 250 km resolution National Centres for Environmental Prediction (NCEP) reanalysis data, to produce three-dimensional fields of mean winds (u, v, w), potential temperature and turbulent kinetic energy (TKE) (McGregor and Dix, 2001; Roux, 2009; Engelbrecht et al., 2013) (Kalnay et al., 1996) to a resolution of 60 km over southern Africa, 8 km over the south western Cape and subsequently to a 1 km resolution over the study area. The model produced hourly estimates on a 1 km \times 1 km spatial grid, which ~~had extent of between~~ extended from 34.5° and to 33.5° south and ~~between from~~ 18.2° and to 19.2° east. ~~These variables were used to drive~~

2.1.4 Jacobian Matrix - H

The Jacobian matrix, H , provides the sensitivities of the concentrations observed at the receptor sites to the surface fluxes and boundary inflows. To generate this matrix in our application the particle counts were processed from a Lagrangian particle dispersion model (LPDM) (Uliasz, 1994). ~~LPDM~~ run in backward mode (Uliasz, 1994). The LPDM was driven by hourly three-dimensional fields of mean winds (u, v, w), potential temperature and turbulent kinetic energy (TKE), which were obtained from the CCAM model. LPDM simulates atmospheric transport by releasing particles from the observational sites and tracking these particles backward in time. These particle counts ~~can be~~ were used to derive the elements of the

Jacobian matrix \mathbf{H} as originally described by Seibert and Frank (2004) and subsequently used in several inversion studies (Lauvaux et al., 2012; Wu et al., 2013; Ziehn et al., 2014; Nickless et al., 2015b; Lauvaux et al., 2016; Nickless et al., 2018; Oda et al., 2018). The details of this as pertaining to the Cape Town reference inversion are described in Nickless et al. (2018). The number of rows in \mathbf{H} are equal to the number of hourly concentrations assimilated into the inversion and the number of columns is equal to the number of sources solved for in the control vector, \mathbf{s} (Lauvaux et al., 2012; Wu et al., 2013; Ziehn et al., 2014; Nickless et al., 2015b; Lauvaux et al., 2016; Nickless et al., 2018; Oda et al., 2018).

Previously we modified the approach of Seibert and Frank (2004) to use particle counts – as produced by our LPDM – instead of mass concentrations which were output by the atmospheric transport model FLEXPART in their study (Ziehn et al., 2014). The elements of the matrix \mathbf{H} corresponding to the surface fluxes in \mathbf{s} were calculated as follows:

$$\frac{\partial \bar{c}_{sf}}{\partial s_{in}} = \frac{\Delta T g}{\Delta P} \left(\frac{N_{in}}{N_{tot}} \right) \frac{44}{12} \times 10^3, \quad (7)$$

where \bar{c}_{sf} is a volume mixing ratio (receptor) expressed in ppm and s_{in} is a mass flux density (source), N_{in} the number of particles in the receptor surface grid from source pixel i released at time interval n , ΔT is the length of the time interval, ΔP is the pressure difference in the surface layer, g is the acceleration due to gravity, and N_{tot} the total number of particles released during a given time interval.

The spatial resolution of the surface flux grid boxes was set to be the same as that of the high-resolution subregion of the atmospheric transport model, resulting in a gridded domain consisting of 101×101 grid boxes (a resolution of $1 \text{ km} \times 1 \text{ km}$). The units of the surface fluxes are given in $\text{kg CO}_2 \text{ m}^{-2} \text{ week}^{-1}$ and are transformed through \mathbf{H} into contributions to the concentration at the measurement site in units of ppm. To solve for the concentrations at the boundary Ziehn et al. (2014) showed that the Jacobian can be calculated as:

$$\frac{\partial \bar{c}_b}{\partial s_B} = \frac{N_B}{N_{tot}} \quad (8)$$

where s_B are the concentrations at the domain boundary, \bar{c}_b is the volume mixing ratios, N_B is the number of particles from the domain boundary, B , and N_{tot} the total number of particles viewed at the receptor site from any of the domain boundaries.

The contribution to the observed concentration at the receptor site can be written as:

$$c_b = \mathbf{H}_B \mathbf{s}_B \quad (9)$$

where \mathbf{H}_B is the Jacobian with respect to the domain boundary concentrations, s_B are the domain boundary concentrations and c_b the contributions from the boundary to the observed concentration at the measurement site in units of ppm. The row elements of \mathbf{H}_B sum to one. Therefore the elements of c_b represent a weighted average of the concentrations at the domain

boundaries, and provide a basis concentration to which the contributions from the surface fluxes are added. Each inversion solves for weekly domain boundary concentrations at the northern, eastern, southern and western borders of the inversion domain box, separated by day and night.

~~The prior fossil fuel fluxes were estimated from a bespoke~~

5 2.1.5 Inventory of Anthropogenic Emissions

~~The inventory analysis carried out for Cape Town. Details are provided in Nickless et al. (2015a) and Nickless et al. (2018). The inventory analysis include fossil fuel emissions from industrial point sources, road vehicle transport emissions~~ CT subdivided ~~the anthropogenic emissions into road transport, airport and harbour emissions, and residential emissions. Residential emissions were based on the assumed use of raw fossil fuels for heating, lighting and cooking. The largest point source was an crude oil refinery plant located north east of the central business district (CBD).~~, residential lighting and heating, and industrial point source emissions (Nickless et al., 2015a). Road transport emissions were derived from modelled values of vehicle kilometres for each section of the road network, based on observed vehicle count data. The vehicle kilometres were scaled for each hour of the day, and separated into week days and weekend days, leading to distinctive vehicle emissions for the week / weekend and day / night periods. Airport emissions were derived from landing and takeoff cycles, as reported by Airports Company South Africa for each month. The IPCC average emission factors for domestic and international fleets (IPCC, 2000) were used to convert the airport activity data into emissions of CO₂. Harbour emissions were derived from gross tonnage of vessels which docked at CT port during each month published by the South African Ports Authority, and emissions derived as described in DEFRA (2010). Residential emissions for lighting and heating were derived from population count data obtained for each of the municipal wards in 2011 (Statistics South Africa, 2011). The South African government reports on the fuel used for domestic heating and lighting (South African Department of Energy, 2009). This was divided between the total population, and then allocated pro rata to each ward. It was assumed that 75% of the annual energy consumed was used for heating, 20% for cooking and 5% for lighting. The majority – 75% – of the emissions for heating were allocated to the winter months. CT provided monthly fuel use for the largest industrial emitters. These were converted directly into CO₂ emissions by multiplying the fuel amount with the DEFRA greenhouse gas emission factors (DEFRA, 2013a). The fuel types that were considered included heavy fuel oil, coal, diesel, paraffin and fuel gas, which was divided into liquid petroleum gas and refinery fuel gas.

~~Uncertainties in these fossil fuel estimates were derived based on error propagation techniques (Nickless et al., 2015a). In the next section we present a comparison between the uncertainties assigned in~~ Based on this inventory analysis, the percentage contribution of industrial point sources to the ~~reference inversion with those assigned to the inversion using the ODIAC fossil fuel fluxes (see Figure 2). The largest uncertainties, as a percentage of the fossil fuel flux estimate, were for those associated with residential emissions, which were spatially distributed according to the 2011 population census. These uncertainties were set at 60% of the domestic emissions estimate. Point sources had relatively smaller uncertainties, as these estimates were based on reported fuel usage data, which was assumed to be accurate, but in absolute terms these uncertainties were large contributors to the total fossil fuel flux uncertainty. Fossil fuel emissions from all sources were summed to provide a total fossil fuel flux for the working week and weekend, separately for day and night. No correlation was assumed between~~ emission for CT was

12.0%, 34.6% from vehicle road transport, 51.0% from the residential sector, and 2.4% from airport and harbour transport. Residential emissions are a large contributor to the fossil fuel emission budget as well as one of the largest contributors to the uncertainties in the fossil fuel sources. ~~This was to avoid creating unlikely correlations between fluxes from different sources. We assumed no correlation in time between fossil fuel fluxes as we were already solving for weekly averaged fluxes, which effectively assumes 100% correlation between fluxes in the same week flux.~~ This is due to the dependency that many people living in CT have on raw fossil fuel burning for heating and lighting. Emissions from power stations are a small component of the total fossil fuel flux from CT as the bulk of the direct emissions from power stations occur elsewhere in the country.

The total fossil fuel CO₂ emissions for the domain were within range of CO₂ emissions reported in the EDGAR (Emission Database for Global Atmospheric Research) (v4.2) database (Nickless et al., 2015a). EDGAR is a global product on a 0.1° × 0.1° grid, which provides the total anthropogenic emissions of CO₂ as estimated from proxy data such as population counts and information on the road transport network (Janssens-Maenhout et al., 2012). The total emissions from the inventory for 2012 were 22% higher than the EDGAR emissions reported for 2010. The emissions in the inventory tended to be concentrated over specific sources, such as over an oil-refinery or along the road network, whereas the EDGAR emissions were smoothed over the city region.

~~Prior estimates of the NEE fluxes were obtained from the land-atmosphere exchange model CABLE (Kowalczyk et al., 2006)~~

2.1.6 Biogenic Emissions

CCAM was dynamically coupled to the land surface model CABLE (Kowalczyk et al., 2006), which allows for feedbacks between land surface and climate processes, such as leaf area feedback on maximal canopy conductance and latent heat fluxes (Zhang et al., 2013). This also has the consequence that the spatial resolution of the biogenic fluxes were at the same spatial resolution of 1 km × 1 km as for the transport model. The model ~~produced~~ produces hourly estimates of NEE net ecosystem exchange (NEE), which were aggregated into weekly (day and night) flux estimates in units of kg CO₂ m⁻² week⁻¹, and used as the prior ~~estimates of terrestrial biogenic fluxes. The spatial resolution of these prior NEE fluxes were kept at a 1 × 1 resolution. We selected CABLE to produce our NEE estimates as CCAM had been dynamically coupled to this land surface model, which allowed for feedbacks between land surface and climate processes, such as leaf area feedback on maximal canopy conductance and latent heat fluxes (Zhang et al., 2013).~~ estimate of biogenic fluxes over the land surface.

The natural areas within the target domain of the inversion are dominated by the fynbos biome. This is a biodiverse biome, with many endemic species, and covers a relatively small area in South Africa, but a large proportion of the area within the domain of the inversion. The fynbos biome is poorly represented by dynamic vegetation models (Moncrieff et al., 2015), and its ability to simulate biogenic fluxes in the fynbos region is largely untested. CABLE was selected as the land atmosphere exchange model to couple with CCAM due to its development for regions in Australia which are similar to the savanna biome in South Africa. In addition to the natural vegetation, a large agricultural sector is within the proximity of CT, particularly vineyards and fruit orchards. The CT region experiences a Mediterranean climate with winter rainfall, with hot and dry summers and mild and wet winters. Significant NEE fluxes take place during both winter and summer periods, as biogenic activity in this region is limited by the amount of water availability, whereas temperatures are usually sufficiently high for plant production

and respiration. The CO₂ fluxes over the ocean were obtained from a study that-which characterised the seasonal cycle of air-sea fluxes of CO₂ in the southern Benguela upwelling system off the South African west coast (Gregor and Monteiro, 2013).
~~Daily-~~

2.1.7 Domain Boundary Concentrations

5 The presence of the Cape Point GAW station provided a source of background CO₂ fluxes-were-derived-from-measurements concentrations for the inversion. The Cape Point station is located approximately 60 km south of CT within a nature reserve, situated on the southern-most tip of the Cape Peninsula at a latitude of 34°21'12.0" south and longitude of 18°29'25.2" east. The inlet is located on top of the 30m measurement tower mounted on a cliff 230 m above sea level. The station observes background measurements of CO₂ when observing maritime air advected directly from the south-western Atlantic Ocean - an
10 extensive region stretching from 20° (sub-equatorial) to 80° south (Antarctic region) (Brunke et al., 2004). Therefore, maritime measurements at Cape Point from the Southern Ocean are well representative of the background CO₂ signal influencing the Cape Peninsula, which are the concentrations expected at the boundary of the inversion domain. The background signal at Cape Point, represented by a subset of the measurements obtained from a percentile filtering technique (Brunke et al., 2004), was used as the prior estimate of the concentrations at each of the four domain boundaries. The percentile filtering technique
15 removes data influenced by the continent or anthropogenic emissions. When applied to the Cape Point CO₂ measurements, approximately 75% of the data are selected. The percentile-filtering technique has been shown to compare well with the more robust method of using contemporaneous radon (²²²Rn) measurements to differentiate between marine and continental air (Brunke et al., 2004).

The Cape Point measurements of the background CO₂ levels meant that we were not dependent on the atmospheric transport
20 model to produce estimates of *p*. These daily fluxes were used to derive weekly flux estimates, which were averaged over a monthly period, and applied as prior estimates to the ocean surface grids CO₂ concentrations at the domain boundary, which are prone to large errors (Lauvaux et al., 2016). The mean weekly background concentrations, separate for day and night, were determined from the percentile filtered measurements at the site, and were used as the prior domain boundary concentrations for each of the four cardinal directions. The prior uncertainty assigned to the boundary concentrations was set at the standard
25 deviation of the measured hourly concentrations for that period, which resulted in a tight constraint on the prior background CO₂ concentrations. Large adjustments by the inversion to the domain boundary concentrations were not expected, including the terrestrial boundaries. The standard deviation in the hourly background CO₂ concentrations ranged between 0.32 and 0.90 ppm, with a mean of 0.62 ppm.

The boundaries of the domain were deliberately set to be far from the measurement sites so that contributions to the CO₂
30 concentration at a measurement site were dominated by the surface fluxes within the domain, rather than by the domain boundary concentrations.

~~As the fynbos biome, which covers a large proportion of the terrestrial surface in our domain, is poorly represented by dynamic vegetation models (Moncrieff et al., 2015)~~

2.1.8 Prior Uncertainty Covariance Matrix - C_{s_0}

Error propagation techniques, as described in Nickless et al. (2015a) and Nickless et al. (2018), were used to estimate the relative uncertainties for each of the sector specific fossil fuel estimates. The relative uncertainties were scaled by a value of 2 in order to ensure that the elements of the covariance matrix were statistically consistent with the assumptions of the inversion (Tarantola, 2005). The resulting uncertainty estimates (expressed as standard deviations) ranged between 6.7% to 71.7% of the prior fossil fuel emission estimate, with a median percentage of 34.9% to 38.4% depending on the month. These values were more conservative compared with uncertainties of Bréon et al. (2015) for the AirParif inventory, which were set at 20% throughout. Since we solved for weekly, rather than daily fluxes, we used a strong assumption that fossil fuel fluxes within the same week were homogeneous over this time. To allow the inversion to react to local conditions within a given week, no temporal uncertainty correlation was assumed between weekly fluxes. Since fossil fuel emissions were expected to be localised in space, we also assumed no spatial uncertainty correlation between fossil fuel fluxes.

The uncertainty in the biogenic prior fluxes was set at the absolute value of the net primary productivity (NPP) as produced by CABLE. Therefore, the uncertainties assigned to the NEE estimates were large. ~~Previous studies, for example, have shown that~~ but there is a great deal of uncertainty in both the productivity and respiration fluxes contributing to the NEE flux (Wang et al., 2011). The estimates of NEE are strongly dependent on the assumed model forms selected for different processes in the CABLE model. For example, the model forms used for the soil temperature-respiration function and the soil moisture-respiration function have large impacts on the NEE estimates, with resulting NEE estimates differing by over 100% compared to ~~with~~ eddy-covariance measurements (Exbrayat et al., 2013). ~~We assigned the value of the NPP associated with the terrestrial NEE estimate as the uncertainty value.~~ The approach of assigning either the productivity or respiration component of NEE as the uncertainty has been used by Chevallier et al. (2010). We wished to avoid assigning fixed proportional uncertainty to the NEE estimates as, particularly for semi-arid regions, small NEE fluxes could occur as a result of both large productivity and respiration fluxes. Proportional uncertainties would lead to unrealistically low estimates of the uncertainty in NEE fluxes. This is different to the approach used by Bréon et al. (2015), where an uncertainty level of 70% was assigned to biogenic fluxes, but in their case absolute NEE estimates were usually large in summer and expected to be small in winter. For the ocean fluxes, the standard deviations in the daily CO₂ fluxes from Gregor and Monteiro (2013) were assigned as the uncertainties. ~~As the uncertainties in NEE estimates were likely to be related, spatial error correlations between NEE fluxes were incorporated in the off-diagonal elements of C_{s_0}~~

To estimate spatial uncertainty covariances in the NEE fluxes, we assumed an isotropic Balgovind correlation model as used in Wu et al. (2013). The off-diagonal ~~elements were calculated in an analogous manner to those for C_{c_1}~~ covariance elements for $s_{NEE;i}$ and $s_{NEE;j}$ were calculated as:

$$C_{s_0,NEE}(s_{NEE;i}, s_{NEE;j}) = \sqrt{C_{s_0,NEE}(s_{NEE;i})} \sqrt{C_{s_0,NEE}(s_{NEE;j})} \left(1 + \frac{h}{L}\right) \exp\left(-\frac{h}{L}\right) \quad (10)$$

where $s_{NEE;i}$ and $s_{NEE;j}$ are NEE fluxes in pixels i and j , $C_{s_0,NEE}(s_{NEE;i})$ and $C_{s_0,NEE}(s_{NEE;j})$ were the corresponding variances in the NEE flux ~~uncertainty matrix for uncertainties in~~ pixels i and j , the characteristic correlation length L was

assumed to be 1 km, and h ~~was is~~ the spatial distance between the centres of pixels i and j . ~~Non-zero error covariances were allowed between NEE estimates from the same week. We assumed no error correlation between fossil fuel and NEE fluxes. Sections 2.2.1 to 2.2.1 describe alterations made to the reference inversion~~

2.1.9 Uncertainty Covariance Matrix of the Observations - C_c

5 The observation uncertainties represented in C_c contain both the measurement error and the error associated with modelling the concentrations. We assigned a minimum uncertainty variance of 4 ppm² for daytime observations and 16 ppm² for night-time observations. These values were assigned as baseline (i.e. minimum) errors, and accounted for measurement errors, atmospheric transport modelling errors, aggregation errors and representation errors. These minimum errors are smaller than those for city-scale inversions conducted in the Northern Hemisphere. We justify the use of these values in our application since CT is
 10 a smaller city compared with the cities considered in the megacity applications, such as Paris and Indianapolis. Measurements of background CO₂ in the Southern Hemisphere have smaller variability compared with measurements in the Northern Hemisphere. For example, for the years 2012 to 2013 the standard deviation between the ~~purpose of sensitivity analyses~~ monthly CO₂ means for Mauna Loa GAW station in the Northern Hemisphere was 2.3 ppm (Tans and Keeling, 2016), whereas for the same time period at Cape Point the standard deviation between the monthly means was 1.6 ppm.

15 We added additional error estimates to these minimum observation errors. We assumed errors in modelled CO₂ concentrations due to the transport model would be larger when the wind speed was lower (Bréon et al., 2015), and this would be compounded at night when the planetary boundary layer height was shallower and more stable (Feng et al., 2016). Additional error ranging between 0 and 1 ppm² was added to the daytime uncertainty variance of 4 ppm², linearly scaled depending on the wind speed, with 0 ppm² added when wind speeds were high (20 m s⁻¹ or higher) and 1 ppm² when the wind speed was close to zero. At
 20 night the additional uncertainty ranged between 0 and 16 ppm². We also accounted for the standard deviation of the measured CO₂ concentrations during each hour. We assumed that variability within the instantaneous measurements at the site during an hour would be associated with larger errors in the atmospheric transport model. The variance of the observed instantaneous CO₂ concentrations within an hour was added to the overall uncertainty. Therefore each hour had a customised observation error dependant on the prevailing conditions at the measurement site. Therefore the total observation uncertainty variance for
 25 hour k is given as:

$$C_c(k, k) = C_{c;base}^2 + C_{c;wind}^2 + C_{c;obs}^2 \quad (11)$$

where $C_{c;base}$ is the baseline observation error of 2 ppm during the day and 4 ppm during the night, $C_{c;wind}$ is the additional error due to the wind speed conditions which ranged between 0 and 1, and $C_{c;obs}$ is the standard deviation of the observed concentrations within that hour. The final observation uncertainties reached up to 15 ppm at night, reducing the weight of these
 30 measurements in the estimation of the prior fluxes.

The off-diagonal elements of C_c were calculated, based on the Balgovind correlation model as used in Wu et al. (2013), as:

$$C_c(c_i, c_j) = \sqrt{C_c(c_i)} \sqrt{C_c(c_j)} \left(1 + \frac{h}{L}\right) \exp\left(-\frac{h}{L}\right) \quad (12)$$

where c_i and c_j are the average concentrations during hours i and j , $C_c(c_i)$ and $C_c(c_j)$ the corresponding error variances for the concentrations in hours i and j , the characteristic correlation length L was assumed to be 1 hour, and h is the length in time between observations i and j . The impact of this, albeit short, correlation length was assessed in a sensitivity tests discussed in the next section. No consensus has yet been reached on how these observation uncertainty correlations should be treated in city-scale inversions (Lauvaux et al., 2016).

2.1.10 Model Assessment

In order to assess the appropriateness of the uncertainty covariance matrices C_c and C_{s_0} , the χ^2 statistic, as described in Tarantola (2005), was calculated as:

$$\chi^2 = (\mathbf{H}s_0 - c)^T (\mathbf{H}C_{s_0}\mathbf{H}^T + C_c)^{-1} (\mathbf{H}s_0 - c) \quad (13)$$

with degrees of freedom equal to ν , the dimension of the data space – in this case the length of observations in the inversion.

The squared residuals from the inversion (squared differences between observed and modelled concentrations) should follow the χ^2 distribution with degrees of freedom equal to the number of observations (Michalak et al., 2005; Tarantola, 2005). The expected value of χ^2/ν is one. Values lower than one indicate that the uncertainty is too large, and values greater than one indicate that the uncertainty prescribed is lower than it should be. The error in the assignment of the uncertainty could be in either C_c or C_{s_0} (or both). In order to ensure the suitability of C_{s_0} , the prior uncertainty variances were multiplied by a factor of two. This ensured that the χ^2/ν statistic was close to a value of one for almost all months of the inversion. These details are provided in Nickless et al. (2018). Due to the length of time it takes to run a single inversion, we did not calculate an individual scaling parameter for each month.

2.2 Alternative biogenic flux product Sensitivity Tests

2.2.1 Alternative biogenic flux product

As part of a project ~~which aimed to assess~~ assessing the carbon sinks of South Africa (DEA, 2015), ~~a report together with~~ monthly 1 km \times 1 km estimates of terrestrial carbon stocks and fluxes were produced (Scholes et al., 2013). To estimate these fluxes, a distinction was made between carbon stocks in natural to semi-natural areas and those on transformed land, such as annually-cropped cultivated land, plantation forests, and urban areas (which was based on the IPCC 2006 value for closed urban forests). ~~We used these estimates of~~ As a sensitivity test, the NEE and NPP ~~in place of those from CABLE (inversion Carbon Assess~~ from CABLE estimates used for the biogenic flux priors and their uncertainties were replaced with NEE and NPP from the carbon assessment product and the inversion rerun with these priors (inversion S1).

To estimate gross primary productivity (GPP), ten years (2001 to 2010) of monthly climatologies (temperature, rainfall, relative humidity) and satellite products for photosynthetically active radiation (PAR) and fraction of absorbed photosynthetically active radiation (FAPAR) were assimilated. Autotrophic respiration (Ra) was calculated based on the inputs for temperature,

above-ground biomass, below-ground biomass and FAPAR. NPP could then be calculated as $NPP = GPP - R_a$. The heterotrophic component (R_h) of Ecosystem respiration (R_e) was based on estimates of soil organic carbon stocks and above-ground litter. The basic calculation to obtain NEE was $NEE = GPP - R_e$, and additional losses of CO_2 through biomass burning, and export and import fluxes from harvest and trade-related activities were accounted for.

- 5 To disaggregate the monthly products into day and night fluxes, it was assumed that all GPP took place during the day, and that half of R_e occurred during the day and half at night. Therefore the weekly NEE and NPP estimates used for the prior information in the inversion were based on the GPP and respiration products from the assessment. The [carbon assessment estimated the](#) GPP flux for the year in the fynbos biome ~~was estimated~~ to be $521 \text{ g } CO_2 \text{ m}^{-1-2} \text{ year}^{-1}$ with a standard deviation of $492 \text{ g } CO_2 \text{ m}^{-1-2} \text{ year}^{-1}$ [across pixels with 1 km² resolution](#). Therefore, as for the CABLE estimates used in the reference inversion, we assign uncertainties to the prior NEE estimates equal to the NPP estimate. A map of the prior daytime NEE fluxes in May 2012 from the CABLE and carbon assessment products is provided in Figure 1.

- [The biogenic \$CO_2\$ fluxes are more homogeneous across the domain in the carbon assessment product. This can be explained by the products used as inputs for the estimation of the carbon stock components, such as FAPAR, which would not be expected to differ considerably from pixel to pixel in this domain. CABLE predicts greater \$CO_2\$ uptake. The average \$CO_2\$ flux over the course of the study period and across the domain, was \$-41 \text{ g } CO_2 \text{ m}^{-2} \text{ week}^{-1}\$ according to the carbon assessment and \$-172 \text{ g } CO_2 \text{ m}^{-2} \text{ week}^{-1}\$ according to CABLE. The true flux is likely to be highly variable but close to carbon neutral over a long period of time \(several years\).](#)
- 15

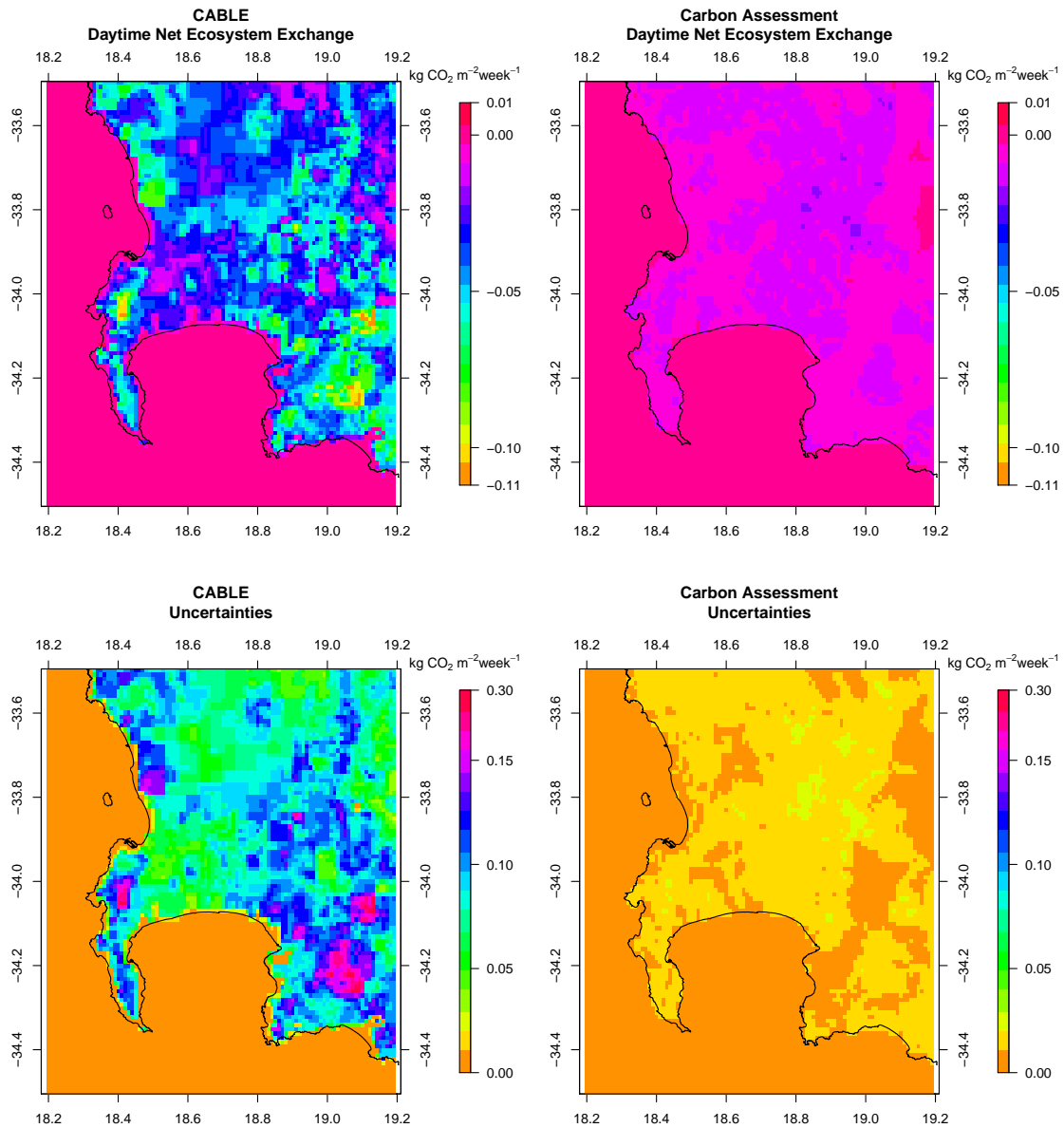


Figure 1. Spatial distribution of the prior daytime NEE fluxes produced by CABLE (top left) and the carbon assessment product (top right) in May 2012, as well as the uncertainty estimates assigned to these fluxes (bottom row).

2.3 ~~Alternative fossil fuel emissions product~~

2.2.1 Alternative fossil fuel emissions product

As an alternative to the inventory analysis of the fossil fuel fluxes, we used current estimates of anthropogenic fossil fuel emissions from the 1 km × 1 km ODIAC product for the years 2012 and 2013 (ODIAC2017) (Oda and Maksyutov, 2011; Lauvaux et al., 2016; Oda et al. , 2017a, b) (inversion ~~ODIACS2~~). The product provides monthly emissions of CO₂ in kt of carbon. The original ODIAC product (Oda and Maksyutov, 2011) made use of global energy consumption statistics and distributed the emissions from these activities based on known point source emitters, such as power plants, and on a global nightlight distribution satellite product. Emissions from point sources, such as those from power plants, were estimated separately from the diffuse emissions, for example those due to transport. These emissions were disaggregated onto to a 1 km × 1 km grid. The updated product has further disaggregated the diffuse emissions to a 30 m × 30 m grid by making use of global road network data, a satellite product on surface imperviousness, and population census data (Oda et al. , 2017a, b). This 30 m × 30 m diffuse emission product together with the point source emission product were aggregated back up to the 1 km × 1 km grid. ~~An inversion carried out for Indianapolis, IN, making use of the updated ODIAC product has shown it to produce similar corrections to the fluxes as those from the inversion making use of the Hestia inventory product (Oda et al., 2017a). The Hestia product is a fine-grained – down to the street/building level – bottom-up emission product which makes use of information from building energy simulation models, traffic data, power production reporting, and pollution reporting (Gurney et al., 2012). This product is available for a few cities in the United States, including Indianapolis.~~ ODIAC has been shown to give comparable flux estimates when used in an inversion as a prior product in place of the ultra high resolution inventory product Hestia (Gurney et al., 2012), carried out for Indianapolis, IN (Oda et al. , 2017a).

The ODIAC monthly estimates were re-scaled according to the day of the week and to the hour of day using scaling factors for South Africa as estimated by Nassar et al. (2013). These estimates were re-aggregated into day and night working week and weekend fossil fuel fluxes in units of kg CO₂ m⁻² week⁻¹. These estimates for the fossil fuel fluxes were used as prior estimates for the inversion in place of the inventory-based estimates used for the reference inversion. The daytime fossil fuel fluxes produced by the inventory analysis and the ODIAC product are provided in Figure 2.

The ODIAC product gave similar fossil fuel fluxes over pixels in the CBD area compared with the inventory estimates. The inventory estimates were concentrated over the road network, point sources, and areas of high population density, whereas the ODIAC product dispersed emissions over the domain, with an area of high concentration over the CT metropolitan area and decreasing emissions away from this region. The average fossil fuel flux for the domain over the study period was 134 g CO₂ m⁻²week⁻¹ according to the inventory and 274 g CO₂ m⁻²week⁻¹ according to the ODIAC product.

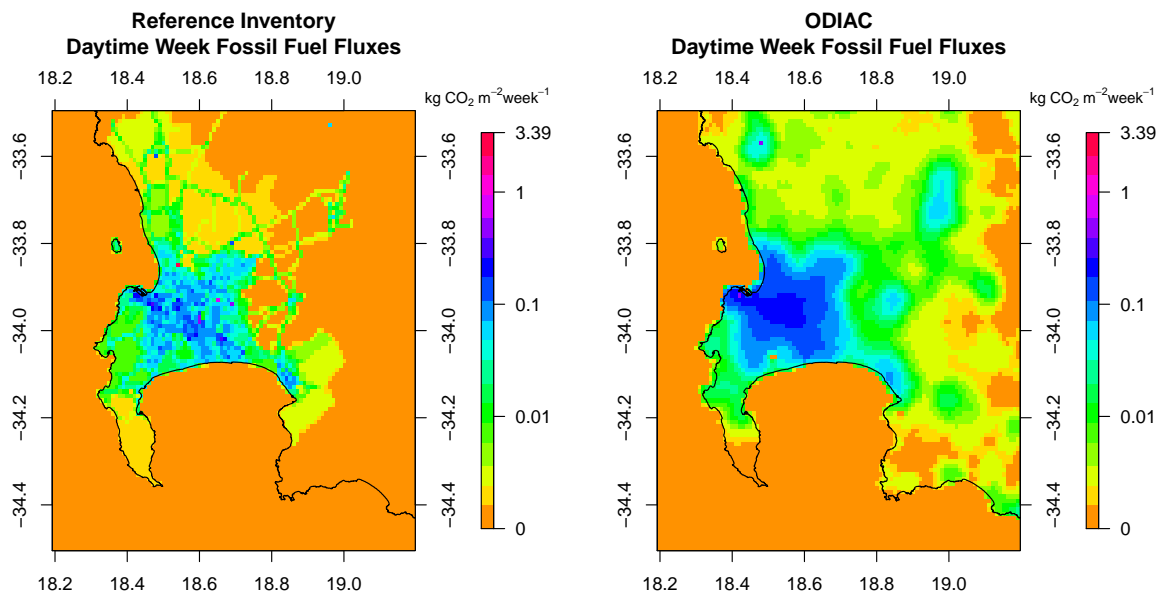


Figure 2. Spatial distribution of the prior fossil fuel fluxes produced from the Cape Town inventory analysis (top-left) and the ODIAC fossil fuel product (top-right) in May 2012, as well as the uncertainty estimates assigned to these fluxes (bottom row): [2012](#).

2.3 Alternative covariance structures

2.2.1 Alternative covariance structures

The specification of the prior uncertainty covariance structures ~~have~~ has been shown to have a ~~significant~~ substantial impact on the pixel-level flux estimates, the total flux estimate for the domain, and on the spatial distribution of the fluxes (Wu et al., 2013; Lauvaux et al., 2016). For example, in the Indianapolis inversion, assuming correlation lengths of 4 or 12 km in the prior uncertainty covariance matrix of the fluxes resulted in total flux estimates for the city that were 17 and 25% larger than the total flux estimate assuming no correlation (Lauvaux et al., 2016). The effect of changing the correlation length had a larger impact on the total flux estimate than changing the prior emission product from Hestia to ODIAC.

To assess the sensitivity of the posterior flux estimates, their uncertainties, and their distribution in space to the specification of the ~~covariance matrix, we considered~~ uncertainty correlations, we ran inversions where the non-zero off-diagonal elements of ~~C_{s_0} and C_c were~~ C_{s_0} and C_c in the reference inversion were systematically set to zero. We considered an inversion which assumed no temporal ~~error-observation uncertainty~~ correlation in the specification of ~~C_c (inversion NEE-Corr)~~ C_c (inversion S3), an inversion where no spatial ~~error-correlation was assumed for~~ C_{s_0} (inversion Obs-Corr) uncertainty correlations were assumed for C_{s_0} (inversion S4), and an inversion which assumed no ~~error-uncertainty~~ correlations in the specification of ~~C_{s_0} and C_c (inversion No-Corr)~~ C_{s_0} and C_c (inversion S5).

We ~~tested what would happen if observation error correlations were set at seven hours (inversion S6) instead of one hour, as was set for the reference inversion. A one hour observation error correlation lengths results in nonzero off-diagonal covariance terms for up to approximately seven hours from the observation. Assigning a seven hour correlation length resulted in non-zero covariances extending through to at least a day away from the observation.~~

We also considered inversions where the prior fossil fuel flux uncertainty was doubled (inversion ~~Double-FFS~~ S7) and where it was halved (inversion ~~Half-FFS~~ S8), and similarly for the NEE flux uncertainties (inversions ~~Double-NEE and Half-NEE~~ S9 and S10). By doubling or halving the uncertainty of the fossil fuel or NEE component of the total flux, we changed the relative uncertainty contribution ~~of~~ each of these ~~had-made~~ to the total uncertainty when compared with the reference inversion.

Due to the large impact that the estimation of the domestic fossil fuel emissions had on the temporal profile of the total fossil fuel fluxes, we considered a modification of the estimated domestic emissions in the inventory product. In the reference inversion 75% of the domestic emissions from heating were assumed to take place during the six winter months. We tested the impact of this assumption by altering the domestic emissions so that they were distributed uniformly through time, but still spatially distributed according to the population size. This ~~changes~~ changed the prior estimates of the fossil fuel fluxes and their distribution through time, as well as their uncertainties, which were set at 60% of the domestic emission estimate (inversion ~~Domestic-Homogenised~~ S11).

Due to the large uncertainty in the modelling of NEE (Zhang et al., 2013; Moncrieff et al., 2015), particularly over the fynbos biome, we considered that perhaps the average of the NEE estimates from CABLE over the domain may be a more reliable representation of the true flux compared with the pixel-level estimates. Therefore we averaged the NEE and NPP estimates

from CABLE over the inversion domain and assigned this average NEE \bar{N}_{EE} and NPP for its uncertainty $\sigma_{N_{EE}}$ as the prior biogenic flux estimates (inversion **NEE Homogenised**S12).

We considered an inversion where the uncertainties in C_c were set at 2 ppm for the day and 4 ppm at night (inversion **Simp-Obs-Error**S13), excluding the additional components for the error due to wind speed and observation variability that were used in the reference inversion. In this case all the errors in the modelled concentrations are contained within these values, and we disregard the climatic conditions under which the measurements were taken. We tested the impact of increasing the night-time uncertainty in the observation errors to 10 ppm (inversion **Simp-Obs with Large Night**S14). We further simplified C_c by performing an inversion which disregarded the temporal correlation which was assumed for the reference inversion (inversion **Simp-Obs No Corr**).

2.3 Alternative control vectors

In the reference inversion the total flux from a single surface pixel for given week was made up of the following individual fluxes:-

$$s_{sf; i} = s_{ff \text{ week day}; i} + s_{ff \text{ week night}; i} + s_{ff \text{ weekend day}; i} + s_{ff \text{ weekend night}; i} + s_{NEE \text{ day}; i} + s_{NEE \text{ night}; i}$$

where $s_{sf; i}$ is the total weekly surface flux from the i^{th} pixel, $s_{ff \text{ week day}; i}$ is the fossil fuel flux during the day during the working week, $s_{ff \text{ week night}; i}$ is the night-time fossil fuel flux during the working week, $s_{ff \text{ weekend day}; i}$ is the weekend daytime fossil fuel flux, $s_{ff \text{ weekend night}; i}$ is the weekend night-time fossil fuel flux, and $s_{NEE \text{ day}; i}$ C_c by using the simplified uncertainties of 2 ppm for the day and $s_{NEE \text{ night}; i}$ are the day and night-time NEE fluxes for the full week from the i^{th} pixel. The inversion solved for each of these fluxes separately and for each of the four weeks in the monthly inversion. Therefore a monthly inversion solved for $10,201 \times 6 \times 4 = 244,824$ surface fluxes. The mean day and night-time concentrations at each of the four domain boundaries for each week were the final components of the control vector. The inversion solved for $4 \times 2 \times 4 = 32$ boundary concentrations ppm at night and also set the temporal observation uncertainty correlation to zero (inversion S15).

2.2.1 Alternative control vectors

As a sensitivity analysis we examined two alternative approaches to the control vector. If we assumed that neither the NEE or nor fossil fuel flux will would change very much from week to week, an option would be to solve for the mean of the six individual fluxes over the four weeks in a given month. We therefore considered a sensitivity test where the inversion solved for one average day and one average night NEE flux within each pixel, and four fossil fuel mean weekly fluxes (day and night working week, day and night weekend) (inversion **Mean-Month**S16). We also considered performing a separate inversion for each week; i.e. four separate weekly inversions in place of each of the monthly inversions (inversion **Week**S17). In this case only the concentration measurements for one week were used and the individual weekly fluxes (two NEE and four fossil fuel) were solved for, and this was repeated for each of the four weeks in the month. The benefit of these two alternative control vectors is that for each individual inversion the resulting C_{s_0} matrix is much smaller compared to with the reference case.

When solving for only one week, or a mean weekly flux for a particular month, the number of surface sources reduced to $10,201 \times 6 = 61,206$. Solving for individual weeks required 4×2 additional boundary concentrations to be added to the control vector, and when solving for the mean weekly flux for the month, we allowed the boundary concentrations to differ for each week, and therefore we still solved for the 32 boundary concentrations as in the reference case. Therefore the $\underline{C}_{s_0} \underline{C}_{s_a}$ for these two alternative control vectors is 16 times smaller than that of the reference inversion.

The benefit of these two alternative approaches is a substantial reduction (at least 75% reduction) in the time taken to perform the inversion. If the results are similar to that of the reference inversion, this type of saving in the computational time and resources would allow more components of the inversion to be tested in a shorter period of time.

2.3 Sensitivity analysis approach

2.2.1 Sensitivity analysis approach

The sensitivity tests were divided into those which assessed alternative products for the prior information; those which assessed an alteration to the structure of the uncertainty covariance matrices; those which assess an alteration to the relative uncertainty specified in \underline{C}_{s_0} ; those which assessed a homogenisation of a component of the prior information; those which considered a simplified version of \underline{C}_c ; and those which solved for an alternative control vector. A summary [A description](#) of the sensitivity tests are presented in Table 1.

The modelled concentrations from each inversion were compared with the observations by assessing the bias and standard deviation of the prior and posterior modelled concentration residuals. Residuals in the prior modelled concentrations were calculated as:

$$\underline{c}_{res\ prior} = \underline{c} - \underline{c}_{mod\ prior}. \quad (14)$$

and residuals-

Residuals in the posterior modelled concentrations were calculated as:

$$\underline{c}_{res\ post} = \underline{c} - \underline{c}_{mod\ post}. \quad (15)$$

where $\underline{c}_{mod\ prior}$ and $\underline{c}_{mod\ post}$ are the CO₂ concentrations modelled from \underline{s}_0 and $\underline{c}_{mod\ post}$ and \underline{s}_0 and $\underline{c}_{mod\ post}$ are the CO₂ concentrations modelled from the posterior estimate of \underline{s} , and $\underline{c}_{res\ prior}$ and $\underline{c}_{res\ post}$ are the respective residuals in the modelled concentrations. The bias, calculated as the mean of these residuals, and standard deviation of these residuals were provided for each inversion. We plotted the time series of the observed and modelled concentrations to assess the skill of the inversion to reproduce the observed concentrations, particularly "local events", which were periods of larger than normal spikes in the observed concentration signal. [These are presented in the supplementary material for all the sensitivity tests.](#)

The posterior fluxes from each inversion were compared with those of the reference inversion in a number of ways. The posterior flux estimates and their spatial distribution were assessed for each inversion by mapping the mean total weekly flux

within each pixel for two months (May and September 2012). We calculated the total flux over the domain, and plotted these weekly total fluxes over time together with the uncertainty bounds. We also considered the total flux over the domain for each month. These total flux estimates are the nett-net flux resulting from the fossil fuel and NEE flux estimates solved for by the inversion. The inversion induces negative correlations between the fossil fuel and NEE flux components from the same week and pixel. When the total flux is considered in a particular pixel, the uncertainty for the total flux will be lower than the sum of the uncertainties for the individual components due to the negative covariance terms. The size of these negative covariances will depend on the prior information specified in the inversion framework. The total estimate gives an indication of the central tendency, which we can compare between inversions, and allows us to assess, for example, if the inversion is predicting the region to be a nett-net source or a nett-net sink. The uncertainties of these posterior total estimates allow us to assess the confidence we can place around these totals, and how this compares to the estimate itself.

In order to assess the goodness-of-fit suitability of the prior uncertainty covariance matrices C_c and C_{s_0} estimates contained in C_c and C_{s_0} , the χ^2 statistic, as described in Tarantola (2005), was calculated \div

$$\chi^2 = \frac{1}{\nu} (\mathbf{H}s_0 - c)^T (\mathbf{H}C_{s_0}\mathbf{H}^T + C_c)^{-1} (\mathbf{H}s_0 - c)$$

where ν is the dimension of the data space, which is the number of observations used in the inversion.

The squared concentration residuals from (see equation 13). We compared these statistics between the different inversions to assess the suitability of the uncertainties prescribed to the prior fluxes. Due to the adjustments made, particularly in cases where the uncertainty covariance matrices were simplified, it was expected that some of the inversion should follow the inversions would have χ^2 distribution with degrees of freedom equal to the number of observations (Michalak et al., 2005; Tarantola, 2005) Dividing this statistic by statistics that deviated from one. We chose not to make additional changes to the sensitivity test inversions to improve these statistics, as it would then not be possible to attribute the sensitivity of the inversion solution between the adjustment tested and the additional adjustment made to the covariance parameters to improve the statistical consistency of the inversion. The number of degrees of freedom of the χ^2 statistic can be divided into the degrees of freedom should yield a χ^2 distribution. We compared these statistics between the different inversions to assess the suitability of the uncertainties prescribed to the prior fluxes for signal (DFS) and degrees of freedom for noise (Rodgers, 2000). The DFS describes the number of independent pieces of information provided by the measurements. The DFS were calculated for the first week of March 2012 for the reference and sensitivity test inversions. These statistics are provided in the supplementary material Section 1 Figure S1.

Table 1. Description of sensitivity tests performed on the Cape Town inversion. Only those aspects which are changed for the sensitivity test are indicated. Other fields are the same as those for the reference inversion.

Sensitivity test abbreviation	Prior NEE product	Prior Fossil fuel product	NEE error correlations	Observation error correlations	Fossil fuel uncertainties	NEE uncertainties	Observation errors	Control vectors
RefS0	CABLE	Cape Town Inventory	Balgovind 1 km	Balgovind 1 hr	Cape Town Inventory Errors	CABLE NPP	2 ppm (day); 4 ppm (night) with wind condition and measurement variance inflation	Six individual weekly fluxes
Carbon-AssessS1	Carbon Assessment Product					Carbon Assessment Estimates $\times 100\%$ NPP		
ODIACS2		ODIAC			ODIAC Estimates $\times 100\%$			
NEE-CorrS3				No observation error correlation				
Obs-CorrS4			No NEE error correlation					
No-CorrS5			No NEE error correlation	No observation error correlation				
Double-FFS6			Balgovind 7 km					
S7					Cape Town Inventory Errors $\times 2$			
Half-FFS8					Cape Town Inventory Errors $\times \frac{1}{2}$			
Double-NEES9						CABLE NPP $\times 2$		
Half-NEES10						CABLE NPP $\times \frac{1}{2}$		
Domestic-HomogenisedS11		Cape Town Inventory with domestic emissions homogenised over the year			Cape Town Inventory Errors domestic emissions homogenised			
NEE-HomogenisedS12	averaged Averaged CABLE weekly estimates over all pixels					average Averages CABLE NPP weekly estimates over all pixels		
Simp-Obs-ErrorS13							2 ppm (day); 4 ppm (night)	
Simp-Obs-withS14							2 ppm (day); 10 ppm (night)	
Large-Night								
Simp-Obs-No-CorrS15				No observation error correlation			2 ppm (day); 4 ppm (night)	
Mean-MonthS16								Six average weekly fluxes for each month
WeeksS17								Separate weekly inversions

3 Results

3.1 Reference inversion

The results of the reference inversion (**RefS0**) are explained in detail in Nickless et al. (2018). The following sections compare the sensitivity tests to **Ref** with respect to the modelled concentrations, pixel-level weekly flux estimates, and aggregated fluxes over each week, month and over the full measurement period. When we refer to the total pixel-level weekly flux, this is the sum of the four weekly and are briefly summarised here. The inversion was able to substantially improve the agreement between the modelled and observed concentrations. The inversion made larger changes to the biogenic fluxes than to the fossil fuel fluxes (week / weekend; day / night) and . Over the Cape peninsula region, where observations made at Robben Island viewed CT central business district (CBD) and harbour emissions as well as biogenic fluxes from the Table Mountain and Cape Point National Park regions, fossil fuel fluxes were adjusted by less than 10%, for example an adjustment from (1.00 to 0.91 kg CO₂ m⁻² week⁻¹). An exception is the two NEE fluxes (day and night) within that pixel. The uncertainty of this total flux is obtained by first obtaining the sum of all the error variance and covariance terms of these six fluxes, and then taking the square root of this total variance term. The aggregated total weekly flux is the sum of all these total fluxes over the full inversion domain for the week in question. The total uncertainty of this aggregated total flux is derived in the same way as for the pixel-level total weekly flux, but now summing over all variance and covariance terms applicable to that week for all pixels in the domain. change to a pixel over a petrol refinery where the inversions made a relatively large change, reducing the total emission in the pixel from 9.43 to 6.62 kg CO₂ m⁻² week⁻¹ for May 2012 and from 9.38 to 7.24 for September 2012. Biogenic fluxes were made more negative over the CBD region, with a maximum adjustment from -0.04 to -0.37 kg CO₂ m⁻² week⁻¹ in May 2012 and from -0.08 to -0.29 in September 2012, and made more positive over the natural areas, but with much smaller adjustments, a maximum adjustment from -0.04 to 0.04 kg CO₂ m⁻² week⁻¹ in May and from -0.11 to 0.08 in September 2012.

Aggregated fluxes are often of interest. For example, we may wish to report the total flux for a region from year to year. As we did not have a contiguous measurement period covering all seasons or over a full year period, which is often reported in these city-scale inversions, we instead aggregated over weekly and monthly periods. The purposes of this is to illustrate how weekly fluxes estimated within the same monthly inversion may differ, and The direction of the differences in aggregated fluxes between different inversions at different times of the year. These aggregated monthly fluxes are calculated in the same way as the aggregated weekly flux adjustments to the prior biogenic fluxes indicated that the CABLE model was overestimating the amount of biogenic carbon uptake over natural areas. Dynamic vegetation models have not been able to simulate fluxes over the fynbos biome well (Moncrieff et al., 2015), and so this result was not surprising. Adjustments to the biogenic fluxes were usually small – ranging between -0.001 and 0.003 kg CO₂ m⁻² week⁻¹. The inversion was able to make larger changes to the biogenic fluxes than to the fossil fuel fluxes because the prior biogenic flux uncertainties were made large and because uncertainty correlations were specified between the biogenic fluxes, whereas fossil fuel flux uncertainties were assumed to be independent.

The biases in the prior and posterior modelled concentrations, together with the standard deviation of the residuals, are provided in Table ???. We supply the time series of the modelled concentrations for each inversion and at both sites in the

Supplement (Sect. 1.1). We provide time series plots of the aggregated weekly fluxes and their uncertainty bounds (Supplement Sect. 1.2) and a table of the aggregated monthly ~~Large uncertainty reductions were made over the natural areas bordering on the CBD, particularly over the Table Mountain National Park, and to natural areas near to the Hangklip measurement site, where the uncertainty was lowered by over 50%. Large uncertainty reductions also occurred over agricultural areas to the north of the CBD region. Uncertainty reductions of up to 60% occurred over a few central CBD pixels, but were generally smaller compared with the uncertainty reductions over natural areas, which reached as high as 92%. When aggregating the fluxes over the full domain for each month (Supplement Sect. 1.3).~~ We also supply maps of the prior and posterior modelled fluxes, together with the uncertainty reduction in each pixel, in the supplementary material for the months of May (early winter) and September (spring / early summer) 2012 (Supplement Sect. 1.4). For the main paper we provide a table of the aggregated fluxes over the full inversion period, together with the ~~and 1.5 kt CO₂ week⁻¹, whereas the posterior uncertainties ranged between 0.9 and 1.5 kt CO₂ week⁻¹. Uncertainties in the prior aggregated biogenic fluxes ranged between 23.6 and 57.3 kt CO₂ week⁻¹ and were reduced to 15.8 and 47.1 kt CO₂ week⁻¹ after the inversion. The median percentage uncertainty reduction in the aggregated flux estimate and the mean χ^2 statistic which provides an assessment of the appropriateness of the prior covariance matrices (Table ??).~~

15 Bias (–) in the prior and posterior modelled concentrations together with the standard deviation of the modelled concentration residuals at the Hangklip and Robben Island measurement sites for the period March 2012 to June 2013. NEE = Net Ecosystem Exchange, FF = Fossil Fuel **Ref** and 50.5 %, with the largest reduction occurring in March 2012.

Prior and posterior total flux estimates of each inversion over the thirteen four-week periods for which observation data were available from March 2012 to June 2013, with uncertainties and the reduction in uncertainty with respect to the prior uncertainty. Total fluxes are expressed as $\text{kt CO}_2 \text{ week}^{-1}$. The mean χ^2 statistic is provided over the thirteen inversion periods. NEE = Net Ecosystem Exchange, FF = Fossil Fuel **Ref**

3.2 Alternative prior information products

The prior biases for both the inversion making use of the carbon assessment for prior NEE flux estimates and uncertainties (which we denote with the emboldened shorthand **Carbon Assess**), and the ODIAC fossil fuel inversion (**ODIAC**) were larger in magnitude and more negative than that of the reference inversion (**Ref**). This indicates that the prior modelled concentrations of from these two inversions were larger on average compared with the observations. The standard deviation in these residuals was larger compared with **Ref** (Table ??). A plot of the modelled concentrations shows that for all three inversions, the prior modelled concentrations only weakly followed the observed concentrations, with modelled concentrations at the Robben Island site too large, and too small at the Hangklip site (Figures 4 and 5). In the case of **Carbon Assess** and **ODIAC**, ~~By assigning spatial correlation between biogenic flux uncertainties of neighbouring pixels and assuming independent fossil fuel flux uncertainties, we attempted to provide the inversion with additional information to allow it to better distinguish between these fluxes. The inversion induced negative correlation between fossil fuel and biogenic flux uncertainties in the same pixel. We demonstrated that the posterior uncertainty of any linear combination of terms from the carbon assessment inversion the prior modelled concentrations were not as underestimated as those from **Ref** at the Hangklip site. The χ^2 statistics indicated that control vector of the fluxes~~

(including the difference between fluxes from the same pixel and the inversion framework specified for the **Carbon Assess** inversion had uncertainties that were too small (Table ??). For **ODIAC**, the χ^2 statistics were slightly closer to one than those for **Ref** (sum of fluxes from the same pixel) will always be unchanged or smaller compared with the prior uncertainty of the same linear combination of elements (Jackson, 1979; Jackson and Matsu'ura, 1985). This means that although negative correlation between the flux components may be introduced through the inversion, the uncertainty in both the difference between fluxes from the same pixel and the total flux within a pixel will be reduced. When we sum all fluxes within the same pixel, the negative correlations created by the inversion resulted in the posterior uncertainty of the total flux being less than the sum of the posterior uncertainty of the individual fluxes. Therefore there is an advantage to solving for these fluxes separately.

The prior total weekly fluxes were notably different compared with **Ref** (Figure 6). The carbon assessment product for NEE fluxes resulted in prior total weekly flux estimates that were always positive and which showed little variation over the year compared with the reference prior. The uncertainty bands were much narrower for the carbon assessment total flux estimates. The resulting posterior weekly fluxes were very similar to the priors.

The ODIAC product for fossil fuel fluxes resulted in prior total weekly fluxes that had a similar pattern of weekly fluxes over time as those obtained by **Ref** (Figure 6), with more positive fluxes between March and June 2012 and March and June 2013, and negative or near-zero total weekly fluxes between August 2012 and February 2013. These summer-time negative fluxes were not as negative as those obtained by **Ref**.

Considering the aggregated flux for each month over the inversion domain, the carbon assessment inversion had larger prior fluxes for every month compared with **Ref**, particularly during the summer months. During these months the discrepancy between the reference and carbon assessment prior aggregated fluxes was between 699. Clearly the inversion result was strongly dependent on the assumptions regarding the prior fluxes and 1386 for a four week period (Supplement Sect. 1.3). The inversion reduced these fluxes and their uncertainties. The results of the sensitivity tests in subsequent sections explore to what degree these assumptions affected the inversion solution. The resulting posterior fluxes were still larger than the reference posterior fluxes by between 400 and 1000 for this same period. The ODIAC prior fluxes were always larger than the reference priors, but consistently for all months by an amount of approximately 690. The posterior aggregated fluxes were still larger than those for **Ref**, but the difference was reduced to 469 on average.

Whereas the aggregated total prior fluxes from **Ref** were generally made more positive by

3.2 Sensitivity tests

To assess the sensitivity of the inversion, there were some months when the total fluxes were made more negative, notably during the winter months. In the case of the carbon assessment inversion, fluxes were made more negative by the inversion for all months. The resulting posterior total fluxes were positive for all months. For **ODIAC**, the posterior fluxes were more negative than their priors, indicating that compared with the reference, the positive fluxes from the fossil fuel sources were specified too large. August and September 2012 were the only months when **ODIAC** made the total posterior fluxes larger than the priors, which agrees with the direction in which **Ref** adjusted the posterior total fluxes.

The aggregated total fluxes of these alternative prior product inversions over the thirteen inversion periods are larger than for **Ref** (Table ??). The uncertainty of the aggregated total flux for **Carbon Assess** was smaller relative to **Ref**, whereas **ODIAC** obtained similar uncertainties in the aggregated total flux. The corrections made by the inversion made the aggregated total flux of **Ref** less negative and closer to zero. When these two we have calculated the aggregated posterior flux across the study period and over the full spatial domain, together with the posterior uncertainty and uncertainty reduction for each of the sensitivity tests, which are presented in Figure 3. The bar charts, also referred to tornado plots, revealed that changing the prior had the largest impact on the resulting posterior fluxes and their uncertainties. Changing to either the ODIAC fossil fuel product or the carbon assessment biogenic fluxes resulted in prior and posterior flux estimates that were much more positive than those for the reference inversion. The inversion appeared to pull the aggregated fluxes towards an ideal position. The reference posterior fluxes were made more positive compared to the priors, whereas for the alternative prior products were used, the inversion corrected the prior drove the posterior fluxes to be less positive, also attempting to make these fluxes closer to zero. The uncertainty reduction achieved over the full inversion period was 25.6% for **Ref** and 23.6% for **ODIAC**, but only 11.9% for **Carbon Assess**. This smaller uncertainty reduction is due to prior biospheric flux estimates from the carbon assessment product being close to one, which corresponding small NPP fluxes, and therefore error correlations much smaller in comparison with **Ref**. The error correlations play an important role in determining the uncertainty reduction achievable by the inversion.

The spatial distribution of the prior and posterior fluxes for May 2012 are provided in Figure ?. **Carbon Assess** has prior total flux estimates that are notably closer to zero and less negative compared to **Ref** across both May and September 2012 (provided in the Supplement Sect. 1.4). **Ref** was able to change. It is hence likely (though not certain) that the true flux is sandwiched between these alternative posterior flux solutions.

The aggregated fluxes were strongly sensitive to the uncertainty spatial correlations specified between the biogenic fluxes. Uncertainty correlations in the biogenic fluxes had a large impact on the spatial distribution of these negative fluxes somewhat, but still maintained these negative fluxes in the posterior estimates. The posterior fluxes of **Carbon Assess** were largely left unchanged, with September 2012 having the most notable adjustments with a small area of negative fluxes created to the east of the oil refinery pixel, to the north of the Cape Town metropolitan area, resulting fluxes, and on the degree to which the inversion was able to make changes across the full domain (Figure 3). Eliminating these uncertainty correlations substantially reduced the inversion's ability to make deviations from the prior fluxes. Therefore, under these sensitivity tests, posterior fluxes were very similar to the prior fluxes, and uncertainty reductions were small.

The map of the ODIAC prior fluxes is distinctly different to those of **Ref** (Figure ??). The reference inventory limited the fossil fuel fluxes to a few specific pixels, with a small number of pixels over point sources with large positive fluxes. The ODIAC product smoothed the fluxes over the Cape Town metropolitan area, covering a larger area with positive fluxes compared with the reference case, and having only three pixels with distinctly larger fluxes than the rest of the region. Although the ODIAC priors do not show any of the very large positive fluxes of the reference, the area of positive flux resulting from the fossil fuel fluxes is focused on the same general area as **Ref**.

With regards to the uncertainty reduction (Figure ??), **Ref** was able to obtain higher reductions than either of these test cases. The spatial pattern of uncertainty reduction was similar between **ODIAC** and **Ref**, whereas for **Carbon Assess** many of

~~the pixels in the domain showed no~~ A short temporal correlation length in the observation uncertainties did not have a large impact on the inversion. Increasing these to seven hours led to greater DFS (see supplementary material Figure S1), but without having an impact on the flux solution or uncertainty reduction. The statistical consistency also fluctuated much more strongly from month to month when the temporal observation error correlation was larger compared to a one hour correlation length or assuming independent observation uncertainties. With a correlation length of one hour non-zero off-diagonal elements persisted for approximately seven hours, whereas these off-diagonal elements persisted for much longer when the correlation was set at seven hours. Long correlation lengths are likely not realistic as wind fields observed at the measurement station during the day may be very different to those observed in the evening, reducing the chance of consistent errors in concentration.

The sensitivity test with the smoothed prior biogenic flux over the full domain produced the only posterior flux solution that was corrected to be further from the reference inversion posterior. This inversion did not assume any knowledge about the spatial variability in the surface fluxes, but it appears that providing at least some prior knowledge of where biogenic fluxes are likely to occur – at least separating the ocean and terrestrial fluxes – was important for a sensible posterior flux solution. The domain is not fully or representatively sampled by the observations. By providing a blanket biogenic flux prior across the domain, areas with large expected biogenic fluxes, which were well sampled by the observation network, had priors that were too carbon neutral, and so biogenic fluxes were made more negative, which was propagated through to neighbouring biogenic fluxes, resulting in a posterior aggregated flux solution that was more negative than the prior. A blanket uncertainty estimate was also used, which meant that the uncertainty associated with the ocean fluxes was much larger compared with the reference inversion, allowing the inversion to make relatively large changes to oceanic pixel fluxes close to the measurement sites.

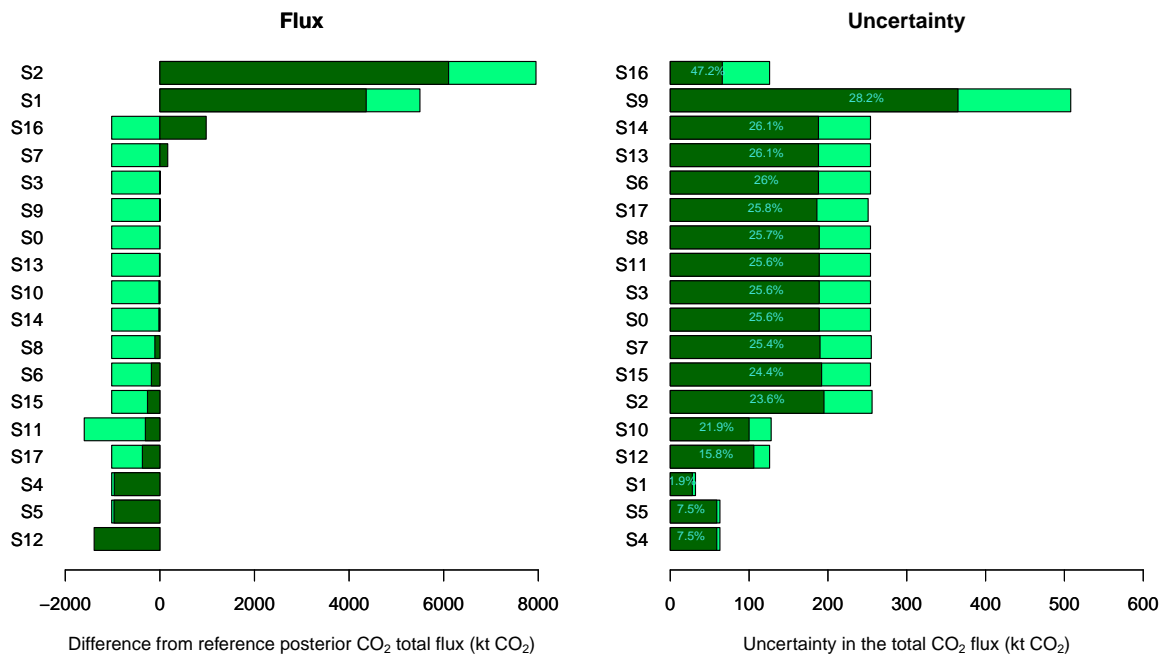


Figure 3. Left: Difference between the reference and sensitivity aggregated posterior fluxes over the domain (100 km × 100 km) for the full study period (16 months), ordered from most positive to most negative difference in posterior estimates. The reference inversion posterior aggregated flux was -317 kt CO₂. Right: Prior and posterior uncertainties in the aggregated fluxes from reference and sensitivity test inversions. The percentage uncertainty reduction is overlaid over each bar. S0 = Reference Inversion; S1 = Carbon Assessment Inversion; S2 = ODIAC fossil fuel inversion; S3 = Correlation for NEE fluxes only; S4 = Correlation for observation errors only; S5 = No correlation specified in prior covariance matrices; S6 = Long observation error correlation length; S7 = Double fossil fuel uncertainties; S8 = Half fossil fuel uncertainties; S9 = Double NEE uncertainties; S10 = Half NEE uncertainties; S11 = Domestic emission homogenised over the year; S12 = NEE fluxes averaged over the domain; S13 = Simple specification of observation error covariance matrix; S14 = Simple observation error covariance matrix with larger night-time error; S15 = Simple observation error covariance matrix with no correlation; S16 = Inversion solving for mean weekly fluxes over the month; S17 = Separate inversions for each week.

3.3 ~~Relative uncertainty in C_{s0}~~ Alternative prior information products

~~In this group of sensitivity tests we assessed how the relative contribution of the uncertainty in the fossil fuel and NEE fluxes affected the inversion results. We considered doubling and halving these uncertainties with respect to **Ref** uncertainties. The impact on the modelled concentrations was small. Biases were similar to **Ref**. While all the sensitivity test inversions produced~~
5 ~~prior modelled concentrations that did not track the observations well (see supplementary material Section 3 Figures S10 to S27), the carbon assessment and ODIAC prior product inversions (S1 and S2) produced prior modelled concentrations that were on average too large compared with the observed concentrations at both sites, and the standard deviation in the residuals of the modelled concentrations were similar (Table ??). The~~
~~whereas the reference inversion (S0) underestimated the concentrations at Hangklip and overestimated the concentrations at Robben Island (Figures 4 and 5) (also supplementary material Section 5~~
10 ~~Figures S37 and S38). The average bias of the prior modelled concentrations from the reference inversion was smaller than the bias for these sensitivity test cases at both sites (see supplementary material Section 3 Figures S11 and S12).~~

~~The carbon assessment total prior fluxes were notably different to those from ODIAC or the reference inversion. There was little seasonal variation, with fluxes remaining net positive throughout the study period. The uncertainty bands were very narrow based on the carbon assessment NPP. The mean χ^2 statistics were larger when the uncertainties were halved, particularly the~~
15 ~~uncertainties in the NEE fluxes (inversion **Half NEE**), indicating that insufficient uncertainty had been assigned to either the fluxes or observations, whereas doubling the uncertainties improved the led to statistic for the S1 inversion of 4.1 (see supplementary material Section 2.1 Table S1) indicated that the uncertainties assigned to the fluxes were too small when compared to the uncertainties assigned to the CABLE NEE fluxes in the reference inversion (χ^2 statistics closer to one (Table ??).~~

~~The pattern in~~
20 ~~statistic of 1.5 on average), which were closer to being statistically consistent with the assumptions of the inversion. The time series of the prior and posterior aggregated fluxes was similar between **Ref** and these test cases. The uncertainty around the weekly aggregated fluxes was strongly dependent on the NEE uncertainty (Table ??)(inversions **Double NEE** and **Half NEE**), whereas it was not noticeably different if the uncertainty in the fluxes from the S0 and S2 inversions were more similar to each other over time than to S1, but with the S2 inversion generally having more positive fluxes compared~~
25 ~~with the reference inversion (Figure 6). These time series indicate that the prior biogenic fluxes drove the temporal variation in the fluxes, whereas the prior fossil fuel fluxes was either double or halved (inversions **Double FF** and **Half FF**). dictated the vertical shift in the flux time series.~~

~~In this group of sensitivity tests, the differences in the aggregated monthly fluxes was more pronounced between months within the same inversion than between inversions performed for the same month. All inversions corrected the prior aggregated~~
30 ~~fluxes to a similar degree and in the same direction. Doubling the uncertainty in the fossil fuel fluxes led to posterior aggregated fluxes that were consistently larger for all months compared with **Ref**, whereas halving this uncertainty led to smaller posterior fluxes. Doubling and halving the uncertainty in the NEE fluxes led to posterior flux estimates that were similar on average to those of **Ref** but with greater variability in this difference between the reference and test inversion posterior estimates from month to month compared with the fossil fuel test inversions.~~

Double NEE obtained the largest uncertainty reduction, but the resulting posterior uncertainty was larger than for **Ref**. Halving the NEE uncertainty led to smaller relative uncertainty reductions for the aggregated monthly fluxes. The reference inversion generally made fluxes more positive, except for a few winter months when the innovations made fluxes more negative. The S2 inversion had innovations that made the fluxes more negative compared to the priors, except for September 2012. S1's innovation was to make the fluxes more negative for each month. The magnitude of the innovations were smaller compared to those made to S0 and S2 prior fluxes, limited by the uncertainty placed on the prior biogenic fluxes. For the S1 inversion, both the biogenic flux uncertainties and the correlation lengths were smaller compared to those for S0, and therefore the posterior fluxes were not allowed to differ much from the prior, leaving the modelled concentration residuals before and after the inversion to be very similar, and posterior uncertainties that were similar in magnitude to the prior uncertainties. The uncertainties in the posterior aggregated monthly fluxes were similar between **Ref** and **Double FF** and **Half FF**. It was always higher for **Double NEE**, and lower for **Half NEE**. The resulting uncertainty in the posterior aggregated flux for **Half NEE** was more similar to **Ref** than **Double NEE**. The aggregated flux over the full inversion period shows that, whereas this estimate was close to the result for **Ref** in the case of the two NEE uncertainty cases (316 and 337), the aggregated flux was more positive when the fossil fuel uncertainty was doubled (-151) and more negative when the fossil fuel flux was halved (-423) (Table ??). On the other hand, changing the relative uncertainty of the fluxes almost as uncertain as the prior fluxes.

The spatial pattern in the fluxes (supplementary material Figures S56 and S57), as reflected in the time series pattern in the weekly fluxes (Figure 6), indicates that prior and posterior fluxes were more positive for the S1 inversion than those of S0 (see also supplementary material Section 2.2 Table S2). The spatial heterogeneity in the S1 fluxes was driven by the fossil fuel fluxes had no impact on the uncertainty in the posterior flux estimate, whereas the doubling or halving the uncertainty in the NEE fluxes led roughly doubling or halving of the uncertainty in the posterior aggregated flux.

The spatial distributions of the, whereas for S0 and S2 this was driven by the biogenic fluxes. The S1 posterior fluxes were similar between the inversions in this group of sensitivity tests. A notable feature largely unchanged from the prior fluxes, except for a notable change made in the September 2012 posterior fluxes is, when NEE uncertainty was doubled, the inversion was able to reduce the aggregated flux with respect to the priors, by creating fluxes where a region of negative flux in an area close to the oil refinery point source to the north of the CBD region (Supplement Figure S42).

Prior and posterior aggregated weekly fluxes over the inversion domain from March 2012 to June 2013 for the reference inversion and the doubled and halved NEE uncertainty test cases.

3.4 Homogenised prior information

In this group of sensitivity tests we looked at the impact on the inversion results of assuming that the domestic emissions were constant through time (**Domestic Homogenised**), and of assuming a spatially homogeneous biogenic flux over the inversion domain within each month (**NEE Homogenised**). The prior modelled concentrations from these two test cases were biased to a similar degree as **Ref**. Homogenising the NEE flux over space led to smaller standard deviations in the prior residuals. The most noticeable difference in the bias was for the Robben Island site, where the modelled concentrations under the homogenised NEE prior were biased by -6 compared to the -3 of **Ref**, indicating that prior fluxes around Robben Island (generally from the

Cape Town central business district area and the Table Mountain National Park area adjacent to this region) were too positive (Table ??). The χ^2 statistics indicated that the inversion framework for these homogenised priors is more suitable than the reference case (Table ??). For the **NEE Homogenised** priors, the statistic was close to one for most months. S2 inversion, the ODIAC fossil fuel emissions were highest over the CBD and diminished at distances further from this centre. The spatial distribution of the S0 inversion fossil fuel fluxes were strongly dependent on the transport network and several point sources. The posterior fluxes around the CBD of the S2 inversion were less radial than those in the prior, taking on a spatial pattern more similar to the reference inversion.

The prior and posterior modelled concentrations for **Domestic Homogenised** are similar to those of **Ref**. In the case of **NEE Homogenised**, the time series shows better agreement between the prior modelled and observed concentrations at the Hangklip site, but worse agreement with respect to **Ref** at the Robben Island site (Figure ??). With regards to the uncertainty reduction, the S0 inversion was able to obtain higher reductions than either S1 or S2 (Figures 6 and 3, 25.6% reduction compared to 11.0% and 23.6% respectively). The spatial pattern of uncertainty reduction was similar between S0 and S2, whereas S1 showed no uncertainty reduction across much of the domain (see supplementary material Figures S54 to S59).

Altering the domestic fossil fuel emissions to be the same over time in S11 had little impact on the inversion results when compared with the wholesale change in the prior product. On the other hand, smoothing the biogenic emissions over space in the extreme manner where it was assumed NEE fluxes were the same throughout the domain (S12) had a large impact on the inversion. This resulted in the only inversion where the aggregated fluxes became more negative. The uncertainty reduction was also small (Figure 3). This represents a fairly extreme change to the assumption regarding the spatial distribution of the prior and posterior weekly aggregated flux between **Domestic Homogenised** and **Ref**. Smoothing NEE over space resulted in less extreme prior NEE and NPP estimates, and therefore the uncertainty around the NEE estimates was smaller than for **Ref**, leading to smaller uncertainties around the aggregated flux (Figure ??). The general pattern in the aggregated weekly fluxes over the course of the inversion period was similar to **Ref**.

Compared to other groups of sensitivity tests performed here, the aggregated monthly fluxes were not very different between the reference and test cases. For **Domestic Homogenised**, NEE fluxes, and illustrates the sensitivity of the inversion to the adjustments made to the prior fluxes by the inversion were generally in the same direction and to the same degree as for **Ref**. The adjustments made by **NEE Homogenised** were not always in the same direction. The resulting posterior fluxes from **NEE Homogenised** were generally more negative than those of **Ref**. This is illustrated in the posterior aggregated fluxes for the inversion period (Table ??).

Differences between the prior and posterior fluxes were small for **Ref** and these changes are consistent with those obtained by **Domestic Homogenised**. In prior information on where fluxes are taking place. In the supplementary material we include timeseries plots of the concentration contributions attributed to the fossil fuel and biogenic fluxes for all the sensitivity test inversions during the month of May 2012, which would have had a smaller domestic emissions specified than in **Ref**, (supplementary material Section 4). Robben Island sees far less of the biogenic influence than Hangklip, so in order to make the modelled concentrations more consistent with the observations, the fossil fuel fluxes were adjusted by the inversion, leading to similar contributions to the concentration from biogenic fluxes before and after the inversion. This was the differences between

~~the prior and posterior fluxes were limited to very few pixels, mainly near the Cape Town CBD area. In September 2012, when the domestic emissions would have been larger than those for **Ref**, the adjustments made by the inversion were more widespread. case for the reference inversion S0 and all other inversions except S12, where the inversion made adjustments to the biogenic fluxes instead of the fossil fuel fluxes in order to reduce the modelled concentrations for Robben.~~

- 5 ~~When NEE was smoothed over the domain with each month. Due to the adjustments made to small number of observations relative to the number of sources solved for in the inversion, it is unsurprising that the posterior solution is strongly dependent on the prior information. The results do show that the inversion brings these different prior estimates closer to each other, and therefore the inversion does assist in taking any selected prior closer to the true state, but this is limited by the prior fluxes were very small in comparison to **Ref**. Changes were restricted to a few pixels in the CBD region and close to the measurement sites.~~
- 10 ~~The uncertainty reduction was concentrated in the regions around the measurement sites and reached over 90% in these areas. Over the Table Mountain National Park, which had some of the highest uncertainty reductions in **Ref**, uncertainty reduction was limited to between 20 to 30% and almost no adjustment to these prior fluxes were made by the inversion (Figure ??) assumed uncertainty limits placed on the priors, as demonstrated in the S1 inversion.~~

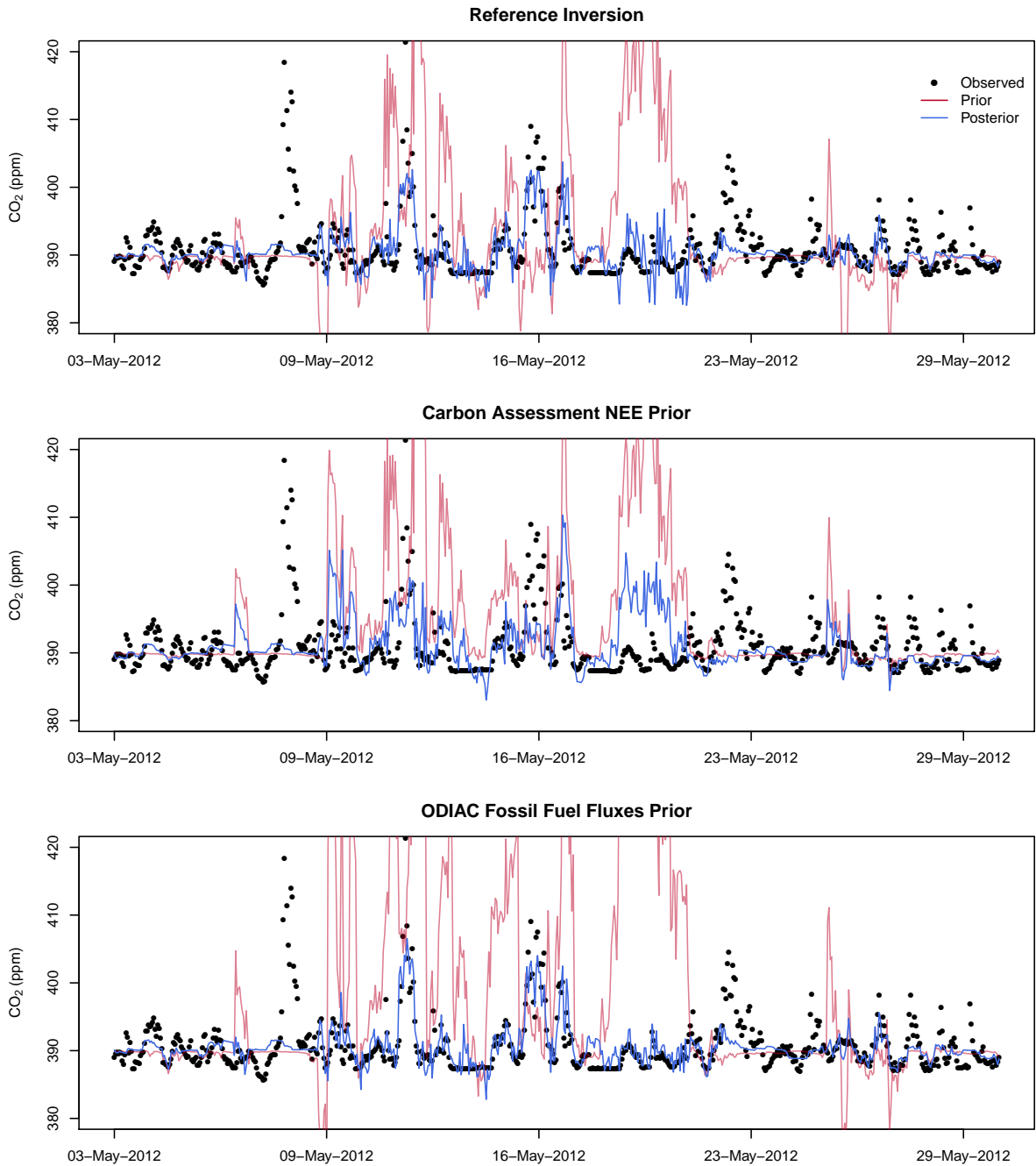


Figure 4. Prior and posterior modelled concentrations when the homogenised-NEE-prior was used for the Hangklip site for the month of May 2012 for the reference inversion (top), carbon assessment inversion (middle), and ODIAC fossil fuel flux product inversion (bottom).

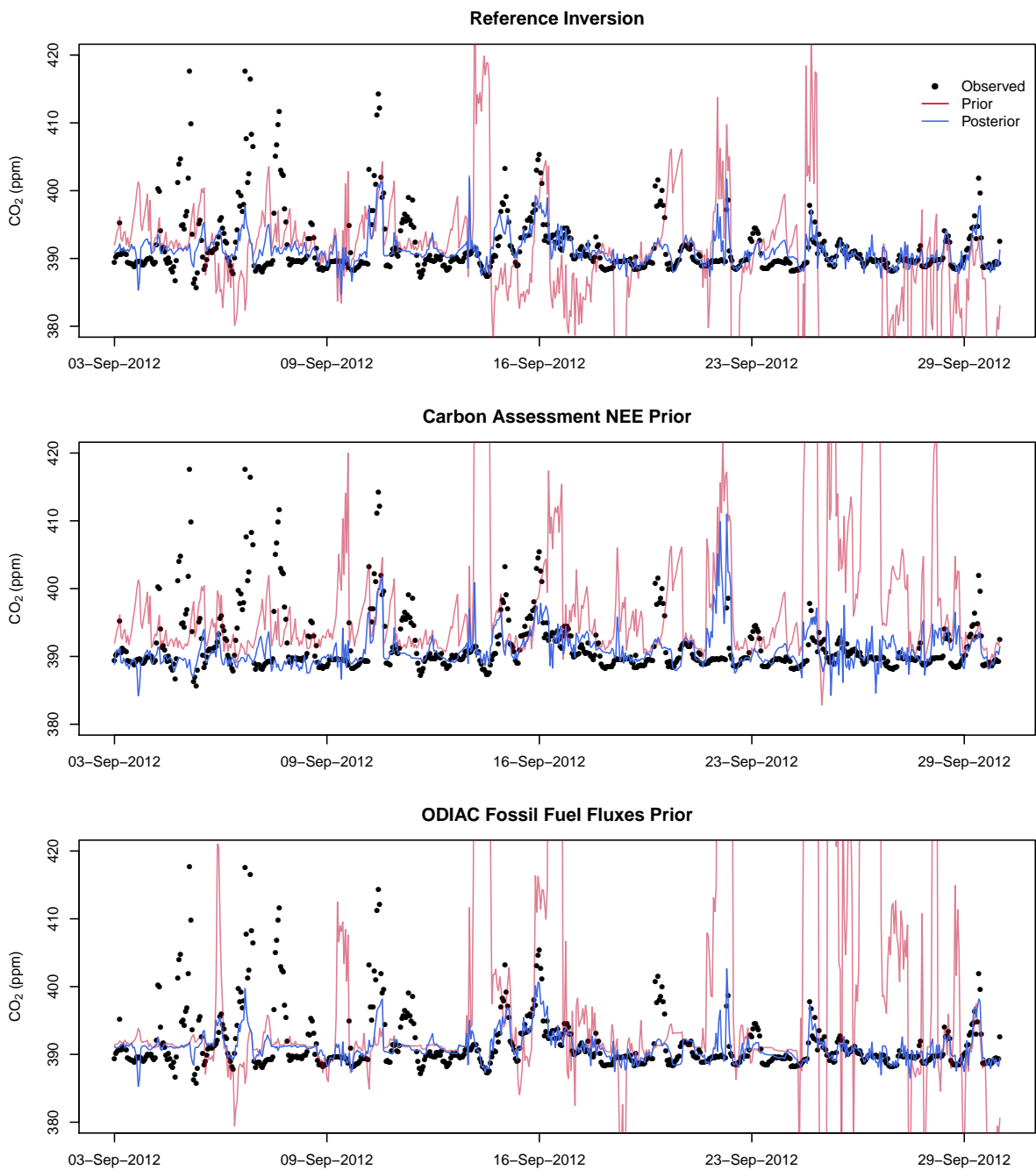


Figure 5. Prior and posterior modelled concentrations for the Robben Island sites over site for the full inversion period from March month of May 2012 until June 2013 for the reference inversion (top), carbon assessment inversion (middle), and ODIAC fossil fuel flux product inversion (bottom).

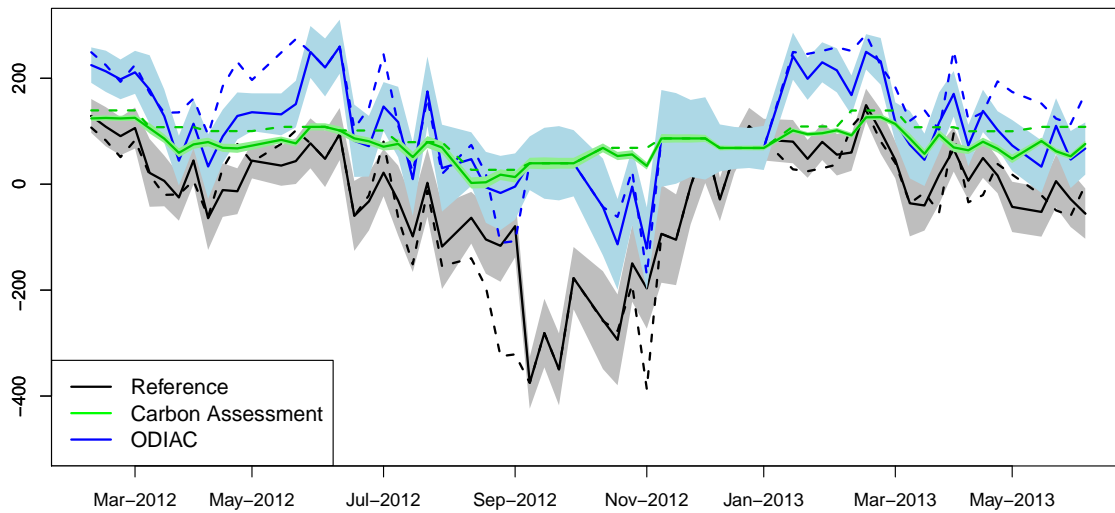


Figure 6. Prior and posterior aggregated weekly fluxes over the inversion domain from March 2012 to June 2013 for the reference inversion, carbon assessment and homogenised NEE-ODIAC inversions. The dashed line represents prior test case flux estimates and the solid line represents posterior flux estimates.

3.4 Uncertainty covariance matrices

The inversion solution was sensitive to the uncertainty spatial correlations assigned to the prior biogenic fluxes. This impacted on the spatial distribution of the ~~pixel-level uncertainty reductions achieved by fluxes~~, the ~~reference inversion~~ magnitude of the total aggregated flux, and the uncertainty reduction achieved by the inversion. By not accounting for the spatial correlations in the biogenic flux uncertainties, this led to uncertainties that were too small, illustrated by average χ^2 statistics above 2 for inversions S4 and ~~homogenised NEE prior test case~~ S5, which set the spatial correlation of the uncertainties in the biogenic fluxes to zero (see supplementary material Table S1). These inversions also showed little innovation or uncertainty reduction in comparison to the reference, leaving the posterior fluxes to be similar to the priors (Figure 7). This is also reflected in the aggregated fluxes over the study period for S4 and S5, as posterior fluxes were similar to the prior aggregated fluxes and uncertainty reductions in these aggregated fluxes were small. Aggregating over the study period led to posterior flux estimates of -317 and -310 kt CO₂ for ~~September 2012~~ S0 and S3, whereas S4 and S5 had estimates of -1281 and -1287 respectively, close to the prior estimate of -1336 kt CO₂. Uncertainty reductions were reduced from 26.6% to 7.6% when biogenic flux uncertainty correlations were removed.

~~Simplified C_c~~ In this group of sensitivity tests, the specification of C_c was simplified to single uncertainty value of 2 during the day or 4 at night (**Simp Obs Error**), or up to 10 for the night-time observations (**Simp Obs with Large Night**). These test cases had uncertainties in the observation errors that were lower than for **Ref**. Removing the correlation assumed in **Ref** was also considered (**Simp Obs No Corr**). ~~The~~ In comparison, the removal of the temporal correlation in the observation errors in S3 had only a small penalty in the χ^2 statistics indicated that simplifying the C_c with smaller errors reduced the goodness-of-fit of the prior uncertainty covariance matrices (Table ??).

The impact on the modelled concentrations was very small, with biases in the prior and posterior modelled concentrations closes to those obtained by **Ref** (Table ??). The bias for the Robben Island modelled concentrations was slightly reduced compared with **Ref** in all three of the simple observation error test cases.

The posterior aggregated weekly fluxes ~~statistic~~. The spatial distribution of the simple observation error cases and their uncertainties were indistinguishable from those of **Ref**. The posterior fluxes, both the spatial distribution in these fluxes and the aggregated fluxes, were similar between all three test cases and when compared with **Ref**. The uncertainty reduction was slightly larger under the simplified (i. e. smaller) observation error covariance matrix, but the spatial distribution in the uncertainty reduction was the same ~~fluxes and uncertainty reductions achieved remained similar to the reference inversion S0 as well~~. Increasing the night-time observation errors to account for greater uncertainty in the atmospheric transport at night led to an aggregated flux estimate over the full measurement period that was more negative than for **Ref**, but with a similar uncertainty in the temporal correlation length in the observation errors from one hour to seven hours for the S6 inversion had little impact on the posterior flux estimates or the uncertainty reduction achieved, with a posterior aggregated flux (Table ??). The aggregated fluxes for this test case were consistently more negative across all months compared with **Ref**. Removing the correlation between observation errors had over the study period of -497 kt CO₂ compared with -317 for S0. The χ^2 statistic

was substantially increased to 7.3 on average, and varied more between months compared to all other inversions. Simplifying the observation errors so that they no longer included terms that depended on the meteorological conditions at the site or on how variable the high frequency measurements were during a given hour (S13 to S15) had very little impact on the inversion results.

5 3.5 **Alternative control vectors**

Performing separate weekly inversions (**Week**) or solving for a mean weekly flux for the month (**Mean Month**) As the flux uncertainties had already been scaled for the reference inversion to improve the statistical consistency of the uncertainty covariance matrices, it was expected that the χ^2 statistic would be too large for inversions where the uncertainties were halved. This was particularly the case for the biogenic flux uncertainties (S10), as these fluxes were throughout the domain whereas the fossil fuel fluxes were assigned to a smaller part of the domain. Halving or doubling the prior biogenic flux uncertainty (S9 and S10 respectively) led to ~~inversions that required less computation resources and time, which meant these inversions could be completed for the full inversion period faster than Ref.~~ posterior uncertainties that were roughly half or double the total posterior uncertainty of the S0 inversion, whereas halving or doubling the fossil fuel flux uncertainties (S7 and S8 respectively) made little change to the uncertainty reduction. On the other hand, changing the fossil fuel uncertainties (S7 and S8) had a larger impact on the aggregated posterior flux (-423 kt CO₂ when halved and -151 when doubled), compared with changing the biogenic flux uncertainties (S9 and S10), where posterior fluxes remained similar to those obtained by S0. Doubling the fossil fuel flux uncertainty led to generally more positive fluxes across all months.

The spatial distributions of the posterior fluxes in this group of sensitivity tests (S7 to S10) were similar to that of the reference inversion S0. A notable feature in the September 2012 posterior fluxes is that when NEE uncertainties were doubled the inversion was able to reduce the aggregated flux with respect to the priors by creating a region of negative flux in an area close to the oil refinery point source to the north of the CBD region (see supplementary material Figure S73).

~~The time series in the posterior modelled concentrations, and the bias and standard deviation in the posterior modelled concentrations were similar between Ref and the two alternative control vector inversions (Table ??). The χ^2 statistics were similar for these three inversions.~~

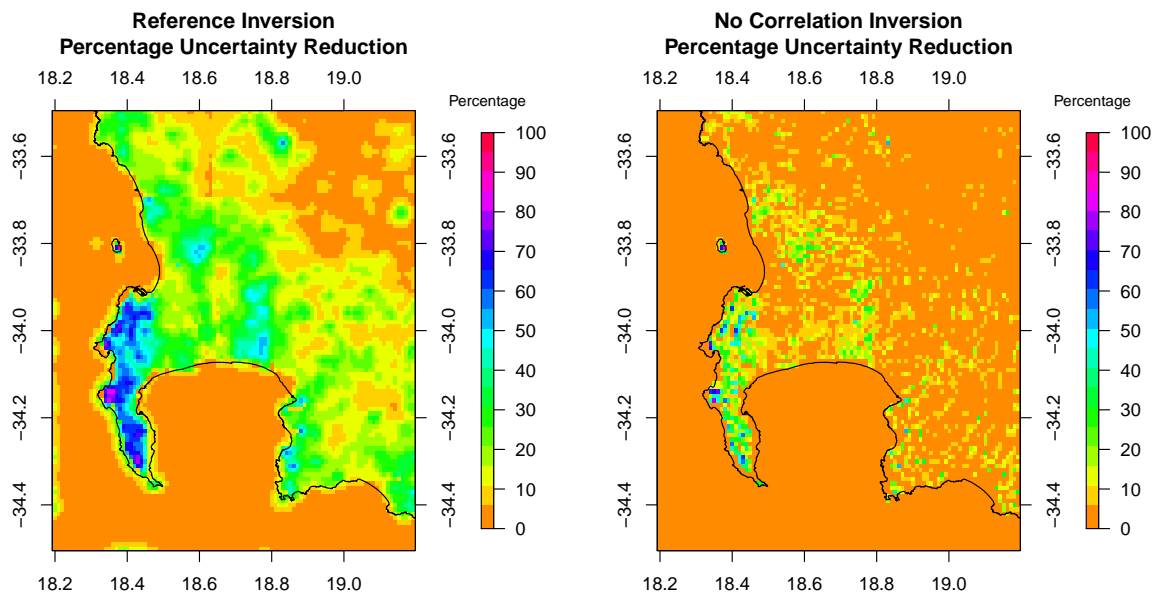


Figure 7. Spatial distribution in the pixel-level uncertainty reduction achieved by the inversion to the prior fluxes in May 2012 for the reference inversion (S0) (left), and to the no correlation inversion (S5) (right).

3.5 Alternative control vectors

- S0 and S17, where separate weekly inversions were performed, had similar aggregated ~~weekly fluxes (Supplement Sect. 1.2)~~ fluxes (Figure 3). For ~~Mean-Month, S16, which forced the fossil fuel and biogenic fluxes to be constant over the month,~~ the ~~weekly aggregated fluxes were forced to be the same within each month, but the~~ general pattern over time was similar to RefS0. For most months the posterior weekly flux was above or below the prior weekly flux to the same degree as RefS0, but the estimates, as expected, were smoother over time –
- (see supplementary material Figure 9). The monthly aggregated fluxes were generally very close to those from Ref S0 except for August, September and November 2012 (~~Supplement Sect. 1.3~~see supplementary material Section 2.2 Table S2). These are ~~the~~ summer months, and there was a great deal of variation in the aggregated fluxes from week to week ~~from the results of Ref in in the S0 inversion during~~ these months. Mean-Month S16 generally had aggregated fluxes that were closer to zero than ~~Ref or Week~~S0 or S17. This had a large impact on the aggregated flux over the full measurement period, due to these less negative posterior aggregated fluxes during the summer months. The aggregated flux for Mean-Month S16 was 662 kt CO₂ compared ~~to with~~ the -317 kt CO₂ ~~of Ref (Table ??)~~. Week for S0, S17 had an aggregated flux of -687 kt CO₂. This discrepancy is partly due to some weeks with missing observations. In Ref S0 these fluxes would have been adjusted by the available observations for neighbouring weeks, but were completely unconstrained by the observations in ~~Week. For those months when all measurements were available, the aggregated totals were similar between Ref and Week.~~S17. The uncertainty reduction in the aggregated estimates was almost double for Mean-Month compared to Ref and WeekS16 compared with S0 and S17.
- The spatial distribution of the posterior fluxes was very similar for ~~Ref and Week~~S0 and S17 (see supplementary material Figure S89), but was distinctly different for Mean-Month S16. Notably, the area around the oil refinery pixel was adjusted to negative fluxes for the month of September (Figure 8). Other areas were made closer to zero compared with Ref. ~~For the month of May the posterior fluxes in the CBD were distributed differently and a new area of relatively large negative fluxes was created north west of the oil refinery pixel (refer to Supplement Figure S55).~~S0. The uncertainty reductions at the pixel-level were large for the Mean-Month compared with Ref, with S16 compared with S0, with more areas of large uncertainty reduction ~~much more widespread~~. In particular, the areas of uncertainty reduction above 90% that were restricted to the area over Table Mountain National Park in Ref S0 were now extended over the CBD area.
- Consequently the aggregated fluxes ~~had uncertainty reduction for S16 had uncertainty reductions~~ that were twice as large as those for RefS0, and uncertainties in the aggregated fluxes ~~that~~ were much smaller. For the aggregated flux over the full period, the posterior uncertainty was 66 kt CO₂ for ~~t~~Mean-Month S16, compared with the uncertainty of 189 and 186 kt CO₂ from Ref and Week respectively (~~Table ??~~S0 and S17 respectively (Figure 3)).

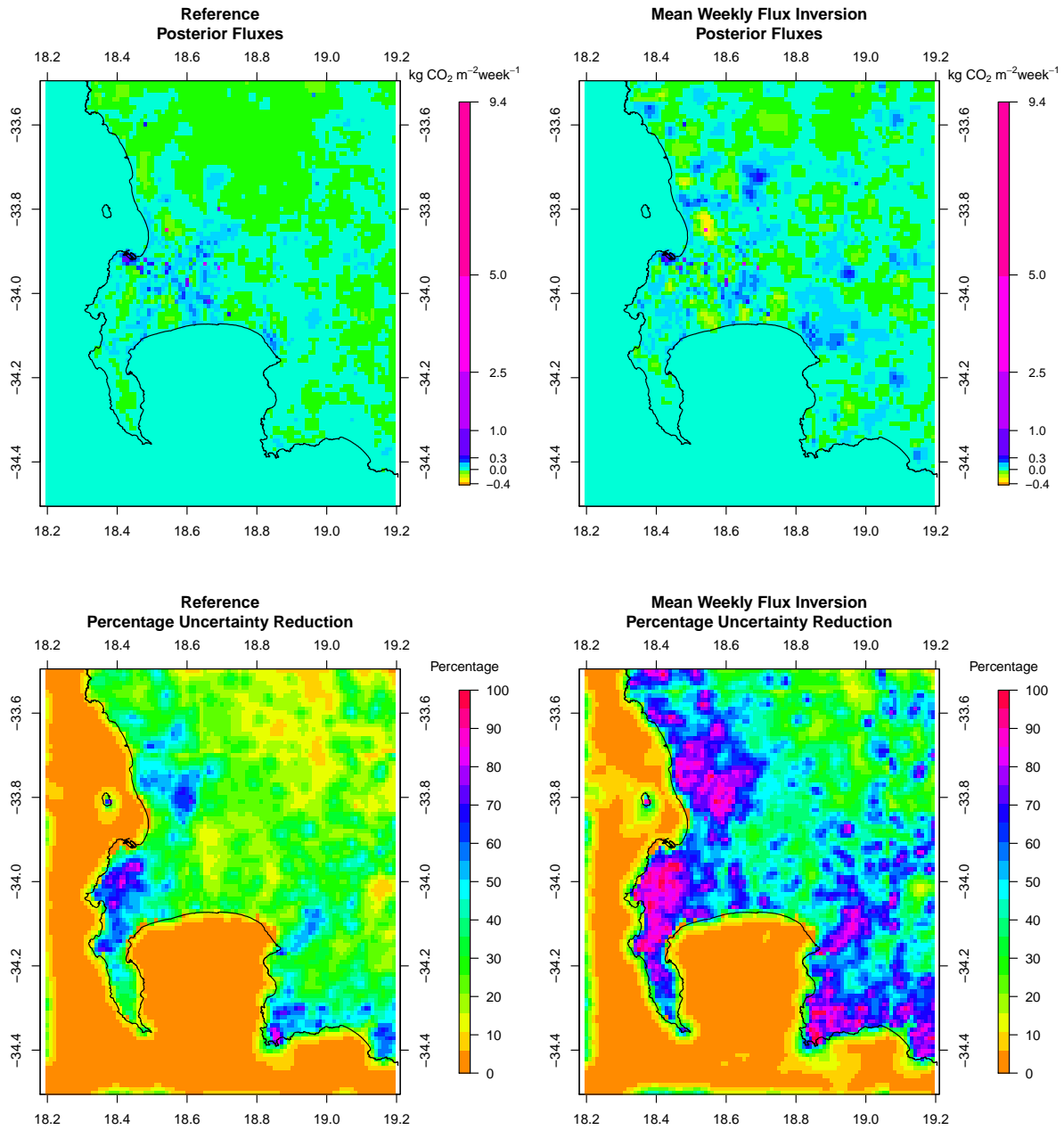


Figure 8. Spatial distribution of the pixel-level posterior fluxes and uncertainty reductions achieved by the reference inversion S0 and homogenised-NEE-prior-test-case-mean monthly flux inversion S16 for September 2012.

4 Discussion

4.1 Alternative prior information products

As Robben Island is dominated by fossil fuel influence from the Cape Town metropolitan area, and Hangklip by biogenic sources from natural and agricultural areas in its vicinity, the discrepancy in the modelled concentrations relative to the observations ~~suggests~~ suggested that the fossil fuel fluxes provided by the prior products are too large in magnitude, and ~~the NEE estimates from CABLE estimate~~ CABLE estimated too much carbon uptake by the biota around the Hangklip site. In the case of the carbon assessment inversion, the bias in the prior modelled concentrations was positive compared ~~to~~ with the negative bias of the reference inversion, indicating that the carbon assessment product was underestimating the uptake by the biota. ~~As the~~ The direction of the correction to the prior fluxes made by the inversion using NEE fluxes from the carbon assessment product ~~was much more homogeneous over space than CABLE, and could not react to local climate conditions, the uncertainty prescribed by using the NPP estimates is most likely too small.~~ suggested that the amount of carbon uptake was insufficient. The NEE fluxes were also smaller compared to those from CABLE, leading to uncertainties that were too small, and therefore an ill-specified inversion. The inversion could not correct the fluxes sufficiently so that modelled concentrations could match better with observed concentrations, and therefore certain localised events (i.e. spikes in the CO₂ signal) were not well represented in posterior fluxes from the carbon assessment inversion.

The comparison of inversion results using different prior products provides useful information regarding which direction the true flux estimates are likely to be. A pixel within the CBD limits had similar fossil fuel flux estimates from the ODIAC product compared ~~to~~ with the reference inventory product. ~~The ODIAC product extended the fossil fuel fluxes much further a field,~~ but the ODIAC product had emissions that were more widespread across the domain away from the CBD region than the reference inventory. This led to aggregated estimates that were ~~much~~ larger under the ODIAC inversion than the reference inversion. ~~The~~ Compared to the reference, the ODIAC inversion attempted to reduce the aggregated flux for most months – and to a greater degree – to better match the observations, indicating that compared ~~to~~ with the reference inventory, the ODIAC prior was most likely overestimating the amount of fossil fuel emissions from Cape Town. ~~It can therefore be deduced that the true fossil fuel~~ to a greater extent for most parts of the study period. When the two prior information products provide divergent prior flux estimates, such that the inversion reduced the flux for one product but increased the flux for the other, it suggests that the true flux lies somewhere between the reference inventory and ODIAC fossil fuel flux estimates. ~~posterior flux estimates from these two inversions. When the posterior aggregated flux was made smaller than the ODIAC prior but larger than the reference prior aggregated flux, such as during February and March 2013, the true aggregated flux should lie between these two posterior estimates. When the posterior flux was made smaller than the prior for both inversions, we could deduce that the true aggregated flux must be below the minimum of these two posterior estimates, and if we have accurate uncertainty estimates, the true flux should be no smaller than the lower uncertainty limit. Making use of the posterior uncertainties and the direction away from the prior in which the inversions made corrections, a region is suggested where the true flux is most likely to lie (Figure 9). For the CT domain, the inversion results suggest that over the spatial domain investigated, the flux is close to carbon neutral for the majority of the year.~~

The comparison of inversion results using different prior products provides useful information regarding which direction the true flux estimates are likely to be.

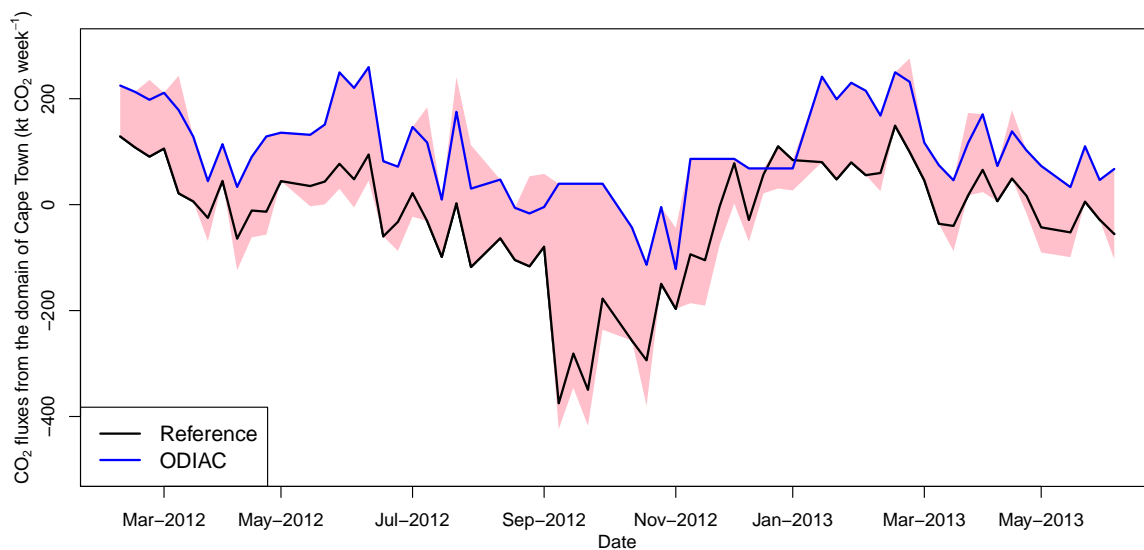


Figure 9. Using the posterior estimates of the reference and ODIAC inversions (S0 and S2) and the direction of change from the prior estimate, a region is inferred where in the true aggregated flux is expected to lie, indicated by the pink shaded area.

4.2 Uncertainty covariance matrix structure: C_{s_0} and C_c

From the analysis of the reference inversion (Nickless et al., 2018), the χ^2 statistics indicated that the reference inversion could be improved by small increases to the uncertainty specified in C_{s_0} , either through accounting for a larger correlation length or increasing the pixel-level uncertainties. Removal of the observation error correlations had a very small impact on the goodness-of-fit statistics, or on the posterior flux estimates and uncertainty reduction achieved by the inversion. To ensure that our reference inversion did not deviate too far from conventions for city-scale inversions where observation error correlations are ignored, we assigned a very short error correlation length to the observations of one hour. ~~If we had assigned a longer length, such as 6 hours, this may have had more of an effect.~~ Although, even with only an hour correlation length, off-diagonal error correlations would have been non-zero for observations at least half a day apart. We considered a longer correlation length in S6, but this had little impact on the inversion and increased the size of the χ^2 statistic, indicating that either the observation errors or flux uncertainties needed to be increased as well to improve statistical consistency. Lauvaux et al. (2009) have shown that observation errors up to 24 hours apart may be strongly correlated. To adequately account for these correlation lengths, a more sophisticated correlation structure may be required where non-zero error correlations are only specified between hours in similar periods of the day, such as afternoon periods for consecutive days, which would be expected to have similar meteorology. The specification of the most suitable observation error length is still under investigation, but the results of these sensitivity tests suggest that this parameter is of less importance than the flux uncertainty correlation lengths.

The impact of the inversion on the posterior fluxes and their uncertainties strongly depended on the specification of the correlation between the uncertainties in the NEE fluxes. In particular, the aggregated fluxes were distinctly different between the reference and test cases ignoring covariances between NEE flux uncertainties, which tended to have aggregated fluxes closer to the priors and uncertainty reductions achieved by the inversion that were much lower (7.6% compared to ~~with~~ 26.6% on average by the reference inversion). This indicates that advantage should be taken of knowledge related to the correlation induced by homogeneity of biogenic productivity in subregions of the domain. If this correlation is correctly specified in C_{s_0} , then the inversion is able to make larger adjustments to the prior fluxes and achieve a larger uncertainty reduction in these fluxes.

4.3 Relative uncertainty in C_{s_0}

Specification of the uncertainties in the prior flux estimates is one of the most challenging tasks in an atmospheric inversion exercise. There is little consensus on the correct approach to follow, and it is difficult to ensure that the most important sources of uncertainty are accounted for.

~~The~~ The χ^2 statistics indicated that for this Cape Town application, further increasing either the uncertainty in the fossil fuel fluxes or in the NEE fluxes led to statistics closer to one. Increasing the fossil fuel flux or NEE uncertainty led to a lower number of DFS. The degree to which the inversion is constrained by the prior fluxes is inversely related to the specified prior uncertainty. If either the uncertainty in the fossil fuel fluxes or in the NEE fluxes was increased, this led to aggregated flux estimates that were more positive as the inversion was apparently attempting to compensate for the overestimation of the NEE

uptake by the CABLE model. When the uncertainties were made smaller, the degree to which the inversion could increase the fluxes was restricted, and the resulting aggregated fluxes were more negative compared with the reference inversion.

~~These sensitivity results illustrate how dependent the uncertainty bounds around the posterior estimates are on the uncertainties specified for the prior fluxes. The inversion relies on the correctness of the uncertainty estimates assigned to the prior fluxes~~

5 An inversion will nudge the flux solution closer to the truth and will always result in reduced uncertainty compared to that which was placed on the prior. If the prior estimates for the fluxes are far from the truth, and the uncertainties are made small, the modelled concentration residuals will be similar before and after the inversion, and uncertainty reduction will be small. Therefore the uncertainties need to be correctly specified to allow the inversion to correct the fluxes as close as possible to the true fluxes. Ideally, large enough to give the inversion the freedom to correct the fluxes towards the truth, but small enough
10 so that the posterior uncertainty is within the required limits. ~~The posterior uncertainties reflect the reduction in uncertainty achieved by the inversion given that the prior uncertainties are accurate.~~ This motivates for the hierarchical Bayesian approach where a distribution is assigned to the uncertainty estimates. It can be shown that in the absence of observation error, doubling or halving the prior uncertainty in the fluxes results in a respective doubling or halving of the posterior uncertainty (see [Supplement Sect. 1.5 supplementary material Section 7](#)). Therefore it is unsurprising that if a prior uncertainty is made
15 larger with respect to a reference inversion specification, that the posterior uncertainty of this inversion will be larger than the posterior uncertainty of the reference.

Normally when an inversion framework is assessed, we are interested in how much uncertainty reduction can be achieved by the available observation network. The uncertainty reduction is dependent on the influence of the observations and on how well the prior information is specified. This set of sensitivity tests demonstrated that if we wish to ensure that the uncertainty
20 bounds around the posterior fluxes are within a prespecified margin, say 10% of the aggregated flux estimate, then we have to ensure that ~~prior uncertainty that~~ we know enough about the sources such that the prior uncertainty we begin with is sufficiently small. Assuming no large shifts in the mean estimate, it can be shown that if we wish to obtain an uncertainty estimate that is within 10% of the aggregated flux estimate, and we are able to reduce the uncertainty by 25% through the inversion as we have achieved in the Cape Town inversion, then the prior uncertainty estimate would need to be within 13.3% of the prior aggregated
25 flux estimate.

4.3 ~~Homogenised prior information~~

~~Applying a spatially homogenised prior for NEE resulted in aggregated prior fluxes with smaller uncertainties, but in aggregated posterior fluxes that were quite different to those of the reference inversion. As the uncertainty was smaller, the degree to which the inversion could adjust these priors was diminished. An alternative sensitivity test could use the mean NEE flux as the prior~~
30 ~~for all pixel, but the maximum NPP as the uncertainty across all pixels. This would have allowed the inversion to adjust the fluxes by a much larger degree allowing us to determine how much the inversion wanted to adjust the prior fluxes. Comparing the results to the reference inversion did illustrate that CABLE was most likely over-estimating the amount of uptake.~~

~~Smoothing the domestic emissions over time had less of an effect on the inversion, with corrections to the prior estimates generally of the same magnitude and in the same direction, and with similar uncertainty reductions.~~

4.3 Simplified C_e

~~Simplifying the C_e~~ Simplifying the C_e had very little impact on the inversion results. Increasing the night-time observation errors caused the aggregated flux to be more negative. Assigning an uncertainty in the night-time modelled concentrations of 10 ppm effectively led to the inversion ignoring most of the information available at night, leaving the posterior night-time fluxes (which are mostly affected by the night-time observations) to be similar to their prior estimates. If the inversion is tending to make large corrections to the daytime fluxes, and is now unable to make large corrections to the night-time fluxes, it implies that the aggregated fluxes will be more in error than if the inversion could be constrained by the observations - provided the constraint is good. The analysis of the misfits in the modelled concentrations from the reference inversion ~~((Nickless et al., 2018))~~(Nickless et al., 2018) demonstrated that the errors in the day and night-time atmospheric transport modelling were not very different, and therefore it is unlikely that assigning errors as large as 10 ppm to all the night-time observations is necessary. ~~The analysis of the errors in the modelled concentrations between day and night for the reference inversion provided confidence that the approach of increasing the errors only when conditions indicated that errors were more likely led model errors that were similar to those obtained during the day (Nickless et al., 2018).~~

4.3 Alternative control vectors

15 The separate weekly inversions obtained similar results to those of the reference inversion. Therefore, if necessary, for example due to computational costs, the separate weekly inversions could have been performed in place of the monthly inversions used in the reference case. In addition to the reduction in computation resources required, this allows additional features of the inversion to be tested more easily.

The large uncertainty reduction achieved by the solving for a mean weekly flux ~~inversion is expected~~is expected, as a mean weekly flux estimate over four weeks has four times as many observations to constrain this estimate ~~than if separately weekly fluxes are solved for~~as separate weekly estimates. The estimates from the inversion solving for a mean weekly flux were consistent with those from the reference inversion, except in the summer months. During these ~~periods~~months observations were often missing ~~during this particular study period, and therefore smaller discrepancies may have been observed if data continuity~~. We would expect smaller discrepancies between mean weekly and separate weekly fluxes if data were complete
25 during these periods ~~was similar to the rest of the inversion study period~~.

An alternative control vector, which could improve on all three of the alternative control vectors used in this study, would be to solve for separate components of fossil fuel and NEE fluxes. For example, if fossil fuel fluxes were split into those fluxes from sectors which change slowly and those which change more quickly, the inversion could solve for a mean weekly flux over the month for the slow fluxes, and for sectors with faster changes, the inversion could solve for individual weekly fluxes. This
30 would allow greater uncertainty reductions for those fluxes for which a mean weekly flux could be solved, which would in turn reduce the overall uncertainty in the aggregated fossil fuel flux. The NEE flux could also potentially be split into a slow and fast component. The fast component responds to local climate conditions and this component could be tightly constrained by the available climate data. The inversion could solve for the slower component which is much harder to model, ~~and to which~~

~~we could assign larger uncertainties than we would need to for the fast component. As this is the slower component, we could solve for a mean weekly flux over the month, which would allow greater uncertainty reduction allowing this estimate to be constant for a relatively long period, thereby allowing for stronger constraint from the observations.~~

4.4 Inversion sensitivity

- 5 If we consider the aggregated ~~flux over the full measurement period presented in Table 3~~ posterior fluxes, the variability between flux estimates across those inversions which used the reference control vector is ~~2024-1962~~ kt CO₂. This is largely driven by the inversions using different prior products, and this ~~uncertainty drops to 487~~ variability drops to 469 if these two inversions are removed, ~~and~~. It drops further to 393-375 if the inversions with the transformed prior information are removed. This represents the variability in the aggregated flux estimate across all inversions which used the same prior information products.
- 10 If we compare this to the uncertainty in the aggregated fluxes, which is approximately 185 kt CO₂, it shows that variability between posterior flux estimates from different inversion frameworks is still very large when compared ~~to~~ with the uncertainty we expect around the posterior flux estimates. If the inversions with no error correlation between biospheric fluxes are removed, then the variability between inversions drops to ~~113-117~~ kt CO₂ ~~--~~ now below the expected uncertainty around the posterior flux from a single inversion. All the inversions that we removed from the estimate of variability were those which had a large
- 15 influence on the error correlations of the NEE fluxes, either because they were specifically manipulated or because they were affected by the choice of prior product. This demonstrates the important role ~~error-uncertainty~~ error-uncertainty correlations in the prior fluxes have on the posterior flux estimates obtained from an inversion.

- Exceptions are the inversions which changed the prior estimates of the fossil fuel fluxes. ~~These~~ The fossil fuel fluxes were not assigned ~~error-uncertainty~~ error-uncertainty correlations. Those inversions which altered the prior estimates of the fossil fuel fluxes also
- 20 had ~~variable aggregated fluxes~~ aggregated fluxes that differed when compared with the reference inversion. This is due to the inversion having limited ability to make large changes to the fossil fuel fluxes. The ensemble of posterior fluxes obtained from inversions with alternative prior fluxes allowed us to determine in which direction the inversion was attempting to adjust these fluxes, and provided us with an interval in which we could deduce the ~~best estimate of the true~~ best estimate of the true aggregated flux would ~~lie most~~ likely be located. Changing the control vector also had a large influence on the aggregated flux, but this was largely due to
- 25 periods with low data completeness.

5 Conclusions

- Sensitivity tests have shown that to improve the inversion results for the Cape Town inversion, two important advancements should be made to the inversion framework. Firstly the NEE estimates need to be improved. The results from the reference inversion and from these sensitivity tests clearly indicate that CABLE is generally overestimating the amount of CO₂ uptake
- 30 in the domain. Where there is more confidence in the estimation of the biogenic fluxes, either from CABLE for an alternative land-atmosphere exchange model, these reduced uncertainties should be incorporated into the prior information, rather than

applying a blanket uncertainty equal to the NPP as done for the reference inversion. For example, over agricultural areas, where the biogenic fluxes may be more reliably modelled, uncertainties may be substantially reduced.

Solving for mean weekly fluxes over a month produced much larger uncertainty reductions. Using an alternative control vector which solves for separate components of the fossil fuel and NEE fluxes that can be split into slow and fast components could take advantage of the larger uncertainty reduction achieved from solving for a mean weekly flux for each month. This could potentially allow the inversion to better distinguish between NEE and fossil fuel fluxes, allowing the inversion to apply corrections to the ~~correct flux~~ right flux component (fossil or biogenic), and at the same time obtain aggregated flux estimates with smaller uncertainties than those obtained for the reference inversion. The estimates of the aggregated fluxes ~~was~~ were shown to be more reliable in the reference inversion than those for the individual fossil fuel and NEE fluxes (Nickless et al., 2018).

The posterior uncertainties are highly dependent on the prior uncertainties. ~~This was shown across several sensitivity tests, including the inversions which used alternative priors, inversions that used homogenised priors and inversions that adjusted the relative uncertainties of the prior fossil fuel and NEE fluxes.~~ Of more concern is the large impact that the uncertainty correlation assumed for the NEE fluxes had on the aggregated flux estimates and on the spatial distribution of the posterior fluxes. This has been observed in previous inversions (Lauvaux et al., 2016). Of all the specifications made, the correlation lengths are the most arbitrary, but ~~can redefine the posterior flux estimates~~ changing this parameter can entirely alter the distribution of the posterior fluxes. The sensitivity tests suggested that correlations between observation errors were of less importance to the inversion result.

Approaches which ~~attempt to solve for the uncertainties rather than relying on prior estimates may provide better estimates~~ allow the data to inform the estimates of the uncertainties and correlation lengths are likely to be more successful at obtaining estimates of the true uncertainty bounds around the inversion posterior flux estimates. Michalak et al. (2005) proposed a maximum likelihood approach to solve for the parameters, and Ganesan et al. (2014) and Wu et al. (2013) ~~propose~~ proposed an hierarchical Bayesian approach to solve for hyper-parameters of the inversion, including the covariance terms, ~~which could reduce the dependency of inversion results on expert opinion estimates of uncertainty.~~ These approaches have required simplifying assumptions in order to use iterative methods to solve for the parameters, such as assuming the uncertainty is the same across all fluxes or groups of fluxes, or solving for a scaling parameter of the fluxes rather than the fluxes themselves.

These sensitivity analyses performed for this paper did not consider alternative atmospheric transport models. Sensitivity tests on previous city-scale inversions have shown this to be an important source of variation between inversion results ~~(Lauvaux et al., 2016; Staufer et al., 2016)~~ (Lauvaux et al., 2016; Staufer et al., 2016; Karion et al., 2019). Future work on the Cape Town inversion will consider ~~multiple atmospheric transport~~ alternative regional climate models, such as the WRF (Weather Research and Forecasting model coupled with Chemistry) regional climate model ~~and alternative atmospheric transport models~~ (Karion et al., 2019).

~~If enough of these sensitivity tests can be performed, and probability distribution around the posterior fluxes can be determined, which may provide better uncertainty limits around these estimates. The ability of running more inversions in a shorter period of time if a more efficient control vector is chosen would make running many more inversion specifications for such an exercise~~

~~possible. Assigning probability distributions to these parameters that we test underpins the hierarchical Bayesian approach in Ganesan et al. (2014).~~

Code and data availability. Data and code related to the Bayesian inversion procedure can be made available upon request

Author contributions. AN installed and maintained all the instrumentation at Robben Island and Hangklip, obtained the measurements and processed these into hourly concentrations, ran and processed the result of the LPDM in Fortran, produced all code and ran the inversion in Python, processed all the inversion results using R Statistical Software, produced all graphics and tables, designed the sensitivity tests, and was responsible for the development of the manuscript which forms part of her PhD. PJR was the main scientific supervisor, oversaw all implementation of the inversion, and provided guidance on the presentation and interpretation of results. FE performed the coupled CCAM-CABLE simulations. BE provided guidance on statistical issues. RJS provided guidance on the location of the sites and provided input on the interpretation of the results. All authors had the commented on the manuscript.

Competing interests. The authors declare that they have no conflict of interest

Acknowledgements. We would like to acknowledge and thank Dr. Casper Labuschagne, [Ernst Brunke](#) and Danie van der Spuy of the South African Weather Service for their assistance in maintaining the instruments at Robben Island and Hangklip, and Dr. Casper Labuschagne for his guidance on processing the instantaneous CO₂ concentration data; Martin Steinbacher for providing guidance and schematics on the calibration system used on the Picarro instruments; Robin Poggenpoel and Jacobus Smith of Transnet for allowing us access to the lighthouses; Peter Saaise of Transnet, the Robben Island lighthouse keeper, (and his daughter) for assisting when the instrument was not responding [and for tolerating the disturbance to the tranquil lighthouse environment](#); Marek Uliasz for providing us access to the code for his LPDM model; Thomas Lauvaux for providing guidance on processing the LPDM results and useful discussion on the boundary contribution in the inversion. Use was made of the University of Cape Town ICTS-HPC cluster. Please see <http://hpc.uct.ac.za/> for details. We would like to thank Andrew Lewis of the University of Cape Town HPC facility for providing useful advice on improving the efficiency of the Python runs. This research was funded by competitive parliamentary grant funding from the Council of Scientific and Industrial Research awarded to the Global Change Competency Area towards the development of the Variable-resolution Earth System Model (VRESM; Grants EEGC030 and EECM066). Additional funding was obtained from the South African National Research Foundation for the Picarro instrumentation.

References

- [Andres, R. J., Boden, T. A., Bréon, F. -M., Ciais, P., Davis, S., Erickson, D., Gregg, J. S., Jacobson, A., Marland, G., Miller, J., Oda, T., Olivier, J. G. J., Raupach, M. R., Rayner, P., and Treanton, K.: A synthesis of carbon dioxide emissions from fossil-fuel combustion, *Biogeosciences*, 9, 1845–1871, doi: 10.5194/bg-9-1845-2012, 2012.](#)
- 5 [Andres, R. J., Boden, T. A., and Higdon, D.: A new evaluation of the uncertainty associated with CDIAC estimates of fossil fuel carbon dioxide emission, *Tellus B*, 66, 23616, doi: 10.3402/tellusb.v66.23616, 2014.](#)
- Archibald, S. A., Kirton, A., van der Merwe, M. R., Scholes, R. J., Williams, C. A., and Hanan, N.: Drivers of inter-annual variability in Net Ecosystem Exchange in a semi-arid savanna ecosystem, South Africa, *Biogeosciences*, 6, 251-266, doi: 10.5194/bg-6-251-2009, 2009.
- Bellassen, V. and Stephan, N.: Accounting for carbon: Monitoring, reporting and verifying emissions in the climate economy, Cambridge University Press, Cambridge, UK, 2015.
- 10 [Boden, T. A., Marland, G., and Andres, R. J.: Global, regional, and national fossil fuel CO₂ emissions, Carbon Dioxide Information Analysis Center, Oak Ridge National Laboratory, U.S. Department of Energy, Oak Ridge, Tenn., U.S.A., doi: 10.3334/CDIAC/00001_V2011, 2011.](#)
- [Boon, A., Broquet, G., Clifford, D. J., Chevallier, F., Butterfield, D. M., Pison, I., Ramonet, M., Paris, J. -D., and Ciais, P.: Analysis of the potential of near-ground measurements of CO₂ and CH₄ in London, UK, for the monitoring of city-scale emissions using an atmospheric transport model, *Atmos. Chem. Phys.*, 16, 6735–6756, doi:10.5194/acp-16-6735-2016, 2016.](#)
- 15 [Bréon, F. M., Broquet, G., Puygrenier, V., Chevallier, F., Xueref-Remy, I., Ramonet, M., Dieudonné, E., Lopez, M., Schmidt, M., Perrussel, O., and Ciais, P.: An attempt at estimating Paris area CO₂ emissions from atmospheric concentration measurements, *Atmos. Chem. Phys.*, 15, 1707–1724, doi: 10.5194/acp-15-1707-2015, 2015.](#)
- 20 [Brioude, J., Angevine, W. M., Ahmadov, R., Kim, S. -W., Evan, S., McKeen, S. A., Hsie, E. -Y., Frost, G. J., Neuman, J. A., Pollack, I. B., Peischl, J., Ryerson, T. B., Holloway, J., Brown, S. S., Nowak, J. B., Roberts, J. M., Wofsy, S. C., Santoni, G. W., Oda, T., and Trainer, M.: Top-down estimate of surface flux in the Los Angeles Basin using a mesoscale inverse modeling technique: assessing anthropogenic emissions of CO, NO_x and CO₂ and their impacts, *Atmos. Chem. Phys.*, 13, 3661–3677, doi: 10.5194/acp-13-3661-2013, 2013.](#)
- [Brunke, E. -G., Labuschagne, C., Parker, B., Scheel, H. E., and Wittlestone, S.: Baseline air mass selection at Cape Point, South Africa: application of ²²²Rn and other filter criteria to CO₂, *Atmos. Environ.*, 38, 5693–5702, doi:10.1016/j.atmosenv.2004.04.024, 2004.](#)
- 25 [Chevallier, F., Ciais, P., Conway, T. J., Aalto, T., Anderson, B. E., Bousquet, P., Brunke, E. G., Ciattaglia, L., Esaki, Y., Fröhlich, M., Gomez, A., Gomez-Pelaez, A. J., Haszpra, L., Krummel, P. B., Langenfelds, R. L., Leuenberger, M., Machida, T., Maignan, F., Matsueda, H., Morgui, J. A., Mukai, H., Nakazawa, T., Peylin, P., Ramonet, M., Rivier, L., Sawa, Y., Schmidt, M., Steele, L. P., Vay, S. A., Vermeulen, A. T., Wofsy, S., and Worthy, D.: CO₂ surface fluxes at grid point scale estimated from a global 21 year reanalysis of atmospheric measurements, *J. Geophys. Res.*, 115, D21307, doi: 10.1029/2010JD013887, 2010.](#)
- 30 [City of Cape Town: State of energy and energy futures report. Cape Town: City of Cape Town, \[http://www.capetown.gov.za/en/EnvironmentalResourceManagement/publications/Documents/State_of_Energy_+_Energy_Futures_Report_2011_revised_2012-01.pdf\]\(http://www.capetown.gov.za/en/EnvironmentalResourceManagement/publications/Documents/State_of_Energy_+_Energy_Futures_Report_2011_revised_2012-01.pdf\), 2011.](#)
- Department of Environmental Affairs (South Africa): South African National Terrestrial Carbon Sink Assessment, Department of Environmental Affairs, Pretoria, South Africa, 2015.
- 35 [UK Department for Environment, Food and Rural Affairs \(Defra\): UK ship emissions inventory. Final report. London: Crown, \[http://uk-air.defra.gov.uk/assets/documents/reports/cat15/1012131459_21897_Final_Report_291110.pdf\]\(http://uk-air.defra.gov.uk/assets/documents/reports/cat15/1012131459_21897_Final_Report_291110.pdf\), 2010.](#)

- UK Department for Environment, Food and Rural Affairs (Defra): Government GHG conversion factors for company reporting: Methodology paper for emission factors, London: Crown, https://www.gov.uk/government/uploads/system/uploads/attachment_data/file/224437/pb13988-emission-factor-methodology-130719.pdf, 2013.
- 5 [Duren, R. M. and Miller, C. E.: Measuring the carbon emissions of megacities, Nat. Clim. Change, 2, 560–562, doi: 10.1038/nclimate1629, 2012.](#)
- [Engelbrecht, F. A., McGregor, J. L. and Engelbrecht, C. J.: Dynamics of the conformal-cubic atmospheric model projected climate-change signal over southern Africa, Int. J. Climatol., 29, 1013–1033., doi: 10/1002/joc.1742.29., 2009.](#)
- [Engelbrecht, F. A., Landman, W. A., Engelbrecht, C. J., Landman, S., Bopane, M. M., Roux, B., McGregor, J. L., and Thatcher, M.: Multi-scale climate modelling over Southern Africa using variable-resolution global model, Water Research Commission 40-Year Celebration Conference, Kempton Park, 31 August - 1 September 2011, doi: 10.4314/wsa.v37i5.2, 2011.](#)
- 10 Engelbrecht, C. J., Engelbrecht, F. A. and Dyson, L. L.: High-resolution model-projected changes in mid-tropospheric closed-lows and extreme rainfall events over southern Africa. Int. J. Climatol., 33, 173–187, doi: 10/1002/joc.3420, 2013.
- [Engelbrecht, F., Adegoke, J., Bopape, M.-J., Naidoo, M., Garland, R., Thatcher, M., McGregor, J., Katzfey, J., Werner, M., Ichoku, C. and Gatebe, C.: Projections of rapidly rising surface temperatures over Africa. Env. Res. Letters., 10\(8\), 085004, doi: 10.1088/1748-9326/10/8/085004, 2015.](#)
- 15 [Enting, I. G.: Inverse Problems in Atmospheric Constituent Transport, Cambridge Univ. Press, New York, 2002.](#)
- Exbrayat, J. -F., Pitman, A. J. Abramowitz, G. and Wang, Y. -P.: Sensitivity of net ecosystem exchange and heterotrophic respiration to parameterization uncertainty, J. Geophys. Res. Atmos., 118, 1640–1651, doi:10.1029/2012JD018122, 2013.
- Feng, S., Lauvaux T., Newman, S., Rao, P., Ahmadov, R. Deng, A., Díaz-Isaac, L. I., Duren, R. M., Fischer, M. L., Gerbig, C., Gurney, K. R.,
- 20 Huang, J., Jeong, S., Li, Z., Miller, C. E., O’Keeffe, D., Patarasuk, R., Ser, S. P., Song, Y., Wong, K. W., and Yung, Y. L.: Los Angeles megacity: a high-resolution land–atmosphere modelling system for urban CO₂ emissions, Atmos. Chem. Phys., 16, 9019–9045, doi: 10.5194/acp-16-9019-2016, 2016.
- Ganesan, A. L., Rigby, M., Zammit-Mangion, A., Manning, A. J., Prinn, R. G., Fraser, P. J., Harth, C. M., Kim, K. -R., Krummel, P. B., Li, S., Mühle, J., O’Doherty, S. J., Park, S., Salameh, P. K., Steele, L. P., and Weiss, R. F.: Characterization of uncertainties in atmospheric
- 25 trace gas inversions using hierarchical Bayesian methods, Atmos. Chem. Phys., 14, 3855–3864, doi:10.5194/acp-14-3855-2014, 2014.
- Gregor, L. and Monteiro, P. M. S.: Is the southern Benguela a significant regional sink of CO₂? S. Afr. J. Sci., 109(5/6), Art. #0094, 5 pages, doi: 10.1590/sajs.2013/20120094, 2013.
- Gurney, K. R., Razlivanov, I., Song, Y., Zhou, Y., Benes, B., and Abdul-Massih, M.: Quantification of fossil fuel CO₂ emissions on the building/street scale for a large U.S. city, Environ. Sci. Technol., 46, 12194–12202, doi: 10.1021/es3011282, 2012.
- 30 [Hutyra, L., Duren, R., Gurney, K. R., Grimm, N., Kort, E. A., Larson, E., Shrestha, G.: Urbanization and the carbon cycle: Current capabilities and research outlook from the natural sciences perspective. Earth’s Future, 2: 473–495. doi: 10.1002/2014EF000255, 2014.](#)
- [Intergovernmental Panel on Climate Change \(IPCC\): Good practice guidance and uncertainty management in national greenhouse gas inventories. Montreal: IPCC, 93–102, <http://www.ipcc-nggip.iges.or.jp/public/gp/english/>, 2000.](#)
- [Jackson, D. D.: The use of a priori data to resolve non-uniqueness in linear inversion, Geophys. J. R. astr. Soc., 57, 137–157, 1979.](#)
- 35 [Jackson, D. D and Matsu’ura, M.: A Bayesian approach to nonlinear inversion, J. Geophys. Res. 90 \(B1\), 581–591, 1985.](#)
- [Janssens-Maenhout, G., Pagliari, V., Guizzardi, D., and Muntean, M.: Global emission inventories in the Emission Database for Global Atmospheric Research \(EDGAR\) – Manual \(I\). Gridding: EDGAR emissions distribution on global gridmaps. Joint Research Centre, Luxembourg: European Union, 33 pp, doi: 10.2788/81454, 2012.](#)

- Kalnay, E., Kanamitsu, M., Kistler, R., Collins, W., Deaven, D., Gandin, L., Iredell, M., Saha, S., White, G., Woollen, J., Zhu, Y., Chelliah, M., Ebisuzaki, W., Higgins, W., Janowiak, J., Mo, K. C., Ropelewski, C., Wang, J., Leetmaa, A., Reynolds R., Jenne, R., Joseph, D.: The NCEP/NCAR 40-year reanalysis project. *Bull. Am. Meteorol. Soc.*, *77*, 437–472, 1996.
- 5 Karion, A., Lauvaux, T., Lopez Coto, I., Sweeney, C., Mueller, K., Gourdji, S., Angevine, W., Barkley, Z., Deng, A., Andrews, A., Stein, A., and Whetstone, J.: Intercomparison of atmospheric trace gas dispersion models: Barnett Shale case study, *Atmos. Chem. Phys.*, *19*, 2561–2576, doi: 10.5194/acp-19-2561-2019, 2019.
- Kort, E. A., Angevine, W. M., Duren, R., and Miller, C. E.: Surface observations for monitoring urban fossil fuel CO₂ emissions: minimum site location requirements for the Los Angeles megacity, *J. Geophys. Res.*, *118*, 1–8, doi: 10.1002/jgrd.50135, 2013.
- Kowalczyk, E. A., Wang, Y. P. and Law, R. M.: CSIRO Atmosphere Biosphere Land Exchange model for use in climate models and as an offline model, CSIRO Marine and Atmospheric Research technical paper xxV ISBN 1 921232 39 0, 2006.
- 10 Lauvaux, T., Pannekoucke, O., Sarrat, C., Chevallier, F., Ciais, P., Noilhan, J., and Rayner, P. J.: Structure of the transport uncertainty in mesoscale inversions of CO₂ sources and sinks using ensemble model simulations, *Biogeosciences*, *6*, 1089–1102, doi: 10.5194/bg-6-1089-2009, 2009.
- Lauvaux, T., Miles, N. L., Richardson, S. J., Deng, A., Stauffer, D. R., Davis, K. J., Jacobson, G., Rella, C., Calonder, G. -P., and DeCola, P. L.: 15 [Urban emissions of CO₂ from Davos, Switzerland: the first real-time monitoring system using atmospheric inversion technique](#), *J. Appl. Meteorol. Climatol.*, *52*, 2654–2668, doi: 10.1175/JAMC-D-13-038.1, 2013.
- Lauvaux, T., Schuh, A. E., Uliasz, M., Richardson, S., Miles, N., Andrews, A. E., Sweeney, C., Diaz, L. I., Martins, D., Shepson, P. B., and Davis, K. J.: Constraining the CO₂ budget of the corn belt: exploring uncertainties from the assumptions in a mesoscale inverse system, *Atmos. Chem. Phys.*, *12*, 337–354, doi: 10.5194/acp-12-337-2012, 2012.
- 20 Lauvaux, T., Miles, N. L., Deng, A., Richardson, S. J., Cambaliza, M. O., Davis, K. J., Gaudet, B., Gurney, K. R., Huang, J., O’Keefe, D., Song, Y., Karion, A., Oda, T., Patarasuk, R., Razlivanov, I., Sarmiento, D., Shepson, P., Sweeney, C., Turnbull, J., and Wu, K.: High-resolution atmospheric inversion of urban CO₂ emissions during the dormant season of the Indianapolis Flux Experiment (INFLUX), *J. Geophys. Res. Atmos.*, *121*, 5213–5236, doi: 10.1002/2015JD024473, 2016.
- Le Quéré, C., Andres, R. J., Boden, T. A., Conway, T., Houghton, R. A., House, J. I., Marland, G., Peters, G. P., van der Werf, G. R., 25 [Ahlström, A., Andrew, R. M., Bopp, L., Canadell, J. G., Ciais, P., Doney, S. C., Enright, C., Friedlingstein, P., Huntingford, C., Jain, A. K., Jourdain, C., Kato, E., Keeling, R. F., Klein Goldewijk, K., Levis, S., Levy, P., Lomas, M., Poulter, B., Raupach, M. R., Schwinger, J., Sitch, S., Stocker, B. D., Viovy, N., Zaehle, S., and Zeng, N.: The global carbon budget 1959–2011](#), *Earth Syst. Sci. Data*, *5*, 165–185, doi: 10.5194/essd-5-165-2013, 2013.
- McGregor, J. L. and Dix, M. R.: The CSIRO conformal-cubic atmospheric GCM, in: IUTAM Symposium on Advances in Mathematical 30 [Modelling of Atmosphere and Ocean Dynamics](#), Limerick, Ireland, 2–7 July 2000, edited by: Hodnett, P. F., Kluwer, Dordrecht, 197–202, 2001.
- McGregor, J. L.: [Semi-Lagrangian advection on conformal-cubic grids](#). *Mon. Weather Rev.*, *124*, 1311–1322, doi: 10.1175/1520-0493(1996)124<1311:SLAOCC>2.0.CO;2, 1996.
- McGregor, J. L.: [Geostrophic adjustment for reversibly staggered grids](#). *Mon. Weather Rev.*, *133*, 1119–1128, doi: 10.1175/MWR2908.1, 35 [2005a](#).
- McGregor, J. L.: [C-CAM: Geometric aspects and dynamical formulation](#). CSIRO Atmospheric Research Technical Paper, No 70, 41, 2005b.

- McGregor, J. L. and Dix, M. R.: [An updated description of the Conformal-Cubic Atmospheric Model](#), in: [High Resolution Numerical Modelling of the Atmosphere and Ocean](#), edited by: Hamilton, K. and Ohfuchi, W., Springer, New York, USA, 51–76, 2008.
- McKain, K., Wofsy, S. C., Nehrkorn, T., Eluszkiewicz, J., Ehleringer, J. R., and Stephens, B. B.: [Assessment of ground-based atmospheric observations for verification of greenhouse gas emissions from an urban region](#), *Proc. Natl. Acad. Sci. U. S. A.*, 109(22), 8423–8428, doi: 10.1073/pnas.1116645109, 2012.
- 5 Michalak, A. M., Hirsch, A., Bruhwiler, L., Gurney, K. R., Peters, W., and Tans, P. P.: Maximum likelihood estimation of covariance parameters for Bayesian atmospheric trace gas surface flux inversions, *J. Geophys. Res.*, 110, D24107, doi: 10.1029/2005JD005970, 2005.
- Moncrieff, G.R., Scheiter, S., Slingsby, J. A. and Higgins, S. I.: Understanding global change impacts on South African biomes using Dynamic Vegetation Models, *S. Afr. J. Bot.*, 101, 16–23, doi: 10.1016/j.sajb.2015.02.004, 2015.
- 10 Nassar, R., Napier-Linton, L., Gurney, K. R., Andres, R. J., Oda, T., Vogel, F. R. and Deng, F.: Improving the temporal and spatial distribution of CO₂ emissions from global fossil fuel emission data sets, *J. Geophys. Res. Atmos.*, 118, 917–933, doi: 10.1029/2012JD018196, 2013.
- Nickless, A., Scholes, R. J. and Filby, E.: Spatial and temporal disaggregation of anthropogenic CO₂ emissions from the City of Cape Town, *S. Afr. J. Sci.*, 111(11/12), Art. #2014 – 0387, 8 pages, doi: 10.17159/sajs.2015/20140387, 2015.
- 15 Nickless, A., Ziehn, T., Rayner, P. J., Scholes, R. J., and Engelbrecht, F.: Greenhouse gas network design using backward Lagrangian particle dispersion modelling – Part 2: Sensitivity analyses and South African test case, *Atmos. Chem. Phys.*, 15, 2051–2069, doi: 10.5194/acp-15-2051-2015, 2015.
- Nickless, A., Rayner, P. J., Engelbrecht, F., Brunke, E.-G., Erni, B., and Scholes, R. J.: Estimates of CO₂ fluxes over the city of Cape Town, South Africa, through Bayesian inverse modelling, *Atmos. Chem. Phys.*, 18, 4765–4801, doi: 10.5194/acp-18-4765-2018, 2018.
- 20 [NRC \(Committee on Methods for Estimating Greenhouse Gas Emissions\): Verifying greenhouse gas emissions: methods to support international climate agreements \(9780309152112\)](#), The National Academies Press, Washington, D.C., 2010.
- Oda, T. and Maksyutov, S.: A very high-resolution (1 km×1 km) global fossil fuel CO₂ emission inventory derived using a point source database and satellite observations of nighttime lights, *Atmos. Chem. Phys.*, 11, 543–556, doi:10.5194/acp-11-543-2011, 2011.
- Oda, T., Lauvaux, T., Lu, D., Rao, P., Miles, N. L., Richardson, S. J. and Gurney, K. R.: On the impact of granularity of space-based urban CO₂ emissions in urban atmospheric inversions: A case study for Indianapolis, IN, *Elem Sci Anth*, 5, 28, doi: 10.1525/elementa.146, 2017.
- 25 Oda, T., Maksyutov, S., and Andres, R. J.: The Open-source Data Inventory for Anthropogenic Carbon dioxide (CO₂), version 2016 (ODIAC2016): A global, monthly fossil-fuel CO₂ gridded emission data product for tracer transport simulations and surface flux inversions, *Earth Syst. Sci. Data Discuss.*, doi: 10.5194/essd-2017-76, in review, 2017.
- 30 [Rodgers, C. D.: Inverse methods for atmospheric sounding : theory and practice](#), World Scientific Publishing, Singapore, 2000.
- Roux, B.: Ultra high-resolution climate simulations over the Stellenbosch wine producing region using a variable-resolution model, MSc Thesis, Faculty of Natural and Agricultural Sciences, University of Pretoria, South Africa, 106 pp., 2009.
- Scholes, R. J., von Maltitz, G. P., Archibald, S. A., Wessels, K., van Zyl, T., Swanepoel, D., and Steenkamp, K.: National Carbon Sink Assessment for South Africa: First Estimate of Terrestrial Stocks and Fluxes, CSIR Technical Report, Pretoria, South Africa, CSIR/NRE/GC/ER/2013/0056/B, 2013.
- 35 Seibert, P. and Frank, A.: Source-receptor matrix calculation with a Lagrangian particle dispersion model in backward mode, *Atmos. Chem. Phys.*, 4, 51–63, doi: 10.5194/acp-4-51-2004, 2004.

- Seto, K. C., Dhakal, S., Bigio, A., Blanco, H., Delgado, G. C., Dewar, D., Huang, L., Inaba, A., Kansal, A., Lwasa, S., McMahon, J. E., Müller, D. B., Murakami, J., Nagendra, H., and Ramaswami, A.: Human settlements, infrastructure and spatial planning, in: *Climate Change 2014: Mitigation of Climate Change. Contribution of Working Group III to the Fifth Assessment Report of the Intergovernmental Panel on Climate Change*, edited by: Edenhofer, O., Pichs-Madruga, R., Sokona, Y., Farahani, E., Kadner, S., Seyboth, K., Adler, A., Baum, I., Brunner, S., Eickemeier, P., Kriemann, B., Savolainen, J., Schlömer, S., von Stechow, C., Zwickel, T., and Minx, J. C., Cambridge, United Kingdom and New York, NY, USA, 2014.
- 5 [South African Department of Energy: Digest of South African energy statistics, Pretoria: Department of Energy. http://www.energy.gov.za/files/media/explained/2009%20Digest%20PDF%20version.pdf, 2009.](http://www.energy.gov.za/files/media/explained/2009%20Digest%20PDF%20version.pdf)
- Staufe, J., Broquet, G., Bréon, F. -M., Puygrenier, V., Chevallier, F., Xueref-Rémy, I., Dieudonné, E., Lopez, M., Schmidt, M., Ramonet, M., Perrussel, O., Lac, C., Wu, L., and Ciais, P.: The first 1-year-long estimate of the Paris region fossil fuel CO₂ emissions based on atmospheric inversion, *Atmos. Chem. Phys.*, 16, 14703–14726, doi: 10.5194/acp-16-14703-2016, 2016.
- 10 [Statistics South Africa: Census 2011 statistical release, P0301.4., Pretoria: Statistics South Africa, 2011.](#)
- [Strong, C., Stwertka, C., Bowling, D. R., Stephens, B. B. and Ehleringer, J. R.: Urban carbon dioxide cycles within the Salt Lake Valley: A multiple-box model validated by observations, *J. Geophys. Res.*, 116, D15307, doi: 10.1029/2011JD015693, 2011.](#)
- 15 [Tans, P. and Keeling, R.: Mauna Loa CO₂ monthly mean data, NOAA/ESRL www.esrl.noaa.gov/gmd/ccgg/trends/ and Scripps Institution of Oceanography scrippsco2.ucsd.edu/, 2016.](#)
- Tarantola, A.: *Inverse Problem Theory and Methods for Model Parameter Estimation*, Society for Industrial and Applied Mathematics, Philadelphia, 2005.
- Turnbull, J. C., Karion, A., Fischer, M. L., Faloon, I., Guilderson, T., Lehman, S. J., Miller, B. R., Miller, J. B., Montzka, S., Sherwood, T., Saripalli, S., Sweeney, C., and Tans, P. P.: Assessment of fossil fuel carbon dioxide and other anthropogenic trace gas emissions from airborne measurements over Sacramento, California in spring 2009, *Atmos. Chem. Phys.*, 11, 705–721, doi: 10.5194/acp-11-705-2011, 2011.
- 20 [Turnbull, J. C., Sweeney, C., Karion, A., Newberger, T., Lehman, S. J., Tans, P. P., Davis, K. J., Lauvaux, T., Miles, N. L., Richardson, S. J., Cambaliza, M. O., Shepson, P. B., Gurney, K., and Patarasuk, P.: Toward quantification and source sector identification of fossil fuel CO₂ emissions from an urban area: Results from the INFLUX experiment, *J. Geophys. Res. Atmos.*, 120, 292–312, doi: 10.1002/2014JD022555, 2015.](#)
- Uliasz, M.: Lagrangian particle modeling in mesoscale applications, in: *Environmental Modelling II*, Computational Mechanics Publications, Southampton, UK, 71–102, 1994.
- 30 [UN-Habitat: Cities and climate change: global report on human settlements 2011, Earthscan, United Nations Human Settlements Programme \(UN-Habitat\), 2011.](#)
- [Wang, Y. P., Kowalczyk, E., Leuning, R., Abramowitz, G., Raupach, M. R., Pak, B., van Gorsel, E. and Luhar, A.: Diagnosing errors in a land surface model \(CABLE\) in the time and frequency domains, *J. Geophys. Res.*, 116, G01034, doi: 10.1029/2010JG001385, 2011.](#)
- Wu, L., Bocquet, M., Chevallier, F., Lauvaux, T., and Davis, K.: Hyperparameter estimation for uncertainty quantification in mesoscale carbon dioxide inversions, *Tellus B*, 65, 20894, doi: 10.3402/tellusb.v65i0.20894, 2013.
- 35 Wu, L., Broquet, G., Ciais, P., Bellassen, V., Vogel, F., Chevallier, F., Xueref-Remy, I., and Wang, Y.: What would dense atmospheric observation networks bring to the quantification of city CO₂ emissions?, *Atmos. Chem. Phys.*, 16, 7743–7771, doi: 10.5194/acp-16-7743-2016, 2016.

Zhang, H. H., Pak, B., Wang, Y. P., Zhou, X., Zhang, Y. and Zhang, L.: Evaluating surface water cycles simulated by the Australian community land surface model (CABLE) across different spatial and temporal domains. *J. Hydrometeorol.*, 14, 1119–1138, 2013.

[Zhang, Y., Gao, Z., Li, D., Li, Y., Zhang, N., Zhao, X., and Chen, J.: On the computation of planetary boundary-layer height using the bulk Richardson number method, *Geosci. Model Dev.*, 7, 2599–2611, doi: 10.5194/gmd-7-2599-2014, 2014.](#)

- 5 Ziehn, T., Nickless, A., Rayner, P. J., Law, R. M., Roff, G., and Fraser, P.: Greenhouse gas network design using backward Lagrangian particle dispersion modelling – Part 1: Methodology and Australian test case, *Atmos. Phys. Chem.*, 14, 9363–9378, doi: 10.5194/acp-14-9363-2014, 2014.